Conceptual Design of an industrial-scale artificial leaf device

PDEng - Chemical Product Design; Individual Design Project - Final Report

Victoria Garcia, Mercedes; Swinkels, Pieter

Publication date
2015

Document Version
Other version

PDEng - Chemical Product Design

Individual Design Project

CONCEPTUAL DESIGN OF AN INDUSTRIAL-SCALE ARTIFICIAL LEAF DEVICE

Final Report

Author:

Mercedes Victoria MSc. TU Delft, Delft Product & Process Design Institute

Supervisors:

prof. dr. Bernard Dam TU Delft, Chemical Engineering Department

dr. ir. Urjan Jacobs TU Delft, Delft Product & Process Design Institute

ir. Pieter Swinkels TU Delft, Delft Product & Process Design Institute

prof. dr. Ernst Sudhölter TU Delft, Chemical Engineering Department

Sander ten Hoopen MSc. Hydron Energy B.V.

Keywords:

Hydrogen, Photo-electrochemical cell, Design

Date issued:

12 August 2015

TU Delft Delft University of Technology

BioSolar Cells

Acknowledgements

I would like to thank in first place the *BioSolar Cells* consortium, for giving me the opportunity to take park on this challenging and aspiring project. Secondly, thanks to prof. dr. Bernard Dam, principal of the project, as well as to the steering committee members: ir. Pieter Swinkels (design coach), prof. dr. Ernst Sudhölter (scientific advisor) and Sander ten Hoopen MSc. (technical advisor). Thank you all for the countless discussions, which resulted in great input for my design.

Special thanks to my daily supervisor, dr. ir. Urjan Jacobs, for his patient guidance and continuous help during this year, which materialized in constant feedback and persistence on details.

I would also like to thank several people that, although were not official advisors of this project, certainly contributed as much as if they were: dr. David Vermaas, dr. Wilson Smith, Moreno de Respinis, Ibadillah Digdaya and Bartek Trzesniewsk. Thanks for the fruitful discussions and for your patience answering my questions.

Thanks to all my fellow PDEng trainees, for being great partners in this demanding programme. Special thanks to those who performed with me the Group Design Project, which set the basis for the present design work: Bengisu Corakci, Nicola Donato, John Paul Garcia, Aurélie Nonclercq and Shriya Reddy Paida. I can't imagine a better group of people to work with. Furthermore, I would like to thank all the *MECs* members for constituting a great environment to work on this design project. I will always remember those coffee breaks that gave me the energy necessary to perform this design.

I could not have performed this *Individual Design Project* without my family and friends who, at a great distance, have been supporting me more than ever on this final step of PDEng traineeship. Thanks for your continuous support in everything I pursue.

Executive summary

Hydrogen, if produced from clean and abundant sources, has the potential for solving the concerns on energy supply security, climate change and local air pollution. Photoelectrochemical (PEC) water-splitting is a promising technology under development for the production of hydrogen from water by using sunlight. This design project aims to investigate the practical implementation of this innovative technology by developing an initial conceptual design of a modular PEC water-splitting device that could be on the market by 2020.

An analysis of the state-of-the-art of the so-called *artificial leaf* technology was used to identify the main design challenges: (a) the need of finding efficient, durable, low-cost, earth-abundant semiconductors and catalysts, (b) the separation of the evolved gases in a reliable way to ensure the safety of the device, (c) the optimization of the components size and relative positioning to minimize internal losses and enhance light absorption, and (d) the optimum operating conditions.

To facilitate the design process of a device that could overcome the identified challenges, a step-wise methodology was applied. In each level, various design alternatives were investigated and evaluated according to technical, economical, safety and sustainability criteria. A device consisting of one photoelectrode and a counter metal electrode facing each other was selected, since this configuration offers low Ohmic losses. Moreover, the photoelectrode is illuminated from the back to minimize the light losses. Low cost and earth-abundant materials were selected for the main components: (i) multifunction a-Silicon for the photoelectrode, (ii) Nickel Molybdenum protection layer for the photoelectrode and (iii) Nickel counter electrode. For these materials to be stable and efficient, the device should operate under alkaline conditions. Moreover, to ensure the separation of the gases, an anion exchange membrane is placed in between the electrodes. Nevertheless, the design offer flexibility to implement material developments.

The economic feasibility of a hydrogen production plant utilising the designed device has been investigated, leading to potential hydrogen cost below 6 \$/kg. This device could be manufactured with commercially available components and manufacturing process, with an estimated cost of ~70 \$/m^2. Moreover, a sustainability life cycle assessment (LCA) showed the potential environmental benefits of this technology, with an energy payback time lower than 2 years, and savings of 2.5 ton CO_2 eq. emissions per m^2 of device during its full lifetime (15 years). It was concluded that the developed conceptual design could succeed in the market, providing a safe and environmental friendly process for hydrogen production.

Nevertheless, some practical issues were identified that need to be resolved before this PEC technology is marketable, and therefore it is recommended that laboratory research focuses on the further development of (a) protection layers to improve the stability of the semiconductor photoelectrodes and (b) anion exchange membranes to minimize the gas crossover and ensure the safety of the device. With respect to engineering development of the device it is recommended to initiate a detailed design project that focuses on the optimization of the operating conditions and the flow management to minimize the internal losses and the gas crossover.

Table of Contents

1

Introduction

This chapter describes the context, the goal and the scope of this project. The main design challenges are outlined and the design solution is briefly described. Lastly, the contents of this report are presented.

1.1 Project Background

The world population and the world economy are expected to increase at 1% and 3% per year until 2035, respectively (European Commission, 2006), which will have as consequence an increase of the world energy demand up to 140,000 TWh (IEA, 2014). If no changes are made in the current global energy system, where fossil fuels provide more than 82% of our energy supply, detrimental consequences are foreseen (IEA, 2014). Not only fossil fuels are a limited resource, but its production and usage are irreversibly harming the environment (EPA, 1999). The global energy sector is responsible for two-thirds of greenhouse gas emissions, which contribute to the climate change and is responsible for more than 150 thousand deaths a year (WHO, 2005). Therefore, it is imperative to make a transition towards sustainable, abundant, carbon-free fuels. Hydrogen is regarded as one of the most promising candidates capable of leading this transition, because it could be used in almost every sector where energy is required, from transportation to industry and households. Furthermore, the utilisation of hydrogen will only produce water as waste. An additional benefit is that hydrogen can be stored, unlike electricity, in either small or large quantities for long periods without significant losses. Finally, hydrogen can be produced potentially from a wide variety of resources, including renewables. However, the production of hydrogen in a sustainable manner, making use of renewable and abundant sources, remains a scientific and engineering challenge (Ball, 2009).

Photoelectrochemical (PEC) water-splitting is a novel and promising way of producing hydrogen in a sustainable way, as it uses sunlight as the only energy input. With this technology solar energy can be stored in the form of chemical bonds, in a similar way as plants do in the photosynthesis process (reason why it is often called *artificial leaf*). The working principle of this technology is described in detail in Appendix A.

In the laboratory-scale solar-to-hydrogen efficiencies of 5% have been achieved (Abdi, 2013), which is almost half of the 10% efficiency target set by the United States Department of Energy (DOE). *BioSolar Cells*, a five-year project funded by Dutch universities, research institutions and industries, envisions that photoelectrochemical production of hydrogen from water will be dominant in 2050 in the highest Technological Readiness Level (TRL). For this reason, *BioSolar Cells* aims to facilitate the rapid development of the technology towards its first commercialization by 2020 and to allow for a technological maturing period toward standardisation of about 30 years (see Figure 1).

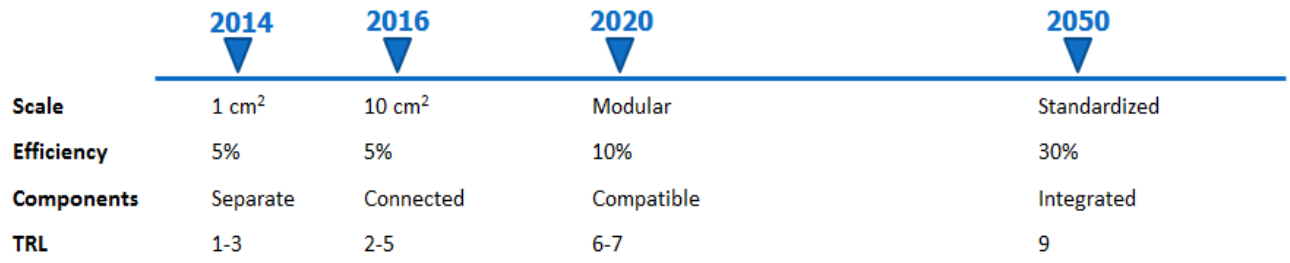

Figure 1. Envisioned timeline for the development trajectory of artificial leaf technology

The current knowledge about the PEC hydrogen production has reached a sufficient level to justify initial investigation into the practical implementation on industrial-scale. Most research on the topic has been focused on specific parts of the PEC cells (mainly in the photoelectrodes) as well as on laboratory-scale configurations. However, very little research has been done on the development of this technology into realistically sized devices for large-scale implementation. To bridge this gap, it is paramount to investigate the engineering and societal hurdles upfront, in order to spur the development of the PEC technology. Developing a conceptual design of an industrial-scale device will shine light on practical issues that need to be overcome before the commercial deployment of this technology.

1.2 Project goal

The goal of this project is to develop a conceptual design of the envisioned PEC water-splitting modular device that could be produced at industrial-scale in 2020.

1.3 Project scope

The tasks that are covered in this project, as well as the ones that are out of the scope, are presented in Table 1.

Table 1. Scope of the project

Inside the scope of this project
- Identification of the most promising application of the PEC technology for its introduction in the market - Literature review of current efforts of scaling up this technology and patented devices - Identification of technical, manufacturability, safety, environmental and economic constraints as well as development hurdles - Proposal of design solutions for identified development hurdles within identified constrains - Selection of the most promising design alternative for development, based on expected technology development, manufacturing feasibility, device operability, environmental impact, flexibility and inherent safety - Conceptual design of the selected modular PEC water-splitting device - The conceptual design of the device will include the following: water-splitting photoelectrochemical solar cell, retrieval of hydrogen and/or oxygen, maintenance of water balance, and storage of hydrogen and/or oxygen - Sustainability Life Cycle Analysis of the selected device - Economic estimation of device costs and hydrogen and/or oxygen production costs

Outside the scope of this project
- Detailed design - Laboratory work - Transportation of hydrogen and oxygen after storage - Device considerations for on-board production of hydrogen for small vehicles - Prototype construction

1.4 Design description

Design problem

This project aims to deliver a conceptual design of a modular PEC water-splitting device. The resulting device should be manufacturable at industrial-scale and it should tackle the technical, economic, environmental and societal challenges of bringing the artificial leaf technology to a commercial scale.

The design challenges that need to be overcome to make the artificial leaf technology into a market competitive technology by the year 2020 are collected in Table 2. The most promising design of a PEC module that tackles all the challenges highlighted in this table is the main question to be answered in the current report.

Table 2. Challenges in the design of an industrial-scale artificial leaf device

ENGINEERING CHALLENGES	- Separation of the gases produced in the cell - Long-term stability of the materials - Light capturing - Optimization of spacing between components - Optimization of operation conditions (pressure and temperature) - Favourable kinetics for the hydrogen and oxygen production reactions - Minimization of the system internal energy loses - Minimization of the environmental impact during its whole lifecycle - Maximization of system durability - Safety of the device - Minimization of the overall device and operating costs
ECONOMIC CHALLENGES	- Use of efficient and low-cost materials - Minimization of the operating cost - Minimization of the hydrogen production cost
ENVIRONMENTAL CHALLENGES	- Use of earth-abundant materials - Use of recyclable materials - Minimizing footprint of the manufacturing process
SOCIETAL CHALLENGES	- Ensure availability of raw materials for the construction of the device - Economic viability and sustainability of the production chain - Safety considerations for production and usage of hydrogen as a fuel

Design solution

The design of the industrial-scale artificial leaf device was the result of a multi-stage design approach, in which each step went subsequently into more detail. The device designed is composed by a back-illuminated tandem photoelectrode, stabilized by a protection layer, and placed in front of a metal counter electrode. A membrane is used to keep the evolved gases separated. A sketch of the design selected can be seen in Figure 2. More details about the materials and the manufacturing of the device are described in Chapter 5.

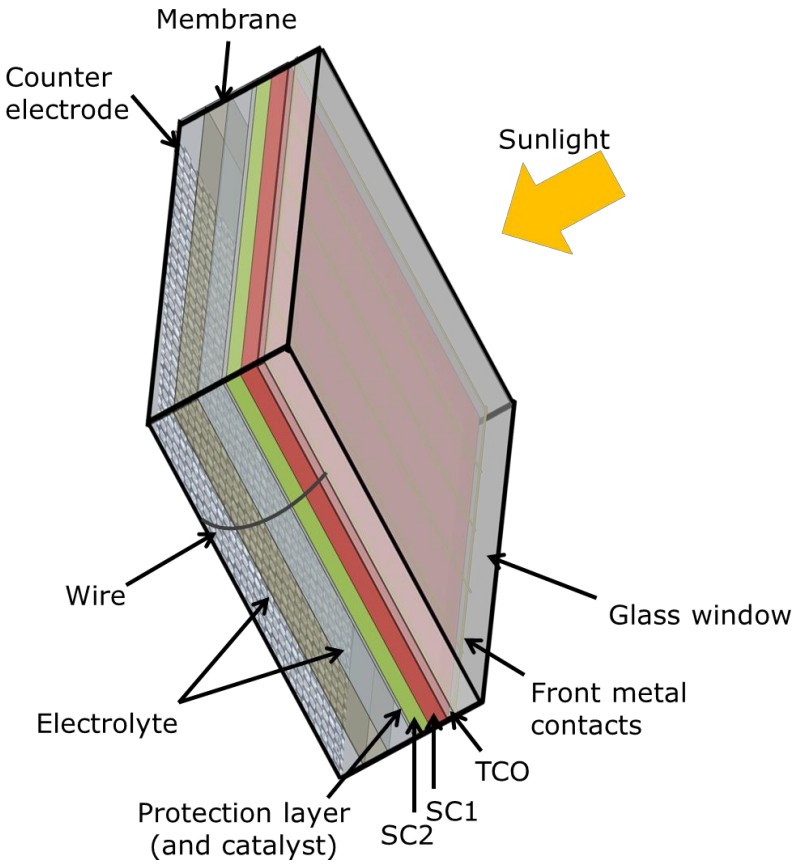

Figure 2. Scheme of the selected design for a scalable artificial leaf device

1.5 Report structure

The report is structured as follows. Chapter 2 describes the *design approach*, containing the design methodology, the modelling tools and the creativity techniques that were used throughout the project. The project organization is also described in this chapter, defining the main milestones and the planning to accomplish them in a period of 12 months. Thereafter, a *market analysis* of the artificial leaf technology is presented in Chapter 3. In this chapter, the opportunities and barriers for the implementation of the technology in the market are described, as well as an appraisal of possible applications for the artificial leaf. The most promising market was further developed with two case studies, and lastly a competitor analysis is presented. In Chapter 4, the *design criteria* for the large-scale artificial leaf device are presented. These criteria were the result of estimations and assumptions that are also described in the chapter. The following chapter (Chapter 5) is focused on the *product design*. The design process is described according to the methodology presented previously in Chapter 2. The selected design is described in detail and the selection of the materials is presented. The envisioned operation of a hydrogen production plant based on the selected design is also described at the end of this chapter. The *economic analysis* of the envisioned PEC water-splitting plant is

presented in Chapter 6. This chapter contains the estimation of the total capital investment as well as the operational expenditures of the hydrogen production plant. A profitability analysis is also presented and the levelized cost of hydrogen was estimated. Lastly, a sensitivity analysis is presented, which shows the effect of several parameters on the cost of hydrogen. Furthermore, the *social and environmental impact* of the device is presented in Chapter 7. A discussion on how the design of the PEC device meets the design criteria is presented in Chapter 8. To finalize, the *conclusions* of this design project are presented in Chapter 9.

2

Design Approach

In this chapter the type and driver of the design project are identified. The design methodology that was followed to facilitate the design process is also explained, together with the modelling tools and the creativity methods that were used. Lastly, the milestones and deliverables of this project are presented, as well as the planning.

2.1 Design type and driver

The design process is related to the type and drivers of the project. This project has *new product* design type, as the project aims to develop a new product family and its manufacturing process. Since this type of innovative design work addresses an unfamiliar product category, there is high risk and many uncertainties involved.

The artificial leaf research has developed towards a stage that the first market evaluation and prototyping is needed for valorisation of the research effort into a marketable product. The technology is able to produce hydrogen and oxygen from water using solar light, but an appropriate market placement of the technology needs to be found. As hydrogen has been identified as the fuel of the future (Ball, 2009; Busby, 2005; Sørensen, 2012), it is expected a high demand of sustainable hydrogen production methods, independently from fossil fuels. In this context, the artificial leaf is not yet at a stage ready to be widespread implemented to supply a large percentage of the hydrogen demand. Therefore, there is a need of finding an appropriate market niche, where the technology could be deployed in the short and medium term. Hence, the design driver of this project is *technology push*, since the primary focus of the project is to find an appropriate market opportunity for the technology and to study the potential commercial viability of an artificial leaf device.

2.2 Design methodology

Design methodologies are an important tool that can largely facilitate the process of designing a new product. Several methodologies were analysed to identify the optimal design approach for this project, and the selected one was based on the *Delft Template for Conceptual Process Design* (Grievink & Swinkels, 2014). This methodology follows an iterative process, on which the level of detail of the design increases in each cycle (see Figure 3).

Each cycle starts with the scope definition followed by a knowledge phase on which the state-of-the art of the technology is studied. In this knowledge phase, a literature study is performed to gather information and the main design constraints are identified. An idea generation phase follows, where solutions to the identified problems are proposed. The ideas are analysed in the next phase, where some characteristics of the design are quantified. According to criteria based on functionality, safety, sustainability, cost and manufacturability, the designs are then evaluated. The most promising design(s) are selected to continue with more detailed design. Before moving forward with the next cycle, a reporting phase is carried out.

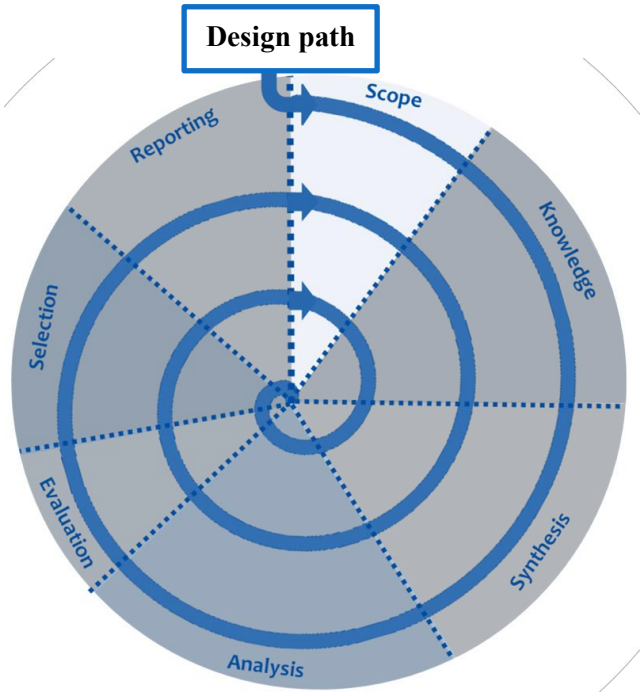

Figure 3. Design methodology to be followed in this project

This stepwise design approach, from scope definition to reporting, was also used for the identification of the market opportunities for the artificial leaf technology.

2.3 Modelling tools

For the performance of calculations and the development of the case studies, Microsoft Excel® was used. This tool was also used for the performance of the economic analysis of the selected design. For design selection, an *evaluation matrix* was used to compare different designs. Once a final design is selected, sketches of the device were done using PowerPoint®.

2.4 Creativity methods

A creativity method called "Mindmap" was used for individual idea generation on the possible market opportunities for the artificial leaf device. The technique consists of writing a central term in the middle of a page and writing many branches around it, and then sub-branches, and so on (Tassoul, 2009).

Another creativity technique used is "Brainwriting" (Tassoul, 2009). This group creativity method was used in parallel to "Mindmap" method to find even more market applications for the technology. Since this technique requires a group of people, the session was organized with the participation of four PDEng trainees and two stakeholders of the project. For this idea generation method, a paper with the layout as shown in Figure 4 is used.

	PROBLEM:		
Person 1 →	Idea 1	Idea 2	Idea 3
Person 2 →	Idea 1	Idea 2	Idea 3
Person 3 →	Idea 1	Idea 2	Idea 3
Person 4 →	Idea 1	Idea 2	Idea 3
Person 5 →	Idea 1	Idea 2	Idea 3
Person 6 →	Idea 1	Idea 2	Idea 3

Figure 4. Brainwriting template

One piece of paper with that layout is provided to each participant. In a maximum time of five minutes, each person writes three ideas (one on each column). Afterwards, the papers rotate and each person writes three new ideas on the new paper. If a person is running out of ideas, he/she can look at the ideas written by previous people for inspiration. The process goes on until the six papers are filled. With this technique, 108 ideas (6 x 6 x 3) are generated in less than 30 minutes.

2.5 Milestones and deliverables

The project was divided in five major milestones, each of them supported by deliverables (see Table 3). The main work content of each milestone is described in this table as well. The first four milestones finish with a meeting where all the stakeholders of the project will be present. In each of these meetings, a presentation by the trainee will be given summarizing the main results, followed by a discussion. A report will be delivered about one week in advance to the meeting. The stakeholders were expected to read the report and bring their questions, comments and suggestions to the corresponding meeting. The last milestone consists on an open presentation of the project, where other PDEng trainees and relevant members of the Chemical Engineering faculty are invited.

Table 3. Milestones and deliverables of the design project

Milestone	Deliverables	Contents
Kick-off	❖ Project brief ❖ Kick-off presentation	• Goal and scope of the project • Planning • Identification of stakeholders and their needs • Market opportunity • Literature study
Basis of Design	❖ Basis of Design report ❖ Basis of Design presentation	• Market analysis of the PEC water-splitting technology and development of at least one case study • Identification of design challenges • Analysis of the identified design constraints • Design criteria
Intermediate	❖ Intermediate Design brief ❖ Intermediate presentation	• Idea generation to meet design challenges • Development of the design concepts • Evaluation of design concepts based on performance, safety, sustainability, cost and manufacturability criteria • Selection of most promising design concept for development
Final	❖ Final Design report ❖ Final presentation	• Improved design concept • Manufacturing of final device • LCA of the device • Estimation of device costs and hydrogen production costs
Colloquium	❖ Colloquium presentation	• Dissemination of the design work through an open presentation

2.6 Planning

All the milestones were executed in a period of 12 months as shown in the project planning (see Figure 5). The dates and time of the milestone meetings with presentation, which were agreed upon during the kick-off, are also shown in this figure.

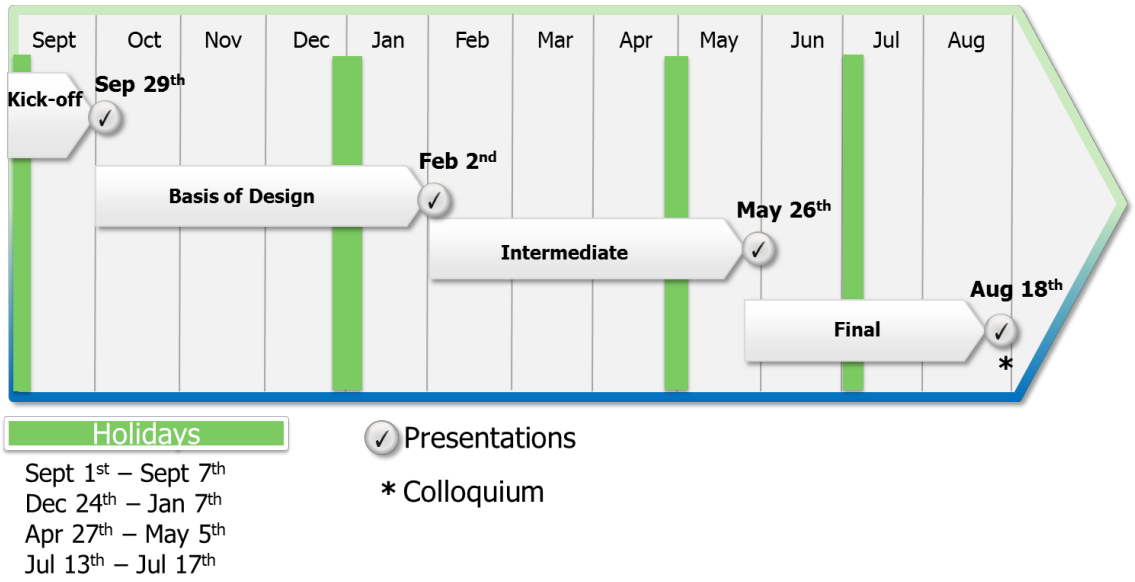

Figure 5. Planning for the project

3

Market analysis

In this chapter, the opportunities and barriers for the artificial leaf technology to enter the market are analysed by using a SWOT analysis. After that, possible markets for the PEC water-splitting device are identified. Many ideas were obtained by literature research and creativity sessions, and were evaluated in order to select the most promising ones. The market of stand-alone power systems seems the best niche for the first commercialization of the artificial leaf device. Two case studies were performed to show the potential of this technology in off-grid power generation. The chapter finalises with the identification of competitors and a deeper analysis on the main competing technology: the combination of PV panels and electrolysers.

3.1 Opportunities and barriers

When analysing the market for a new product, it is important to identify its opportunities and barriers. In order to do so, a SWOT analysis of the artificial leaf was performed (Appendix B). In this analysis, the strengths, weaknesses, opportunities and threads are identified.

Strengths are positive aspects of the technology that are inherent to it. The main strength of the artificial leaf is the possibility of storing solar energy in the form of a clean fuel allowing for an energy system independent from fossil fuels. The modular configuration of the artificial leaf allows for easy adaptation of the capacity to the customer needs. Moreover, possible on-site generation has the advantage of eliminating the cost of hydrogen transportation. Other strengths are the potential for using earth abundant and low cost materials, which could result in a low capital investment. Moreover, the maintenance costs have the potential for being very low.

There are some external issues that constitute *opportunities* for the artificial leaf. One opportunity is the increasing public acceptance towards hydrogen, due to an increase in environmental awareness. Currently, the public knowledge is low, specifically about the artificial leaf technology. To mitigate this, it is necessary that the public understand the need for a transition to a hydrogen economy. When the time comes to bring the artificial leaf to a point to penetrate the market, it is needed that a marketing campaign shows the benefits of this technology. The depletion of fossil fuels is another issue that will help the development of the required market environment.

The development of hydrogen fuelled cars, such as the new Toyota Mirai (http://www.toyota.com/fuelcell/), states the need of hydrogen fuelling stations, which is a possible market for the artificial leaf. Moreover, the cost of delivering hydrogen and the complex logistics involved is the main challenge in the development of a hydrogen economy based in centralized production of hydrogen. Building a new pipeline network for hydrogen is prohibitively expensive in the short to medium term (Ball, 2009). This constitutes an opportunity for the hydrogen production technologies with possible on-site generation, such as the artificial leaf. Lastly, the difficulty in economically and efficiently capturing CO_2, which results as by-product in the production of hydrogen via steam reforming and coal gasification - the two most economical methods of hydrogen production nowadays (see section 3.4) - poses an advantage for the artificial leaf, where no CO_2 is produced.

On the other hand, *weaknesses* of the artificial leaf technology are its technology immaturity and the need of finding cheap, efficient and stable earth-abundant materials for the system components. Moreover, due to the low efficiency of the device, of about 15%, large areas will be needed to produce a significant amount of hydrogen. Lastly, the inexperience in recycling the systems components is an issue to be solved before the commercial implementation of this technology.

In the SWOT analysis several *threats* have been also identified. These threats to the artificial leaf technology come from external issues such as the need for further improvement and cost reduction of fuel cells and hydrogen storage technologies. The implementation of the artificial leaf as part of a hydrogen economy will depend on these systems. Another threat is related to the development of competing technologies. Moreover, possible regulatory and institutional barriers constitute a potential threat for the PEC hydrogen production technology.

3.2 Identification of possible markets for the artificial leaf

The function of the artificial leaf is to provide hydrogen in a sustainable way, in order to positively contribute in the development of a *hydrogen economy*. However, the transition towards a hydrogen economy is expected to be gradual and long (HyWays, 2008). In this transition period it is important to identify niche markets for the first hydrogen applications to develop its techno-economic potential. The development of initial markets for the technology will help in (a) the development of the product, (b) lowering of manufacturing cost, and (c) increasing public awareness on hydrogen as an energy carrier (Ball, 2009).

In order to identify possible markets for the artificial leaf, several applications of hydrogen and oxygen were identified. A literature research was first performed to identify applications. A mindmap was then created, to enhance creativity and find new ideas over the ones found in literature. A brainstorming session was hold with the goal to identify new and creative markets.

3.2.1 Idea generation

Mindmap

The mindmap creativity method (Tassoul, 2009) was used to generate ideas of possible applications for this technology. The central word was “artificial leaf”, out of which branches with the words hydrogen, oxygen, sunlight and water, represent the outputs and inputs of a PEC device. From these four words, different word associations were written and expanded into new related words and so on. The resultant mindmap can be found in Appendix C.

Brainstorming session

To generate more ideas to find markets for the PEC water-splitting technology a *brainwriting* session (Tassoul, 2009) was held. Six people from different backgrounds attended the session. After the introductions and an icebreaker activity, the problem was explained. The main question posed to the attendees was “*where could you use a PEC cell?*”, which was also presented as “*where could oxygen and hydrogen be used?*”. After making sure that everyone had a clear understanding of the problem and the goal of the session, the idea generation was performed, following the method explained in Chapter 2. After the idea generation phase, the ideas were clustered in different groups and repeated ideas where removed. When all the ideas were organized, there was time for more idea generation and combination of ideas. A total of 84 ideas were generated and can be found in Appendix D.

3.2.2 Idea evaluation

A total of 15 ideas were selected as the most attractive from the results of the brainwriting and the mindmap methods. An evaluation matrix was used to identify the most promising applications. The matrix can be found in Figure 6.

The evaluation criteria were the following:

- **Mid-term implementation.** If the implementation of the artificial leaf requires the development of a different technology that will not be ready by 2020, then the market is not attractive. To illustrate this criterion the idea of fuelling stations for boats is evaluated. Currently, there are no boats running on hydrogen and it is not expected to become a firmly established market by 2020. Hence, the idea is unattractive for mid-term implementation.
- **Possibility of using both gases.** If the market allows the utilization of oxygen as well as hydrogen, it will make the artificial leaf a more economically attractive technology.
- **Already expensive market.** It is expected that the first artificial leaf devices will provide hydrogen at a high cost. Therefore, an application where the price of hydrogen or the supply of electricity is already expensive will be easier to enter.
- **Governmental subsidies.** As mentioned before, this technology will require a high capital investment. For this reason, the possible economic help of the government will facilitate the implementation of this technology.
- **Environmental concern.** There are much cheaper ways of producing hydrogen than using a PEC cell, such as steam reforming or coal gasification (European Commission, 2006). However, these technologies produce large amounts of CO_2. The environmentally friendliness of the PEC technology will pose and advantage of this technology over the cheaper but "dirtier" technologies, in a market where pollution is an important concern.
- **Low complexity of the infrastructure.** Producing and storing hydrogen remains a technical challenge. If to that, the construction of a hydrogen distribution infrastructure needs to be added, the implementation time will be extended. This is the case, for example, of centralized hydrogen production facilities. For mid-term implementation localized facilities are a more reasonable market.

	Mid-term implementation	Possibility of using both gases	Already expensive market	Possible Government Subsidies	Environmental concerned	Complexity of infrastructure
On a hospital						
On a University						
Offshore fuelling for boats/ submarines						
On a harbor (fuel for boats)						
Fuelling station buses						
On a house (residential area)						
Isolated mountain (house or other)						
Island (house/commercial)						
Weather stations						
Remote villages in Africa						
On the side of a road						
On an industrial site						
Centralized facility						
On a water treatment plant						
Electronic industry						

Figure 6. Evaluation matrix for ideas generated with the creativity methods. Green indicates that the application meets the requirement; red indicates that the criterion is not met.

3.2.3 Idea selection

It can be observed in the evaluation matrix (see Figure 6) that the application of the artificial leaf to provide energy on difficult to access locations such as islands, mountains or weather stations seems most promising in light of the criteria. These promising applications are part of the stand-alone power systems market.

Moreover, it can be seen in the evaluation matrix that Universities are also a promising market. Although for these buildings the obtainment of energy is not too expensive, their openness to innovation and sustainability makes them a promising market for initial investigations of the implementation of the artificial leaf in a stand-alone power system.

All in all, the market of stand-alone power systems is considered as the best niche for the first commercialization of the artificial leaf technology.

3.3 Artificial Leaf in stand-alone power systems

In Europe, around 300,000 houses are not interconnected to the main electricity grid (Lymberopoulos & Zoulias, 2008). These houses are located in remote areas such as islands and mountains. Currently, fossil fuel based generators do the electrification of these households, which face problems with onsite fuel availability, noise and local emissions. Sometimes the generators are supplemented with renewable energy based systems (e.g. PV solar panels or wind turbines). However, these systems have to deal with the intermittency of the natural source, such as wind or sun. The disadvantages of both systems could be potentially overcome with the introduction of the artificial leaf technology for fuel production, since the energy provided by the natural intermittent source (i.e. the sun) could be stored in the form of a clean fuel, providing a reliable and sustainable power system.

On the other hand, it is expected that one of the most important barriers in the introduction of the artificial leaf technology in a hydrogen-based power systems is its high cost. Since these off-grid power systems already have a high energy cost – usually more than 1 €/kWh (Lymberopoulos and Zoulias, 2008) – it makes this a promising market niche.

The future potential markets for hydrogen-based stand-alone power systems can be divided in two main groups: customers already connected to the grid and customers without access to grid (see Figure 7). The customers already connected to the grid are a least promising market segment for the short term. However, willingness to investigate the novel implementation of stand-alone renewable-energy-based power systems could persuade these customers (e.g. universities or early adopters). Other potential customers that have access to the grid are people that only have access to electricity at a premium price. For example, in certain rural isolated areas, it might therefore be possible to enter the market.

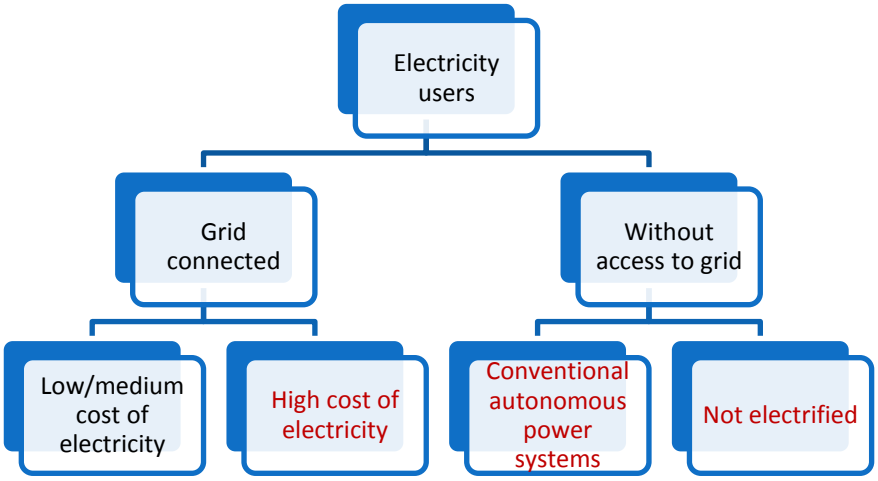

Figure 7. Identification of customers for stand-alone power systems based on the artificial leaf technology

Customers that are not connected to the grid constitute a more promising niche market for the early implementation of the artificial leaf technology. These customers can be divided into two segments: those with access to electricity thanks to conventional (fossil fuel based) autonomous systems, and those with no access to electricity.

An estimation of the market size for stand-alone power systems in Europe was performed by Lymberopoulos and Zoulias (2008), concluding that the total annual energy demand for these systems is of ~1.7 TWh, being the largest market segment in residential applications in rural villages. National and local authorities provide financial support for the electricity supply in rural villages, because a reliable electric grid in rural villages is an important measure to avoid depopulation of these areas.

To show the potential of the artificial leaf technology in the selected market of stand-alone power systems, two case studies were developed, and they can be found in Appendix E.

It should be noticed that the envisioned hydrogen-based stand-alone power systems, uses a combination of PV panels and PEC water-splitting devices. It is believed that this combination of devices would give a more efficient and economic system than using solely PEC panels. Commercial PV panels convert sunlight into electricity with an efficiency of ~20% (Luque & Hegedus, 2011). On the other hand, the production of electricity using a PEC cell with an efficiency of 15% (Lewerenz, 2013) and a fuel cell with 60% efficiency (Larminie, 2013) will result in less than 9% solar-to-electricity efficiency. For this reason, it is more efficient to convert sunlight directly into electricity while the sun is shining, and use the hydrogen fuel only when the

PV panels cannot provide electricity. The area of PV panels should be sized according to the energy demand during daytime (while sunlight is available). During this time, the PEC modules will be producing hydrogen that will be stored and used to cover the electricity demand when the sun is not available. The design capacity for both PV and PEC panels will vary according to the application and the sizing will require information on the electricity load profile.

The first case study analyses the possible substitution of a diesel generator by the artificial leaf in an island of Greece (without access to the grid). It was concluded that a small community at the Greek island of Kythnos could in principle be powered by a stand-alone power system that relies solely in the solar energy, by using a combination of 73 m^2 of solar panels and 71 m^2 of PEC modules.

Furthermore, the implementation of the PEC water splitting technology at the campus of Delft University of Technology (grid connected), was investigated in a second case study. It was shown that a combination of 1,800 of PV panels and 2,800 m^2 of PEC panels, that provide hydrogen for fuel cells, could supply the electricity consumed at the Sports Centre. This area is indeed available in the roofs of the building and in the unutilised area of the surroundings. This preliminary analysis showed the feasibility of providing electricity to the Sports Centre solely with solar energy. A more detailed study should be performed in order to optimize the combination of PEC and PV panels and to size the hydrogen storage capacity. For this, the hourly electricity demand at the building and the hourly irradiation profile should be known. Lastly, although the utilisation of oxygen has not been considered in this study, oxygen could be used at the TU Delft for laboratory purposes, providing additional economic benefits to the system.

3.4 Competitor analysis

The artificial leaf will compete with other hydrogen production technologies on the market. According to the European Commission, in their World Energy Outlook 2050, the most representative and promising hydrogen production technologies over the next fifty years are steam reforming of natural gas, coal gasification, biomass gasification and electrolysis of water (European Commission, 2006). A brief description of these hydrogen production technologies can be found in Appendix F. Table 4 shows the main advantages and disadvantages of each of the technologies.

In the short term, steam reforming and coal gasification will be the main competitors of the artificial leaf. However, increasing environmental concerns and need for energy security, avoiding the dependence on fossil fuels, will make these technologies unattractive in the long term. Biomass gasification seems to be a promising technology for hydrogen production with potentially no net CO_2 emissions. However, this technology is still under development and will be limited by available biomass (waste or from non-food crop yielding lands) in order to avoid competition with food production.

For the specific application of the artificial leaf technology in stand-alone power systems, the only competitor is electrolysis of water, since the other technologies are too expensive to scale-down. If the electrolyser is powered with electricity coming from a solar panel, it could serve the same function as the PEC water-splitting technology Therefore, the combination of PV and electrolysis will be the main competitor for the artificial leaf. The combination of these two technologies is further analysed in the following section.

Table 4. Comparison of different hydrogen production technologies (European Commission, 2006)

Technology	H_2 cost	Advantages	Disadvantages
Steam reforming of natural gas	5 – 8 €/GJ *0.6 – 1 €/kg*	- Mature technology - Easily scalable - Good safety records	- Emission of CO_2 - Dependence on natural gas - Low purity of hydrogen - Expensive to scale-down and need of large area
Coal gasification	8 – 10 €/GJ *1 – 1.2 €/kg*	- Mature technology - Large scale production	- Emission of CO_2 - Dependence on coal - Low purity of hydrogen - Expensive to scale down
Biomass gasification	9 – 12 €/GJ *1.1 – 1.4 €/kg*	- No net CO_2 emissions	- Biomass is a complex and variable feedstock - Complex gas cleaning needed - Difficult to scale down - Immature technology
Electrolysis of water	22 – 25 €/GJ *2.6 – 3 €/kg*	- Easy to scale to large and small facilities - Mature technology - High purity of hydrogen - Possible zero emissions, if electricity is provided from renewable source	- High consumption of electricity

3.4.1 Solar-to-hydrogen via PV + electrolysis

The main competitor for the artificial leaf technology is the production of hydrogen combining an electrolyser and solar panels. The first obvious difference between the two hydrogen production technologies is that the artificial leaf integrates the entire process of solar absorption and water splitting in one single device. The integrated device has the potential to be simpler and cheaper than two separated devices, namely the PV panel and the electrolyser.

For a better understanding on the opportunities of the artificial leaf to outcompete the PV and electrolysis system, the electrolysis technology was further investigated (Appendix G). Alkaline electrolysers are a well stablished technology, with a relatively low cost since they use non-noble catalysts. However, the hydrogen output of these electrolysers has a low purity, because the diaphragm does not completely avoid the crossover of gases, especially at low loads (Carmo, 2013). Low purity of hydrogen will involve safety concerns and lower efficiency of the fuel cell. On the other hand, PEM electrolysers deliver high purity hydrogen. However, the technology is still maturing, with the main focus in development on lowering the cost of the device and extending its lifetime. Another disadvantage that both type of electrolyser face is the use of highly corrosive liquid electrolyte, which could have large environmental impacts in case of leakage. This concern will be of great importance if the electrolyser is to be placed in a protected area such as islands and natural parks. For this reason, the PEC could present an advantage if less corrosive electrolytes are used.

The integrated device (PEC) could be a more economical option than the separated PV and electrolysis. The DOE recently reported the current (2013) and future cost (2025) of hydrogen production from PEM

electrolysis, for a decentralised and centralise facility (DOE, 2014). The cost of the decentralised facility is the one that PEC technology should outcompete in the short term. The cost of hydrogen by PEM electrolysis depends on several parameters, being most sensitive to the cost of electricity (see Figure 8).

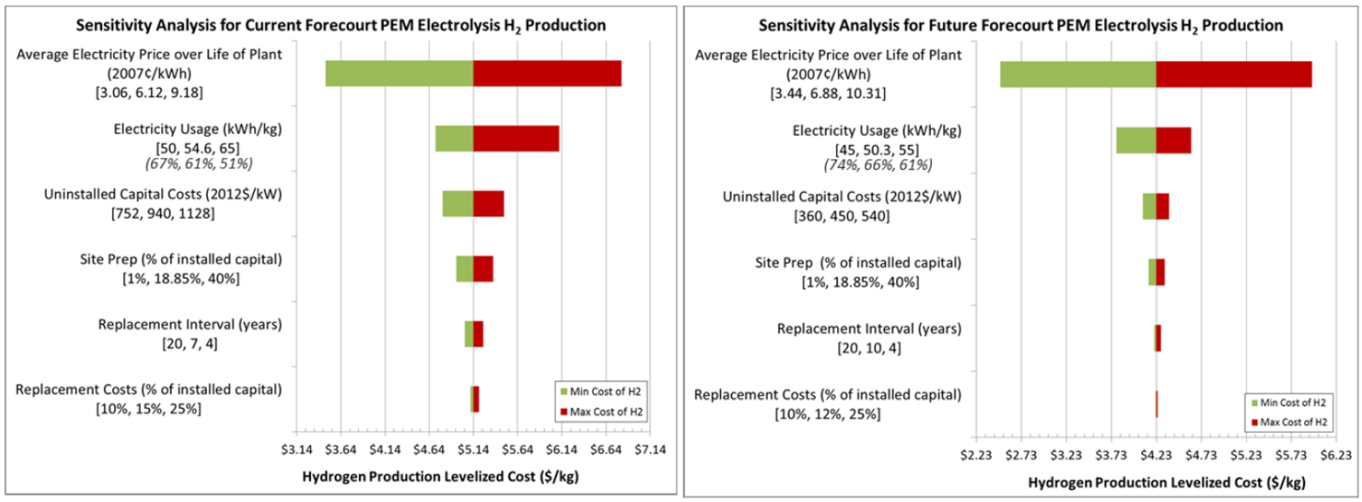

Figure 8. Sensitivity analysis of the cost of hydrogen for current (left) and future (right) decentralised PEM electrolysis hydrogen production facilities (with capacity of 1,500 kg/day) (DOE, 2014)

It was estimated that the current cost of hydrogen is in the range of 3.41 to 6.82 $/kg, for a cost of electricity of 0.031 to 0.093 $/kWh. However, that cost of electricity seems too optimistic, if compared with the forecast by the Fraunhofer institute (Figure 9. Forecast of the levelized cost of electricity from renewable and conventional energy technologies in Germany (Fraunhofer, 2013). For the *future case* (2025), it was estimated that the cost of hydrogen from PEM electrolysis could be 5.95 $/kg for an electricity price of 0.103 $/kWh.

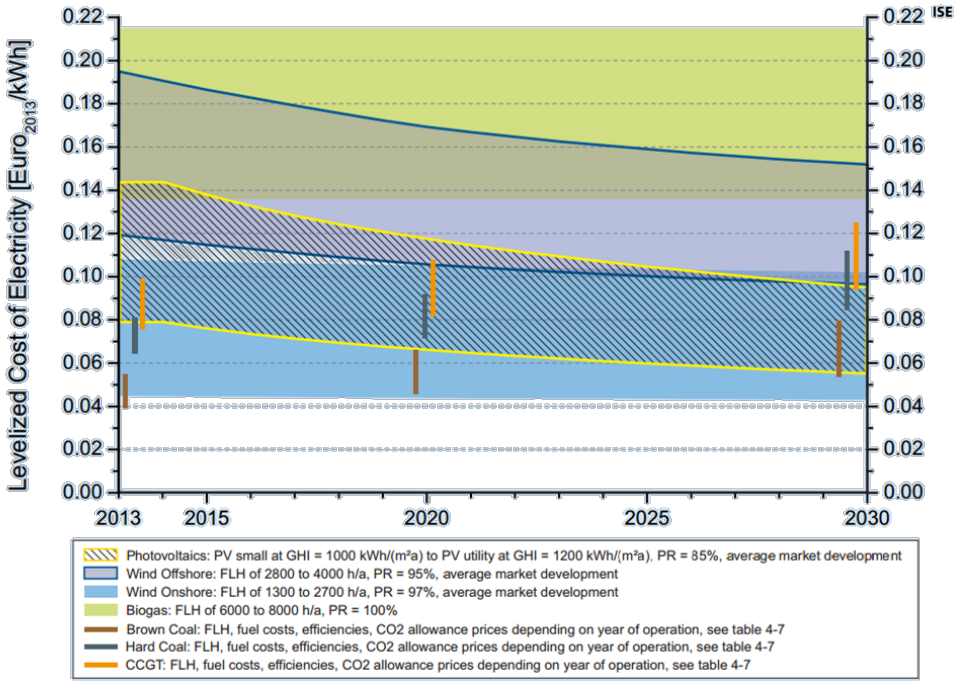

Figure 9. Forecast of the levelized cost of electricity from renewable and conventional energy technologies in Germany (Fraunhofer, 2013)

It should also be noted that these estimations assume a plant capacity of 1,500 kg/day, which is a much higher capacity than the estimated for stand-alone power systems (<100 kg/day). For example, the plant at the Kythnos Island shown described in Section 4.3.1, produces ~2 kg/day; and the plant at the Sports Centre produces less than 70 kg/day (Section 4.3.2).

Economic analysis has shown that PEC water-splitting could be a cheaper option for hydrogen production. Xu (2014) estimated the cost of hydrogen from PEC technology for a plant with capacity of 50 tons per day with 10% STH efficiency. The analysis showed that the cost of hydrogen could be lower than 3 $/kg. Again, it should be pointed out that this cost estimation corresponds to a much larger scale facility than the ones for stand-alone power systems. Figure 10 shows the sensitivity of the hydrogen cost to several parameters. It can be observed that the cost of electrodes will play an important role.

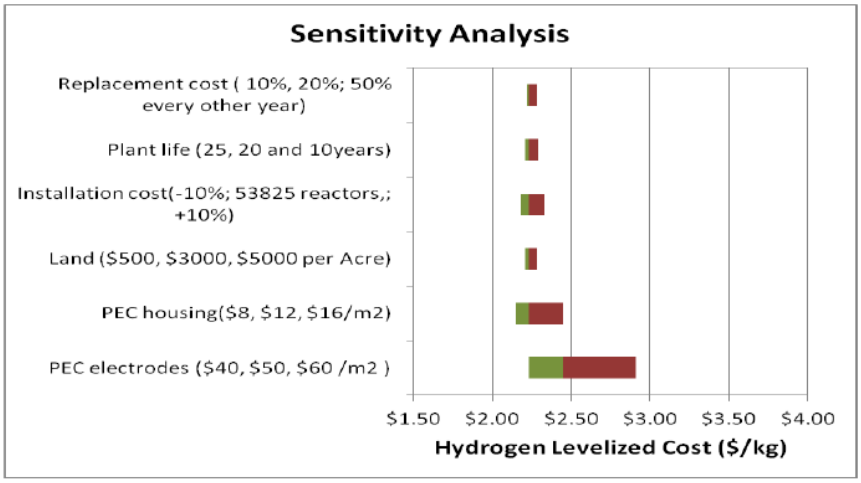

Figure 10. Sensitivity analysis of the cost of hydrogen from a PEC water-splitting facility (with capacity of 50,000 kg/day) (Xu, 2014)

However, it should be considered that the economic analysis of a new technology in such an early stage involves large uncertainty due to the amount of assumptions that need to be done to carry out the analysis. Industrial-scale production and materials to be used, among others, is information that requires assumptions for these analyses. Nevertheless, there is a potential for the artificial leaf to outcompete the *PV + electrolysis* technology in terms of cost.

Regarding the performance, a recent study compares the performance of a PV+electrolyser system and compares it to the performance of an integrated system (Haussener, 2013). The overall efficiency for the production of hydrogen via PV and electrolyser ($\eta_{PV/Electrolyser}$) was calculated using the following formula:

$$\eta_{PV/Electrolyser} = \eta_{PV} \cdot \eta_{DC-DC\ converter} \cdot \eta_{Electrolyser}$$

where η_{PV} is the efficiency of the PV cell, $\eta_{DC-DC\ converter}$ is the DC-DC converter and $\eta_{Electrolyser}$ is the efficiency of the electrolyser.

Haussener *et al.* (2013) used an efficiency of a DC-DC converter of 85%, which is in accordance with values found on literature (Keeping, 2012); and an electrolyser efficiency of 75%, which corresponds to state-of-the-art electrolyser efficiencies (Carmo, 2013). From the equation shown before, it can be calculated that a PV cell with an efficiency of 23.5% would give an overall efficiency ($\eta_{PV/Electrolyser}$) of 15%, equal to that targeted for the PEC cell.

In his study, Haussener *et al.* (2013) used a Si/GaAs as a dual absorber system for both the PV and PEC cells, and showed that an optimized PEC design could outcompete the PV and electrolyser system. For the production of the same amount of hydrogen, the PV and electrolyser system needed 13% more area than the integrated system. The difference was even larger at higher temperatures. However, it should be noticed that the selected Si/GaAs system does not represent the highest achievable efficiency of a tandem-cell PV.

The influence in irradiation and temperature was also investigated for an optimized integrated PEC system, and an optimized PV+electrolyser system. The integrated system outperformed the separated PV+electrolyser under the conditions investigated in the report (temperature variations from 300 to 360 K and variation of the irradiation from 0 to 1 kW/m^2) in terms of annual production of hydrogen in kg per year. The reasons of the better performance of the integrated system are the lower operating current density, which in turn reduces resistive losses, especially at low illumination intensities. Moreover, the integrated device shows enhanced kinetics and transport at elevated temperatures (Haussener, 2013).

It can be concluded that the integrated device has the potential of producing hydrogen at a lower cost and with higher efficiency than the PV+electrolysis system if an optimized PEC device is achieved were the resistive loses are minimal.

4

Design Criteria

Several challenges that need to be overcome before the PEC water-splitting technology can be implemented in commercial-scale have been identified and are presented in the first section of this chapter. Among the large amount of parameters that need to be considered in the design of the device, some of them are considered fixed and others are estimated. These first estimations lead to the design criteria, presented at the end of this chapter, which set the requirements that the device should meet to be functional, as well as economically attractive, sustainable and safe.

4.1 Design challenges

Several challenges for the design of an industrial-scale artificial leaf have been identified. These are mainly related to the need of efficient and stable materials that can be easily scaled-up, and the lack of research performed on the optimum operating conditions of a large-scale device.
All the identified challenges can be summarised as follows:

- Finding low-cost earth-abundant semiconductor materials that can provide a large solar-to-hydrogen efficiency.
- Separation of the evolved gases in a reliable and economic way.
- Enhancement of gas bubble removal.
- Optimization of components size and relative positioning.
- Minimization of light losses.
- Optimization of the operating conditions.
- Improvement of lifetime of the individual components as well as the overall system.
- Minimization of the environmental impact of device during its life cycle.
- Ensuring safe operation of the device.

For a more detailed explanation of the challenges please refer to Appendix H.

4.2 Assumptions

In this project, the solar-to-hydrogen efficiency (η_{STH}) of the commercial-scale device is assumed to be equal to 15%. This parameter can be used to compare the performance of different materials (Chen, 2010) and is defined as follows:

$$\eta_{STH} = \frac{P_{output}}{P_{light}} = \frac{\Phi_{H2} \cdot G^0_{f,H2}}{P_{light}}$$

where Φ_{H2} is the hydrogen evolution rate in mol/s m^2, $G^0_{f,H2}$ is the Gibbs free energy of formation of hydrogen (237 kJ/mol) and P_{light} is the light irradiation (W/m^2).

Although 10% STH efficiency has been considered as an acceptable efficiency in literature (Chen, 2010), the

techno-economic analysis performed by the DOE showed that larger efficiencies will be needed for a commercially viable PEC device (James, 2009). Based in this analysis, it can be concluded that the efficiency of the industrial-scale device should be at least 15% (Parkinson & Turner, 2013).

Since the goal of the device under consideration is to produce hydrogen solely from solar energy, it is assumed that the PEC cell is bias-free, and thus no bias potential will be applied to the device.

4.3 Estimations

4.3.1 Estimations of technical parameters

Photocurrent density

The photocurrent density generated in the PEC cell is related to the power output according to the following expression (Chen, 2010):

$$P_{output} = \mathrm{j_{sc}} \cdot \mathrm{V} \cdot \eta_{\mathrm{F}}$$

where $\mathrm{j_{sc}}$ is the short-circuit photocurrent density normalized to the illuminated electrode area ($\mathrm{A/m^2}$), V is the standard reduction potential of water at 25°C (1.23V), and η_{F} is the faradaic efficiency for hydrogen evolution. Assuming a faradaic efficiency of 100%, the STH efficiency can be expressed as a function of the photocurrent using the following formula:

$$\eta_{\mathrm{STH}} = \frac{\mathrm{j_{sc}} \cdot 1.23}{\mathrm{P_{light}}}$$

In order to achieve an efficiency of 15% STH efficiency in a device working under one sun illumination (1 $\mathrm{kW/m^2}$), the photocurrent density should be 122 $\mathrm{A/m^2}$ (12.2 $\mathrm{mA/cm^2}$).

Hydrogen and oxygen evolution rates

The volume of the gases evolved from the system is an important parameter to consider when designing the device, especially for the gas storage. The hydrogen evolution rate can be calculated for a certain efficiency and light intensity according to the following formula:

$$\eta_{STH} = \frac{\Phi_{H2} \cdot G^0_{f,H2}}{P_{light}}$$

where Φ_{H2} is the hydrogen evolution ($\mathrm{mol/s\ m^2}$), $G^0_{\mathrm{f,H2}}$ is the Gibbs free energy of formation of hydrogen (237 kJ/mol), and $\mathrm{P_{light}}$ is the light intensity. Assuming an efficiency of 15% and a light intensity of one sun (1 $\mathrm{kW/m^2}$), the hydrogen evolution would be 0.63 $\mathrm{mmol/s\ m^2}$.

$$0.15 = \frac{\Phi_{\mathrm{H2}} \left(\frac{\mathrm{mol}}{\mathrm{s \cdot m^2}}\right) \cdot 237\ \mathrm{kJ/mol}}{1\ \mathrm{kJ/s \cdot m^2}} \rightarrow \Phi_{\mathrm{H2}} = 6.3 \cdot 10^{-4}\ \frac{\mathrm{mol}\ H_2}{\mathrm{s \cdot m^2}}$$

According to these calculations, the amount of hydrogen produced in a 1 $\mathrm{m^2}$ PEC cell of 15% STH efficiency under a sun irradiation of 1 $\mathrm{kW/m^2}$ is 4.6 g/h. The volume occupied by this amount of hydrogen depends on the pressure of compression. At standard ambient pressure and temperature (1 atm and 25°C), the volume of the evolved hydrogen is 0.056 $\mathrm{m^3/h}$ per $\mathrm{m^2}$ of cell. If the hydrogen is compressed at 20 bar, the volume

occupied by the H_2 produced is 0.28 m^3/h per m^2.

The molar relation between hydrogen and oxygen generation is 2:1. This means that the oxygen evolution rate will be half of the hydrogen one.

$$\phi_{O2} = 3.17 \cdot 10^{-4} \frac{\text{mol } O_2}{\text{s} \cdot \text{m}^2}$$

The volume of the evolved oxygen, at standard ambient temperature and pressure is 0.028 m^3/h per m^2 of cell, working under 1 kW/m^2 with an efficiency of 15%. In terms of mass, the amount of oxygen produced in this cell is 37 g/h per m^2.

Water consumption rate

The water consumption rate in the PEC cell can be calculated considering that one mole of water is consumed to produce one mole of hydrogen.

$$\phi_{H2O} = 6.3 \cdot 10^{-4} \frac{\text{mol } H_2O}{\text{s} \cdot \text{m}^2} = 41 \frac{g\ H_2O}{h \cdot m^2}$$

Considering the density of water (1 kg/l), the water consumption rate in a device of 1 m^2 (with 15% STH efficiency and under a sun irradiation of 1 kW/m^2) is 41 ml/h.

To put in perspective the availability of water consumed in the production of hydrogen, every year 110,000 km^3 of water comes from rainfall, 61% of which is evapotranspirated by forests, natural landscapes or rain-fed agriculture (FAO, 2015). Therefore, 42,920 km^3 are available for human uses. If hydrogen produced from PEC water-splitting was to supply the world energy demand 104,426 TWh (IEA, 2014), 28.2 km^3 of water would be needed. This represents only 0.066% of the annual rainfall. It should be noted that under real conditions with lower sun irradiation, these volumes would vary accordingly.

Resistances

Several resistances limit the efficiency of the device. Understanding these resistances, which originate from several sources as described below, is important in order to find a way of mitigating them. The total resistance found in a photoelectrochemical water splitting system can be described, similarly to those in a typical electrolysis system, as the sum of the following resistances (Santos, 2013):

$$R_{total} = R_{anode} + R_{cathode} + R_{bubble,O2} + R_{bubble,H2} + R_{ions} + R_{membrane} + R_{electric}$$

where,

- R_{total} is the total resistance found in the system
- R_{anode} is generated from the overpotential of the oxygen evolution reaction (OER) at the anode
- $R_{cathode}$ is generated from the overpotential of the hydrogen evolution reaction (HER) at the cathode
- $R_{bubble,O2}$ is the resistance due to partial coverage of the anode by the oxygen bubbles
- $R_{bubble,H2}$ is the resistance due to partial coverage of the cathode by the hydrogen bubbles
- R_{ions} is the resistance due to the ion transport through the electrolytic solution
- $R_{membrane}$ is the resistance due to the ion transport through the membrane
- $R_{electric}$ is the resistance due to the transport of electrons through the transparent conductive oxide layer and the metal contacts

Reaction resistances (R_{anode}, $R_{cathode}$)

This type of resistances come from the barriers encounter due to the activation energies of the hydrogen and oxygen evolution reactions (HER and OER) at the cathode and anode surfaces, and result in an increase of the overall cell potential. These are inherent energy barriers that can be minimized by the use of good electrocatalysts that can decrease the electrodes' chemical overpotentials. Figure 11 shows the overpotential for the state-of-the-art HER and OER catalysts in both alkaline and basic conditions (McCrory, 2015). According to the values in this figure, it can be predicted that the resistance losses would be in the order of ~ 0.6 V (0.4 V for OER plus 0.2 for HER).

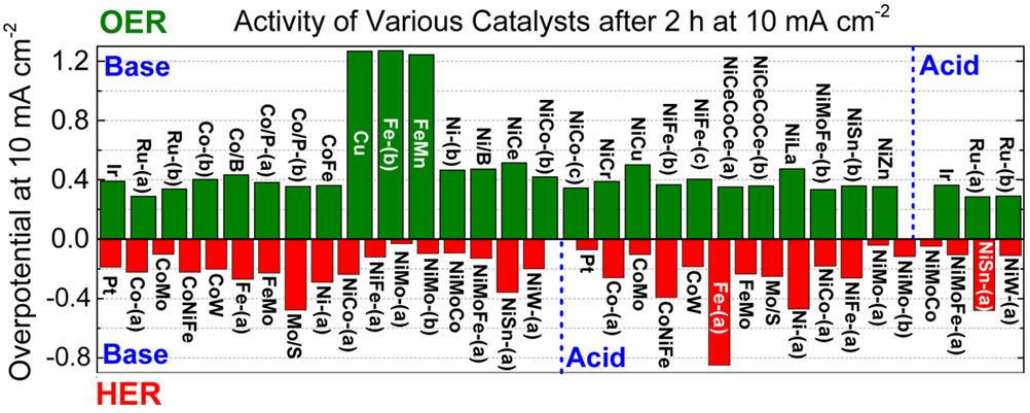

Figure 11. Overpotentials of different catalysts for HER and OER for both pH acid and alkaline (McCrory, 2015)

Transport resistances ($R_{bubble,O2}$, $R_{bubble,H2}$, R_{ions} , $R_{seperation}$)

These types of losses come from transport resistances due to the area of the electrodes covered by gas bubbles and the ion transport within the electrolyte and the separation element (e.g. membrane).

A quantification of the resistances due to the coverage of bubbles at the electrodes surface of a PEC device has not been found in literature. In commercial alkaline electrolysers, it is common practice to stir the electrolytic solution to enhance the removal of the bubbles (Santos, 2013). This is also the case for the lab-scale experiments carried out by most researchers. The presence of a stirrer in the lab-scale devices minimizes these resistances making it neglectable. In the large-scale device, similarly to commercial scale electrolysers, a flow of the electrolyte solution should be induced to enhance the removal of the gas evolved at the electrode's surface. In this report it is assumed that they would be low (< 0.05 V), since proper flow management could minimize the losses.

Other types of resistance are the result of the transport of ions through the electrolytic solution and membrane. These losses, which can be calculated using Ohms law, have been recently modelled for two different configurations of PEC cells: side-by-side and back-to-back photoelectrodes (Haussener, 2012). From the results of their model it is concluded that the resistances of the electrolyte and the membrane could lead to large ohmic drops, although providing short ionic path and high ionic conductivity of the solution and membrane, the losses can be kept below < 0.15 V.

Electrical resistances ($R_{electric}$)

The electrons need to travel through metal contacts and wires, as well as through transparent conductive oxides (TCOs). The latter are used to transport the electrons towards the metal contacts, while providing high transparency to maximize the amount of light that reaches the semiconductor photoelectrode. In this transport there will be losses due to the resistivity of the materials. While the resistivity of metals such as silver, copper or nickel is in the order of 10^{-6} Ωcm, that of TCOs is about 10^{-4} Ωcm (Delahoy, 2011). Therefore, the distance

that the electrons need to travel through the TCO should be minimized, since this material involves the largest losses.

An estimation of the magnitude of the losses due to sheet resistance of the TCO films can be found in Appendix I. These preliminary calculations showed that, using a 600 nm TCO film with a resistivity of 10^{-4} Ωcm, in a 1 m^2 cell of 15% STH efficiency under one sun illumination (1 kW/m^2), and placing the metal contacts at a distance of 2 cm will result in a voltage loss of 41 mV. A feasible target for the electrical resistance losses has been set as < 0.1 V. Therefore, the allowable losses due to the transport of electrons through wires and contacts are about 0.05 V.

Total resistance losses

Adding the losses due to reaction resistances and transport of ions and electrons, the total losses are estimated as ~0.9 V. This means that the PEC device should produce at least 2.2 V in order to be able to carry the water splitting reaction (1.23 V) and overcome the losses.

Light losses

Any component placed in front of the semiconductor photoelectrode will bring about losses: counter electrode, membrane, electrolytic solution, gas bubbles, electrocatalyst layer, etc. Since the amount of hydrogen produced is directly related to the amount of incoming photons and their intensity, the light losses should be minimized. The only component that is unavoidable to be placed in front of the semiconductor photo-absorber is the glass window, which has a maximum transmission of about 92% (Arkema, 2000). Therefore, a target of light losses lower than 10% has been set, meaning than at least 90% of the incoming light should reach the semiconductor photoelectrode.

Operating conditions

As mentioned earlier in the section of *design challenges*, the optimum operating conditions of the large-scale PEC cell are still uncertain. While most research has been focused on finding an efficient, cheap and stable semiconductor material for the PEC cell, very little research has done on the effect of the operating conditions on the performance of the process.

The *Joint Center of Artificial Photosynthesis* (JCAP) recently modelled the effect of the temperature on the performance of the PEC cell, showing that temperature changes in the range of 300 – 360 K weakly affect the efficiency (Chen, 2014). Two competing effects explain the small influence of the temperature on the performance of the cell. On one hand, an increment in temperature increases the radiative recombination (Shockley & Queisser, 1961), which negatively affects the performance of the cell since the operating current density is equal to the current density produced by the solar radiation and the thermal radiation minus the current density from radiative emission. On the other hand, the ion transport is enhanced and the overpotential of the electrocatalysts is decreased at higher temperatures (Chen, 2014). As shown in more detail in Appendix J, the effect of temperature on the performance of the device will depend on the materials that compose the PEC cell (light absorbers, electrolyte, etc.). These preliminary studies performed at the *JCAP* used well-studied materials, for example Pt as catalyst or Si/GaAs as dual-absorber tandem photoelectrode (Haussener, 2013). Although the operating temperature should be optimised when the system components are specified, this design work gave a first estimation of the range of temperatures that could be used for the device, i.e. 300 – 360 K.

Regarding the operating pressure, up to now the PEC devices used in the lab-scale have been run at atmospheric pressure. The effect of working at higher pressure on the performance of the device is still unclear. In the techno-economic analysis performed by the DOE, one type of reactor design comprises pressurized cells at ~20 bar (Pinaud, 2013). Working at this high pressure precludes the need for a separate

compressor, which carries economic benefits (James, 2009). Moreover, pressurizing the device brings other benefits such as minimization of the water vapour loss and reduction of the bubble size, which reduces photon scattering and increases overall device efficiency (Pinaud, 2013). Nevertheless, no study has been found in literature that models the effect in the performance of the device by increasing the operating pressure. For this report it is assumed that the PEC device would be able to work under pressures that range from atmospheric pressure to 20 bar.

The effect of the irradiation in the performance of the PEC cell has been recently studied at the *JCAP*. On one hand, Haussener *et al.* (2013) modelled the performance of a system with a dual-absorber Si/GaAs as a function of the solar-radiation intensity in Barstow, Southern California (US). They showed that the system efficiency varied significantly during the day and over a year, exhibiting local minima when the solar irradiation is most intense (at midday and a global minimum at midyear). However, the variations in instantaneous efficiency could be reduced or even eliminated, by the use of designs that produce low total overpotentials (Haussener, 2013). Another study carried by Chen *et al.* (2014) modelled the performance of a PEC cell using concentrated sunlight up to 20 suns (20 kW/m^2). The STH efficiency exhibited a significant dependence on the optical concentration factor of the incident solar illumination. The efficiency decreased with increasing the optical concentration. This effect was explained by the increase in the kinetic overpotentials of the OER and HER resulting from a higher operational current density as the optical concentration increase (Chen, 2014).

These results showed that the artificial leaf device could work in a wide range of solar irradiation (50 – 1000 W/m^2). Moreover, the use of solar concentrators can be considered to increase light intensity up to 20 suns in order to decrease the area needed for the PEC device.

4.3.2 Estimation of economic parameters

The main economic figure for the PEC water-splitting device is the cost of hydrogen per unit weight. The hydrogen cost goal has been set by the US Department of Energy (DOE) to match that of hydrogen produced by steam reforming (~2 $/kg). However, it has been argued that a more realistic metric would be affordability, taking as reference the price of gasoline (4 $/gallon) and a fuel economy of 30 mpg (Lewerenz, 2013). The equivalent price for the same distance per kg of H_2 would be 8 $/kg, considering that fuel cell vehicles have a more efficient fuel utilization. Since the cost of hydrogen should include ~2 $/kg for storage and dispensing, the price of the hydrogen produced by the PEC cell should be closer to 6 $/kg.

A recent analysis commissioned by the DOE estimated the cost of the produced hydrogen in four different engineering designs, leading to hydrogen costs from 2 to 10 $/kg (James, 2009), showing that the PEC technology has the potential of meeting the target of 6 $/kg.

To set a realistic target for the cost of the reactor, the cost estimations of the DOE on the flat panel type of reactor was taken as reference (Appendix K). According to this analysis, the normalized cost of a PEC reactor of 15% efficiency would be 180 $\$/m^2$, being around 64% of this cost from materials and manufacturing (120 $\$/m^2$) (James, 2009). An investment payback time target has been set at 7 years, which is in the same order as current solar panels payback (Luque & Hegedus, 2011). Keeping the sales price of hydrogen at 6 $/kg, the operating cost should be lower than \$16 /year $/m^2$ (see calculations on Appendix K).

4.4 Design criteria

The following table collects the design parameters that should be taken into account in the design of a functional, economically attractive, sustainable and safe PEC water-splitting device.

Table 5. Design criteria for the large-scale PEC water-splitting device

Design parameter	Value	Comments
Technical parameters		
η_{STH} (%)	15 %	
Lifetime	15 years	
Photocurrent density	122 A/m^2	Maximum value
Operating temperature	293 – 360 K	To be optimized
Operating pressure	1 – 20 bar	Working at high pressures has not been proven in literature
Solar irradiation	50 – 1000 W/m^2	Use of solar concentrators might be considered
Hydrogen evolution rate	0.63 mmol/s m^2	At 15% η_{STH} and 1 kW/m^2
Oxygen evolution rate	0.32 mmol/s m^2	At 15% η_{STH} and 1 kW/m^2
Water consumption rate	0.63 mmol/s m^2	At 15% η_{STH} and 1 kW/m^2
R_{total}	< 0.9 V	Considering that 2.2 V are produced in the cell and 1.23 V are needed for water splitting
R_{anode}+$R_{cathode}$	< 0.6 V	Overpotentials at the cathode and anode
$R_{bubble,O2}$ +$R_{bubble,H2}$	< 0.05 V	Voltage loss due to the coverage of bubbles in the electrodes' surface should be neglectable
$R_{electrolyte}$+$R_{membrane}$	< 0.15 V	
$R_{electric}$	< 0.1 V	
Light losses	< 10 %	> 90 % of the incident light reaches the absorbing material
Economical parameters		
Cost of hydrogen	< 6 $/kg	
Capital cost PEC cell	< 180 $/m^2	Based on DOE analysis
Cost of materials	< 120 $/m^2	Based on DOE analysis
Operating cost PEC cell	< 16 $/year/m^2	
Payback time	< 7 years	
Environmental parameters		
% of recyclable materials	> 90%	
Availability of materials	Earth abundant	
Energy payback time (EPBT)	< 2 years	The EPBT of thin film solar cells is below 1.5 years (Luque & Hegedus, 2011)
H_2 leakage	< 1 %	
Safety parameters		
% H_2 in O_2 stream	<< 4 vol%	The flammability level of hydrogen in oxygen is 4-94 vol% at NPT (McCarty, 1981)
% O_2 in H_2 stream	<< 6 vol%	

5 Product design

In this chapter the design methodology described in Chapter 2 is applied to come up with a device the most promising design for a large-scale artificial leaf device, meeting the criteria established (Chapter 4).

A first loop in the spiral-like design process was used to identify the best reactor type among the four options available. The result of this design step was that a reactor based on planar electrodes is the most promising. A second loop was then performed to identify the best device configuration among the different alternatives for planar devices. A device with configuration of two electrodes facing each other is selected as the most favourable. A third loop was completed to further design the layout of the device with faced electrodes. It was concluded that a back-illuminated tandem photoelectrode with a counter metal electrode is the most promising device configuration for an industrial-scale artificial leaf device. The selected device was further developed by selecting possible materials.

5.1 Design alternatives

Around 30 design alternatives have been identified. Some of these ideas came from literature and patent research, others arose during a group creativity session, and some other designs were developed during the course of this project. These alternatives are collected in Appendix L, and they will be grouped and analysed in the next section in order to select the most promising design.

5.2 Design selection

To facilitate the design selection process, the spiral-like design methodology defined in Chapter 2 was applied. Sequential "design loops" were performed, increasing the level of detail: from type of reactor to configuration and selection of materials. In each loop, design steps were taken as shown in Figure 12.

Figure 12. Steps followed in each "design loop"

1st design loop: Selection of the reactor type

The scope of the first *design loop* is to identify the best type of reactor for the industrial-scale artificial leaf device. The knowledge phase leads to the definition of four types of reactors, which at the same time are split in two groups: particle-based and flat semiconductor based reactors (Figure 13).

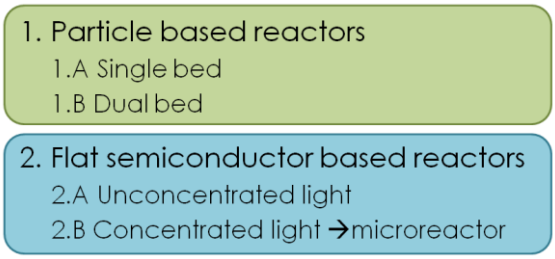

Figure 13. Types of PEC water-splitting reactors

Analysis of reactor types

A short description of each type of reactor, together with their main advantages and disadvantages is presented below.

1.A. Single bed particle-based reactor

This type of reactor, shown in Figure 14, consists of photoactive particles in an electrolytic solution, contained in a transparent plastic bag (Pinaud, 2013). The particles can be conductive spherical cores coated with photoanodic and photocathodic materials as islands, particles or thin film shells. Another particle geometry could be a photoabsorbing core with co-catalysts for both the HER and OER. Under illumination, water-splitting reactions happen at the surface of the particles, evolving hydrogen and oxygen within the same chamber. The gases must be separated in a posterior step.

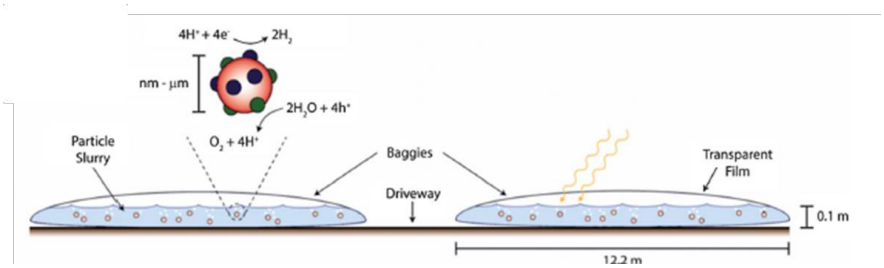

Figure 14. Scheme of a single bed particle-based reactor (Pinaud, 2013)

The main advantage of this type of reactor is its potential low capital cost, which could result in a hydrogen production cost lower than 2 $/kg according to Pinaud *et al.* (2013). However, the production of H_2 and O_2 within the same chamber involves unsafe operation. Moreover, the need of an external gas separation unit will increase the cost and the technical complexity of the process.

1.B. Dual bed particle-based reactor

Similarly to the previous reactor, the dual bed consists of plastic bags that contain photoactive particles in an electrolytic solution. In this case, separate beds connected via a porous bridge are used for hydrogen and oxygen production; see Figure 15 (Pinaud, 2013). The particles can be conductive spherical cores coated with photoanodic or photocathodic materials as islands, particles or thin film shells.

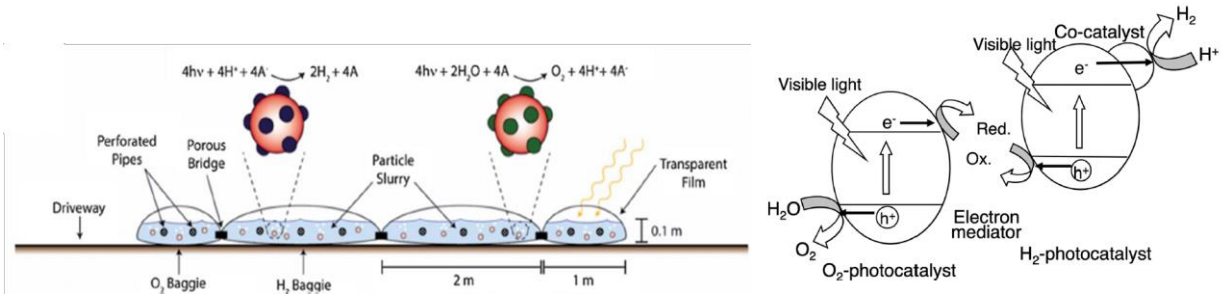

Figure 15. (Left) Scheme of a double bed particle-based reactor (Pinaud, 2013); (Right) working mechanism of the particles, the so-called Z-scheme (Sasaki, 2013)

The dual bed reactor is based on a two-step photoexcitation (called Z-scheme), shown in the right-side of Figure 15. The system is composed by a H_2 evolving photocatalyst, an O_2 evolving photocatalyst and an electron mediator that travels within the H_2 and O_2 compartment and completes the overall water splitting reaction (Sasaki, 2013).

This reactor presents low capital cost, potentially providing a cost of H_2 of about 3 $/kg (Pinaud, 2013). Compared to the single chamber reactor, this type of reactor is safer to operate, since the two product gases evolve in separated chambers. However, there are many uncertainties concerning this type of system. First, the size of the reactor "baggies" envisioned by the DOE (2 meters long) is unrealistically large. It is foreseen that the ohmic losses due to the transport of the redox mediator from one chamber to the other will be unacceptable, leading to a non-functional device. If smaller chambers are considered, in the rage of centimetres, the cost of such reactor should be recalculated. Secondly, the "porous separator" that would allow the transport of the redox mediator has not been thoroughly studied yet, and the membrane with 10 µm porous size used by Sasaki *et al.* (2013) will not avoid the crossover of dissolved gases. Finally, the efficiency proven in the laboratory-scale is in the range of 1% (Sasaki, 2013), and thus a considerable amount of for materials research and system design is still needed.

A new concept that can be considered a variation of the dual bed particle-based reactor can be found in Figure 60 in Appendix L. This concept was inspired by photocatalytic reactors for water treatment and it consists of a tubular reactor where the particles with OE catalyst and HE catalyst are placed in opposite sides of the tube, which is split in half by a membrane. A mirror placed in the back of the tube allows for the light absorption of the particles placed at the back-side. The main advantage of this tubular reactor over the dual chamber "baggie" reactor is the much shorter ionic path between the O2 and H2 evolution chambers. However, this type of reactor would involve a higher capital cost, due to the use of glass tubes, larger membrane area and mirrors.

2.A. Planar semiconductor based reactor with non-concentrated sunlight

This reactor uses planar (photo)electrodes immersed in an electrolytic solution (Figure 16). The reactor can use one or two photoactive electrodes that can be integrated or spatially separated. The working principle is that of a common photoelectrochemical cell. Under illumination, electron-hole pairs are generated at the semiconductor(s). The charged species travel to the semiconductor(metal)-electrolyte interface where the water-splitting half reactions take place. The evolved gases are kept apart thanks to a separator, which must allow the transport of ions from one electrode to the other in order to complete the water-splitting reactions. This reactor allows for multiple (photo)electrodes configurations, and the final design should be such that minimizes the internal loses in the device (Pinaud, 2013).

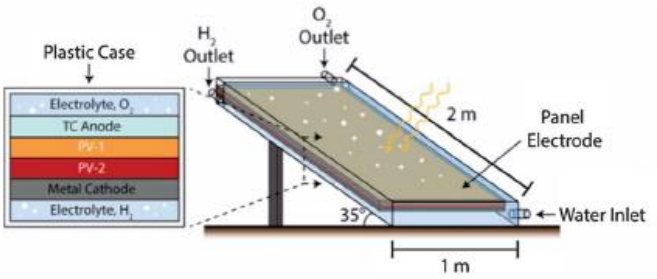

Figure 16. Schematic representation of the flat semiconductor based reactor under un-concentrate sunlight (Pinaud, 2013)

The main disadvantage of this reactor is the estimated high capital cost, with an estimated hydrogen cost of more than 10 $/kg for a device with 10% STH efficiency (Pinaud, 2013). However, one advantage of this type of reactor is the wider experience in the flat semiconductor manufacturing from the photovoltaic industry. Potentially, low cost large-scale manufacturing techniques (such as roll-to-roll) could be used. Another advantage is the more advanced state-of-the-art, with efficiencies over 18% proven at laboratory-scale (Licht, 2001).

2.B. Planar semiconductor based reactor with concentrated sunlight

Similarly to the previous type, this reactor uses planar (photo)electrodes (integrated or spatially separated) immersed in an electrolytic solution. Additionally, a highly reflective material is used to concentrate light onto the photoactive material. One or two photoactive electrodes can be used. The working principle is the same as for the non-concentrated light reactor.

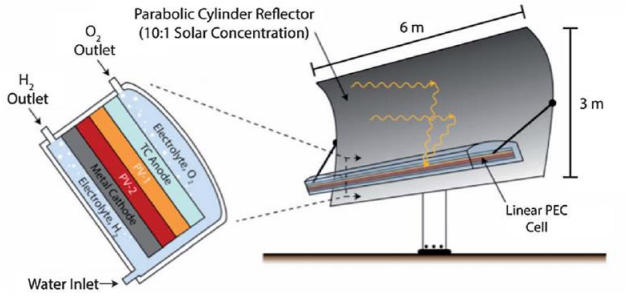

Figure 17. Schematic representation of the flat semiconductor based reactor under concentrate sunlight (Pinaud, 2013)

The use of solar concentration in PEC cells has been investigated by Chen *et al.* (2014) and it was observed that the distribution of the current density along the electrodes was non-uniform, due to the much larger current densities of this system, leading to a large overpotential difference along the electrode width. They concluded for this reason that the width of the electrode needs to be kept in the range of mm in order to have acceptable ohmic losses. Such device can be thus considered a "micro-reactor". The manufacturing of this type of micro-reactor, which involves the placement of many small components (membrane, electrodes, electrolyte, gas collection, etc.), is foreseen to be complex and costly. Therefore, the main goal of using solar concentrator (i.e. reducing the cost due to less use of expensive semiconductor material) is probably hindered by the higher cost of manufacturing. Thus, the cost of hydrogen production by this type of reactor, estimated as 4 $/kg by the DOE (Pinaud, 2013), should be revised accounting for the complexity manufacturing process.

Evaluation of reactor types

The four types of reactors were compared qualitatively in order to select the most promising one. The parameters used for the selection of the design were related to the cost, the state-of-the-art of the technology, the scalability and the potential of low cost manufacturing.

Firstly, the group of particle-based reactors were compared to the planar electrodes reactors (Table 6). Although the particle-based reactors could potentially provide a lower cost of hydrogen, their state-of-the-art is in an embryonic state and there is not enough understanding of the technology. Moreover, the experience on the large-scale fabrication of flat semiconductors is much larger than that for large-scale manufacturing of particles. For these reasons, the planar electrodes based reactors are a better option for the industrial-scale artificial leaf device to be built by 2020. Nevertheless, if breakthroughs on particle-based reactors are achieved in the laboratory and the large-scale particle production technologies are further developed, this argumentation should be reconsidered.

Table 6. Comparison between particle-based and planar electrodes based reactors [(+) Better; (-) Worse]

	Particle-based	Planar electrode
Potential low cost	+	-
Efficiency demonstrated at lab-scale	-	+
Understanding of the technology	-	+
Large-scale manufacturing	-	+

Secondly, a comparison between the two options for planar electrodes reactor, i.e. concentrated and non-concentrated sunlight, was performed using the same criteria as before (Table 7). Estimations performed by the DOE showed a lower H_2 production cost by using concentrated reactors (Pinaud, 2013). However, these calculations have not considered the complexity of manufacturing a device based on electrodes with widths in the millimetre scale. The low experience in large-scale manufacturing of such type of reactors and the lack of understanding of the concentrated systems in the laboratory scale make them unsuitable for this project.

Table 7. Comparison between non-concentrated and concentrated planar electrodes reactors [(+) Better; (-) Worse]

	Non-concentrated	Concentrated
Potential low cost	-	+
Efficiency demonstrated at lab-scale	+	-
Understanding of the technology	+	-
Large-scale manufacturing	+	-

Selection of reactor type

For the reasons stated in the previous section, it is concluded that **planar electrodes based reactor without solar concentrator** is the best option for the initial commercialization of the artificial leaf technology.

2nd design loop: Selection of device configuration

After the selection of planar electrodes based reactor, the second design loop is now focused on defining the device configuration, i.e. the placement and relative positioning of the components.

Many design alternatives have been found for planar electrodes-based PEC water-splitting devices (Appendix L). The different ideas can be clustered in five groups according to the placement of the (photo)electrodes (Figure 18).

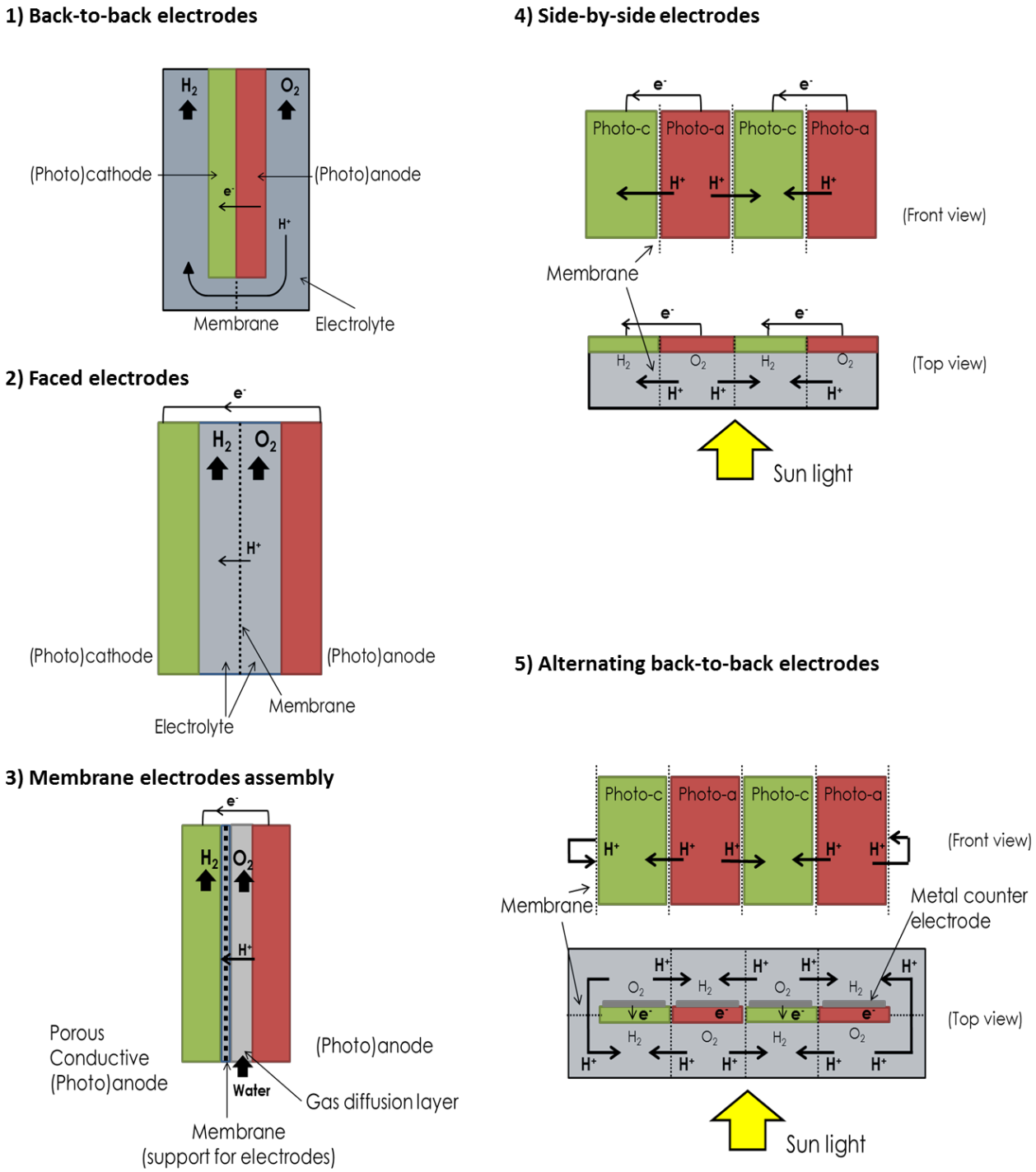

Figure 18. Five types of PEC water-splitting configurations

Analysis of device configurations

The design alternatives regarding the configuration of the device are described here and their main advantages and disadvantages are analysed.

1. Back-to-back electrodes

In this configuration, the electrodes are monolithically integrated, evolving hydrogen and oxygen at opposite sides (Figure 18.1). No external wires are needed, since the electron transfer is achieved through the bulk of the electrode (for this reason, this configuration is usually called "wireless"). A pathway for the transport of ions has to be provided and should be minimized in order to avoid large ohmic losses.

The main advantage of this configuration is the potentially simple manufacturing of the electrodes, since multilayer thin film deposition could be done by several scalable production technologies. This advantage, however, is lost once the ohmic losses are considered. In order to scale-up this device providing a short ionic path, the electrodes' width should be kept in the order of few centimetres (Haussener, 2012). Therefore, the manufacturing of such device is envisioned to be rather complex, since the device would be built with alternating parts of membrane and electrodes. Moreover, the large amount of sealing areas will jeopardize the safety of the device. Figure 19 shows a possible industrial-scale PEC device based on this configuration (Haussener, 2013).

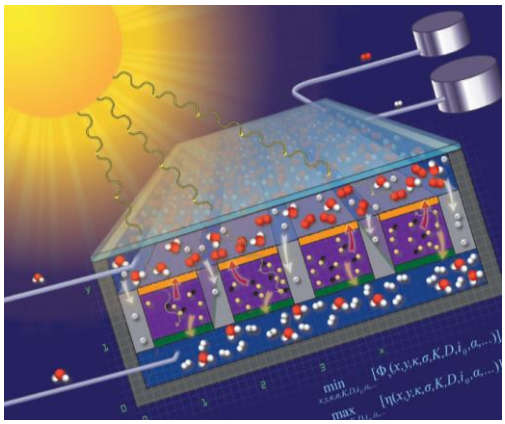

Figure 19. Large-scale PEC water-splitting device based on back-to-back electrodes configuration (Haussener, 2013)

The model by Haussener *et al.* (2012) highlighted another important drawback of this configuration. The size of the membrane should be about the same as the electrode (both in the order of < 5 cm) to have acceptable ohmic losses. This means that half of the device's area exposed to light is occupied by a non-photoactive component (i.e. the membrane). Therefore, in terms of hydrogen production per area this device offers low efficiency.

2. Faced electrodes

In this configuration, electrodes are facing each other, separated by the electrolytic solution (Figure 18.3). A separator is also placed between the electrodes to avoid mixing of the evolved gases. Both electrodes are electrically connected via an external wire to allow the transport of the electrons from the anode to the cathode (reason why this configuration is also called "wired").

One advantage of this configuration is that it offers a short ionic path within the electrodes, resulting in lower ohmic losses. Moreover, most laboratory-scale devices work with this configuration and thus there is more experience on this type of systems, with proven efficiencies of more than 15% (Khaselev, 2001). Another advantage is the potential simple manufacturing, due to the possibility of increasing the photoelectrode area

without inferring larger ohmic losses. The main challenges with this design are the placement of the light-absorbing electrode in such a way that the light losses are minimized, as well as the electrical connection between the electrodes ensuring low ohmic losses.

3. Membrane Electrodes Assembly

Membrane Electrodes Assembly (MEA) is a widely used configuration in fuel cells (Larminie, 2003) and PEM electrolysers (Godula-Jopek, 2015). In this configuration, the electrodes are directly deposited on opposite sides of an ion exchange membrane, leading to very low ohmic losses due to the proximity between the electrodes. Fast and low cost deposition methods based on spraying are commonly used, which is a potential advantage of this configuration. A gas diffusion layer is used for the fast removal of the gases evolved at the electrodes. For this configuration to work, a porous and conductive electrode that allows the transport of ions and electrons is needed. Attempts to a working PEC device using this configuration have been reported (Jeng, 2010; Hernández, 2014), however low efficiencies where achieved and a large effort on materials development should still be done to further develop this configuration.

4. Side-by-side electrodes

In this configuration, a photocathode and a photoanode are placed side-by-side, being electrically connected via their back contact. A membrane is placed perpendicularly in between the two electrodes to ensure the gas separation while allowing the transport of the ions needed to complete the electrochemical reactions (Figure 18.4).

A potential advantage of this system is that the membrane is not on the light path towards the photoelectrodes, which allows the use cheaper non-transparent membranes. The main disadvantage of this configuration is that only half of the device's area exposed to light is actually used for hydrogen production. Therefore, the hydrogen production per device area is halved. Moreover, a similar disadvantage to that of the back-to-back electrodes is encounter here: in order to ensure low ohmic losses, the electrodes' width must be kept in the order of ~5 cm (Haussener, 2012), which will involve a complex assembly of the device's components and lower inherent safety due to the large amount of sealing areas.

5. Alternating back-to-back electrodes

This innovative configuration is a combination of the side-by-side and back-to-back electrodes configurations. It is meant to tackle the problem of the poor area utilization of the side-by-side electrodes, while taking advantage of lower ohmic losses when compared to the back-to-back electrodes. In this device, a photoanode and a photocathode are placed next to each other, but each of them is electrically connected to the corresponding counter electrode situated at their back (Figure 18.5). To our knowledge, such configuration has not been proven in the laboratories yet, therefore many uncertainties remain regarding the performance of this device. Although this configuration offers improved area utilization compared to the side-by-side and back-to-back electrodes configuration, the issue of complex manufacturing remains.

Evaluation of the configurations

Each design has been analysed according to the design criteria, established in the previous chapter. Parameters that could apply equally to all design have not been considered for the selection. For example, regarding the resistances of the device, only the ones related to the transport of ions through the electrolyte and membrane are considered here. The overpotential at the electrodes is independent on the positioning of the electrodes, and therefore this parameter is not relevant in the selection. The loss due to the bubbles sticking to the surface is an issue that has not been quantified or deeply studied yet and it is believed that the problem will be of the same magnitude for all configurations, and thus it is not taken into account for the device selection. Besides, the electric losses due to the transport of electrons are foreseen to be very low compared to the losses due to

the ion transport (since the conductivity of the metal wires and contacts is three orders of magnitude larger than that of the electrolyte and membrane).

The parameters taken into account for the design selection are (a) the ohmic losses due to ion transport, (b) the area utilization for hydrogen production, (c) the manufacturability and (d) inherent safety of the device, (e) the state-of-the-art and (f) the potential low cost of the device. The results are collected later on Table 8.

Table 8. Comparison of the different device configurations

	Faced electrodes	Electrodes side-by-side	Electrodes back-to-back	Alternating back-to-back	MEA
Ohmic losses (Max 200mV)	100 mV (2cm separation)	120 mV (4cm electrodes)	190 mV (4cm electrodes)	120 mV (4cm electrodes)	0.2 mV
Photoactive area for H_2 / total area	~1	~0.5	~0.6	~1	~1
Manufacturability	+	-	-	- -	+ +
Inherent safety	+	-	+	-	+ +
State-of-the-art	+ +	+	+	-	- -
Cost	+	-	-	-	+

The ohmic losses were calculated for each design taking as reference the model performed by Haussener *et al.* (2012), adopting the same values of conductivity of electrolyte (40 S/m) and membrane (10 S/m), as well as current density (20 mA/cm^2). As it can be seen in Table 8, all the configurations can potentially meet the design criteria of providing ohmic losses lower than 200 mV. It should be noticed that the losses in the faced electrodes configuration could be easily reduced by placing the electrodes closer to each other. On the other hand, the reduction of the losses in the back-to-back or side-by-side electrodes configuration will imply having smaller electrodes.

Selection of configuration

After evaluating each design for all the parameters mentioned before, it is concluded that the **faced electrodes** configuration is the most promising for the large-scale PEC water-splitting device , and it is further developed in the following design phase.

The side-by-side and back-to-back configurations are rejected because of the low ratio of the photoactive area for H_2 production over the total area of device. Considering the low efficiency of the process, the area needed for producing a significant amount of hydrogen constitutes already an issue; even in an ideal scenario in which 100% of device area is photoactive for hydrogen production. Therefore, this is considered a decisive parameter for rejecting the two configurations. Furthermore, the alternating back-to-back configuration is rejected for the envisioned complex manufacturing, safety and cost.

The MEA is a very promising configuration that offers low ohmic loses, easy manufacturing and potential low cost. However, a large effort on material research should be done to develop such device. Due to the embryonic state-of-the-art of this configuration, it is decided to reject this configuration for this project that aims for manufacturability in 2020. Nevertheless, the scientific community is encouraged to develop porous and conductive photoelectrodes that would allow for the manufacturing of a MEA PEC device. The faced electrodes configuration is thus left as the most promising configuration.

3rd design loop: Selection of the type of electrode materials

Now that the considered design alternatives have been narrowed to planar electrodes type of reactor with two electrodes facing each other, a third "design loop" was performed to design in more depth the device. The scope of this design level is to define the type of electrode materials, which will depend on the direction of the illumination.

It is accepted by the PEC scientific community that at least two semiconductors will be needed in order to achieve high efficiencies. A single semiconductor would give a maximum efficiency of 11.2%; whereas efficiencies of 22% could be achieved if two semiconductors are employed (Seitz, 2014). For this reason, it is assumed that two semiconductors will be used in the industrial-scale PEC device, called for now SC1 and SC2 being the bandgap of SC1 larger than the one of SC2. An important consideration is that the top absorber should be the material with larger bandgap (i.e. SC1), in order to efficiently absorb the high-energy photons before the lower-energy photons can be absorbed in the following layer.

Keeping these considerations in mind, six different alternatives are presented according to the role of the tandem photoelectrode (cathode or anode) and the direction of the illumination (Figure 20).

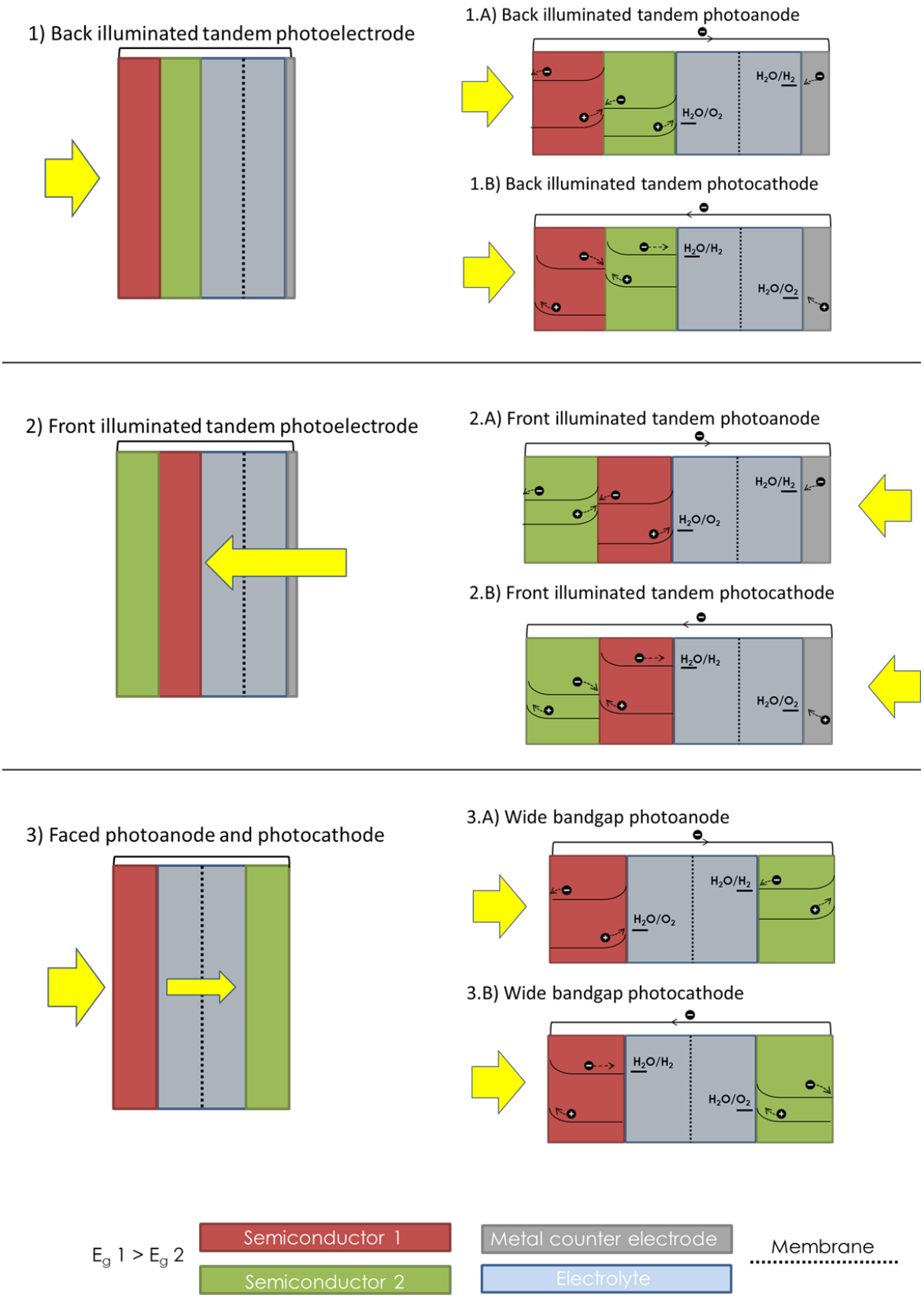

Figure 20. Design alternatives for faced electrodes

Analysis of design alternatives for faced electrodes configuration

The design alternatives for the selected faced electrodes configuration are described here.

1. Back photoelectrode

This design uses a tandem photoelectrode that is illuminated from the back, which means that the light enters through the opposite side of the electrolyte-semiconductor junction. Therefore, the small bandgap material is the one in contact with the electrolyte. A metal counter electrode is used to complete the electrochemical reactions. The two electrodes are connected via an external wire to transport the electrons to the cathode. Depending on the type of semiconductor (p or n type), the tandem photoelectrode could act as photoanode (Figure 20.1.A) or as photocathode (Figure 20.1.B).

This configuration has been mainly used with buried junctions (i.e. the semiconductor is not in direct contact with the electrolyte, but rather a protective metallic layer is placed in between). Example of efficient devices ($\eta_{STH} > 7\%$) using this configuration can be found in literature (Khaselev, 2001; Miller, 2003; Urbain, 2014).

2. Front photoelectrode

The structure of this design is similar to the previous one, with the difference that the tandem photoelectrode is illuminated from the front (i.e. from the side of the electrolyte-semiconductor junction), and thus the wide bandgap material is the one in contact with the electrolyte. Similarly to the previous design, the selection of different semiconductors could lead to a tandem photoanode or photocathode (see Figure 20.2.A and Figure 20.2.B). This configuration has been widely used in the laboratory scale, showing good STH efficiencies (>4.5%) (Reece, 2011; Abdi, 2013; Han, 2015).

It should be noted that in this type of devices, light needs to go through the glass panel, the metal counter electrode, the electrolyte and the separator before being absorbed by the photoelectrode. A critical step is the transmission through the counter electrode, since even very thin metal layers such as 10 nm thin Pt absorbs about 55% of the photons coming from an AM1.5 spectrum (Seger, 2014). In the laboratory-scale the counter electrode, usually a small wire placed on the side of the illuminated photoelectrode, does not constitute a light loss issue. However in large-scale, where large areas of counter electrode are needed, light losses by shading from these components on the photoelectrode can seriously damage the efficiency of the device.

Therefore, for this configuration to be realised, a “transparent” counter electrode is needed. A possible solution is to use a low loading of electrocatalyst patterned on a transparent conductive oxide (Figure 21).

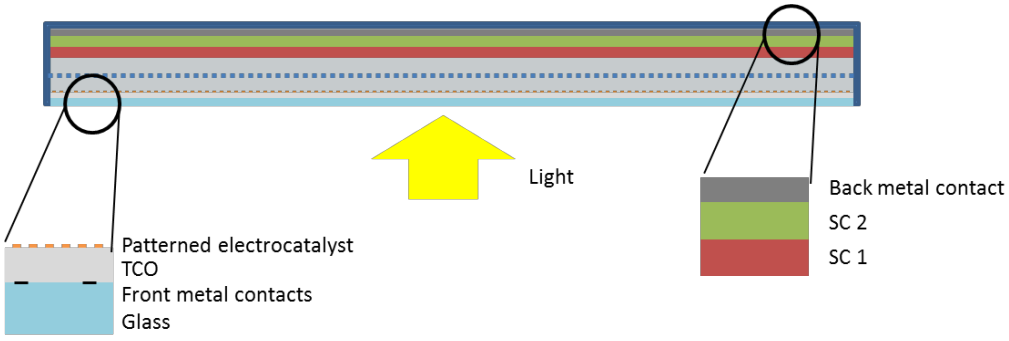

Figure 21. Possible design for a device with a front illuminated tandem photoelectrode and a "transparent" counter electrode

Chen *et al.* (2015) studied the trade-off between optical obscuration by a patterned catalyst and its overpotential. In their study, the overpotentials were modelled for a Pt patterned catalyst on a TCO layer for different filling factors (defined as the geometric area of the catalyst over the total area of the electrode) and concluded that the use of too low filling factor (< 0.01) leads to very high ohmic losses. A good trade-off

could be achieved with, for example, a filling factor of 0.07 that offers an overpotential of 66.5 mV, at expenses of 7% of photoactive area loss (Chen, 2015).

3. Separated photoelectrodes

In this design the two semiconductors needed to achieve a high enough efficiency are not integrated in one unique photoelectrode. In contrast, the two semiconductors are in contact with the electrolyte, acting as photoanode and photocathode. Two alternatives can be found for this system setup depending on the type of semiconductors used: the wide bandgap material could act as photoanode (Figure 20.3.A) or as photocathode (Figure 20.3.A). It is noticeable that the light that has to reach the second semiconductor photoelectrode will face large losses, travelling through the first semiconductor, the electrolyte and the membrane on its way. Examples of this type of configuration can be found in literature (Lin, 2012; Jang, 2015), reaching efficiencies lower than 1%.

Evaluation of the design alternatives for faced electrodes

The three designs presented (each of them with two options according to the type of semiconductor materials) will be evaluated regarding their potential implementation in large-scale with low light losses and large stability. Notice that the ohmic losses, although being an important parameter for the design of the device, it is not considered here as decisive parameter since they will be the same for all six options, and the same measures of minimization of ohmic losses could be applied to all of them.

a) Light losses

It can be easily predicted that the lowest light losses will be obtained in the *back photoelectrode* device, since light needs to travel just through the front glass panel before reaching the semiconductor absorber. If the front panel material is PMMA, the transmission would be of 92% (http://www.plexiglas.com/en/).

On the contrary, in the *front photoelectrode* device light needs to go through several components of the device before being absorbed by the photoelectrode. As explained before, the main concern is the counter electrode, as this component should absorb as little light as possible. Let's consider that a "transparent" counter electrode could be fabricated, and evaluate the losses due to the different layers that the light needs to pass before reaching the semiconductor in this "best case scenario". One type of light loss evaluated is the so-called Fresnel losses, which are present at the boundaries of two materials with different refractive index due to reflections at the optical boundaries, and can be calculated as described in Appendix M. For an estimation, common materials have been assumed for the different layers, such as PMMA for the front panel, In_2O_3 as TCO material and Nafion® as membrane, leading to a transmission value of 83%. A sensitivity analysis showed that changing the materials of the front panel, TCO or membrane will not lead to a large improvement in the transmission (Appendix M). On the other hand, a significant improvement could be achieved by reducing the refractive index of the semiconductor. However, this would imply the use of a larger bandgap semiconductor, which is not desirable in terms of efficiency. Further reduction of the light loss could be achieved by employing an intermediate layer between the semiconductor and the electrolyte with a lower refractive index.

Another type of light losses is due to the bulk absorption, which depends on the absorption coefficient of the material as well as its thickness. As explained in more detail in Appendix M, the bulk absorption losses will be significantly lower than the losses at the optical boundaries. It can be then estimated that accounting for the two types of light losses, only about 80% of the irradiance will reach the surface of the semiconductor photoanode. Although not performed here, a similar analysis could be done for the *separated electrodes* device. It can be predicted that similar losses will occur in order to reach the second semiconductor.

b) Potential stability

The stability of the tandem photoelectrode is a big challenge that needs to be overcome to ensure the long lifetime of the device. Metal oxides have been widely investigated as potential stable photoanode materials, although they are susceptible to degradation if the energy levels for anodic and cathodic decomposition do not fall within the valence and the conduction band (van de Krol & Grätzel, 2011). For this reason, the generally accepted trend is that larger bandgaps result in higher stability of the material. In this line, it should be then considered that the front illuminated device has potential for a higher stability, since the wide bandgap material is the one in contact with the electrolyte. In the case of separated photoelectrodes, both components are in contact with the electrolyte and thus to ensure the stability of this device will be more challenging. Nevertheless, the efficiency of some photoelectrode materials have been largely improved – from minutes to days – by the use of protection layers (Seger, 2014).

Table 9 summarizes the results of the analysis on light losses and potential stability of the three faced electrodes design alternatives.

Table 9. Evaluation table of the faced electrodes design alternatives based on light losses and potential stability

	Back photoelectrode	Front photoelectrode	Separated photoelectrodes
Light losses	~ 8%	> 20%	> 20%
Stability	-	+	- -

Selection of a design

The back photoelectrode design offers a clear advantage in terms of low light losses. Potentially, in this design only 8% of the light would be lost, compared to more than 20% in the front photoelectrode device, and a similar loss in the device with separated photoelectrodes. Furthermore, back photoelectrode design would allow for the use of cheaper non-transparent membranes and counter electrodes without providing further light loss.

Although the front photoelectrode device offers the advantage of a (potential) larger stability due to the placement of the wide bandgap material in contact with the electrolyte, current developments on protection layers for the photoelectrodes are showing a big improvement of different material's stability. Moreover, protective materials based on conductors (non-transparent) that could act as catalyst as well, are a promising approach to improve the stability of the device (Seger, 2014), which could be only implemented in a device with back illumination.

Therefore, the **back photoelectrode** is selected as the most promising device for commercial scale application.

4th design loop: Materials selection

The scope of this design loop is to select materials for the different components of the PEC water-splitting device, namely the photoelectrode and counter electrode, the membrane and the electrolyte. The material selection started by the most challenging component, the back-illuminated photoelectrode. Thereafter, an appropriate protection layer and counter electrode were selected by their expected performance and cost. The selection of these components, is directly related to the type of electrolyte used, which at the same time guides the selection of the membrane.

Back-illuminated photoelectrode

The design selected offers two possibilities according to the semiconductor materials used: back illuminated photocathode or photoanode. The decision of using either a photoanode or a photocathode is based on the available earth-abundant and inexpensive materials possibilities.

Figure 22 shows the cost of common materials used for photoelectrodes and catalysts. The abundancy of different elements is shown in Figure 23. Note that both graphs are in logarithmic scale.

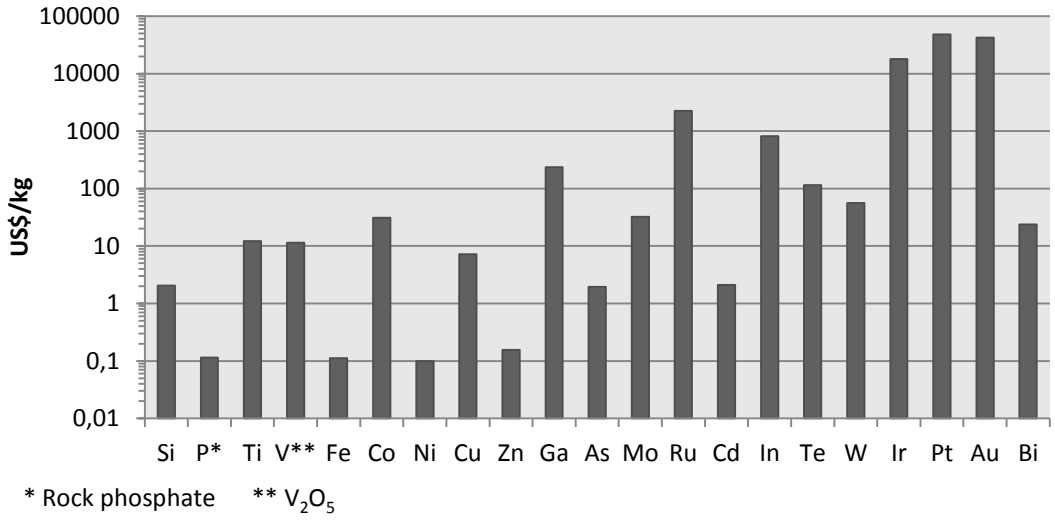

Figure 22. Price per kg of common elements used for photoelectrodes and catalysts. (Prices obtained in www.metalprices.com)

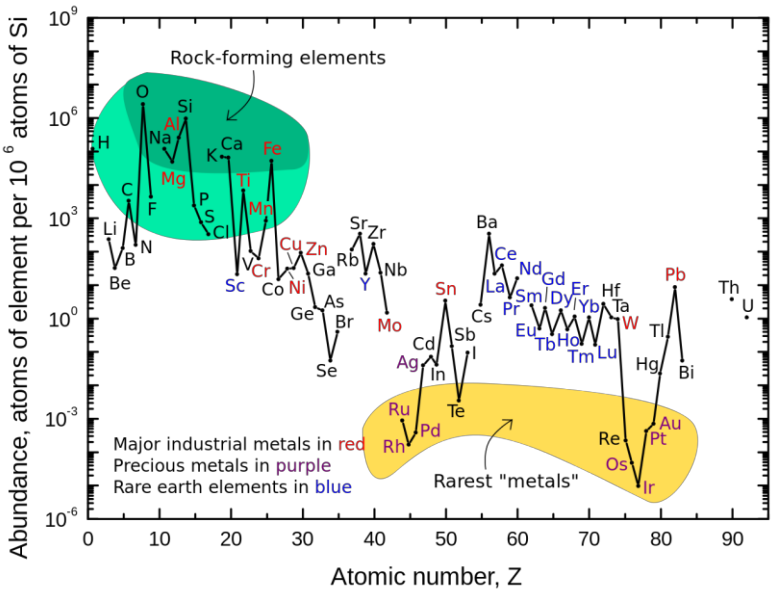

Figure 23. Abundance of elements.

For the materials for the photoelectrode, a semiconductor that meets both requirements, i.e. cost and abundancy, is Silicon. This is the second most abundant element, and its price is 100 times lower than other studied materials like GaAs. Moreover, Si has been widely used in the PV industry, reaching high solar conversion efficiencies. Other common semiconductor is CdTe. However, the high cost and low abundancy of Te, together with the toxicity of Cd, makes this material unattractive for employing it on the PEC technology.

Therefore, a promising option is to use only Si-based semiconductors, due to their low cost and availability together with a wide experience from the photovoltaic industry. Si thin films can largely vary their bandgap from 2.2 to 1.1 eV according to the doping used (Luque & Hegedus, 2011). In order to have an efficient charge separation, thin film Si solar cells are built using p-i-n junctions as shown in Figure 24 (n-i-p junctions are also possible). Multiple p-i-n (n-i-p) junctions can be used in order to increase the voltage and the efficiency of the device. Also, the TCO layer is usually textured to provide a rough surface to the following deposited layers, increasing light trapping (Müller, 2004).

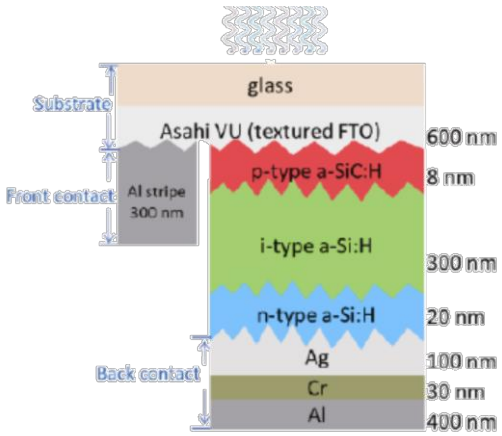

Figure 24. Single junction a-Si solar cell (Abdi, 2013)

It should be noted that superstrate configurations are needed, since the device is illuminated from the glass substrate side. Commercial superstrate a-Si solar cells are based on p-i-n junctions, rather than n-i-p, due to the lower efficiency of the latter one. Keeping these considerations in mind, the **multi-junction Si-based** photoelectrode with superstrate configuration should act as **photocathode**.

Protection layer

A passivation layer should be used to protect the surface of Si in contact with the electrolyte. Protection materials can range from conductors, semiconductors and insulators (Seger, 2014). The two last ones had attracted more research attention due to their lower light absorption. However, since the device selected is back illuminated and the light absorption of the protection layer is not an issue, using non-transparent conductor material is a plausible option. Moreover, the metallic protection layer could enhance the light absorption of the semiconductor by providing back reflection. Ni, Ni-Fe and Ni-Mo are good candidates for such protective layer, since besides protecting the photocathode, they will act as catalyst for hydrogen evolution reaction. Ni-Mo has shown a low overpotential for hydrogen evolution, similar to that of Pt in alkaline conditions (McKone, 2011), while being much cheaper and more abundant. Hence, **Ni-Mo** is selected as most promoting material for the protective layer.

Counter electrode

Regarding the metal counter electrode, which acts as anode in the design under consideration, Nickel is an especially attractive material, not only for its low cost (Figure 22) and abundancy (Figure 23) but also for its performance. **Nickel** is recognized as one of the best materials for OER, due to its good corrosion resistance in alkaline solutions and electrochemical activity (Godula-Jopek, 2015).

Electrolyte

In order to use low cost and earth-abundant materials, the pH of the electrolyte solution should be alkaline. Common electrolytes in commercial alkaline electrolysers are KOH and NaOH, although the latter is preferred due to the higher specific conductivity (Guillet, 2015). Concentrations of 20 – 30 wt%, which have a

conductivity of 60 S m^{-1}, are commonly used in this type of electrolysers (Guillet, 2015). However, 1M NaOH solutions (i.e. 2.6 wt%) have been used for catalyst characterization, offering low overpotentials (McCrory, 2015), and their conductivity is high enough (~14 S/m) to provide low ohmic losses (Appendix N). Although further optimization of the electrolyte solution should be done in the laboratories, and its compatibility with all the materials should be tested, an electrolyte of **1M NaOH** is suggested here as promising option.

It should be pointed out that the proposed device configuration could work under acidic conditions. However, the materials selection must be reconsidered.

Membrane

The water-splitting reactions in alkaline medium are the following:

$4e^- + 4\,H_2O \rightarrow 2H_2 + 4OH^- \quad [E^0_{red} = -0.828\,V]$ Reaction at the cathode

$4h^+ + 4OH^- \rightarrow O_2 + 2H_2O \quad [E^0_{ox} = -0.401\,V]$ Reaction at the anode

Based on the water-splitting half reactions in alkaline conditions, an anion exchange membrane is needed, to allow the transport of OH^- ions while keeping the gases apart. The membrane should be chemically stable in contact with water and during operation, it should have a high ionic conductivity and minimal permeability to gases, and it should be inexpensive. Although anion exchange membranes are not as developed as proton exchange membrane, a large research effort is currently focused on the development in these membranes, with the main goal of reducing the cost of fuel cells and PEM electrolysers (Arges, 2010; Faraj, 2012; Merle, 2011). Guillet *et al.* (2015) recently compiled a list of commercial suppliers of **anion exchange membranes**. One possible supplier is Tokuyama Corporation (http://www.tokuyama.co.jp), who developed stable anion exchange membranes with conductivity about 42 mS/cm.

5.3 Final design: Back-illuminated photoelectrode with buried junction + metal counter electrode

In the selected device setup (Figure 25), light enters through the glass window, which is also the support of the tandem photoelectrode, and a protection layer is used to avoid corrosion of the small bandgap material. This protection layer acts as catalyst for the corresponding water-splitting half-reaction. The counter electrode is a metallic mesh that provides high surface area for reaction. Both electrodes are in contact with the electrolyte and an ion exchange membrane is placed in between the electrodes providing separation of the evolved gases while allowing the transport of ions. An external pump will be used to provide flow of the electrolyte. This flow enhances the removal of the gases from the surface of the electrodes.

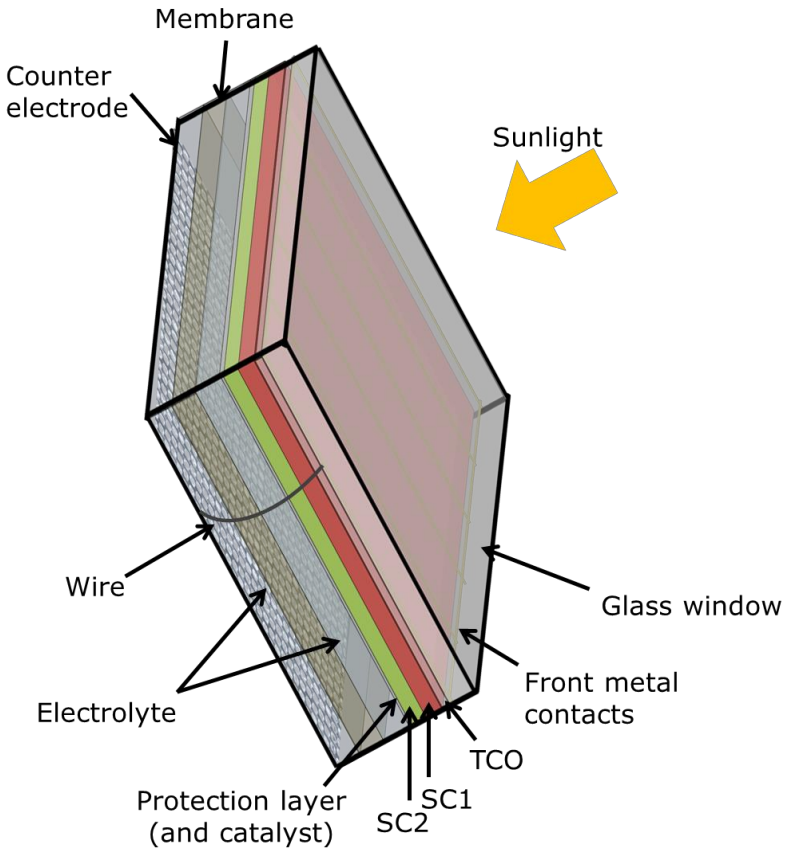

Figure 25. Scheme of the envisioned large-scale artificial leaf device

Figure 26 shows a sketch of the design selected with the proposed materials for a sustainable and economic device.

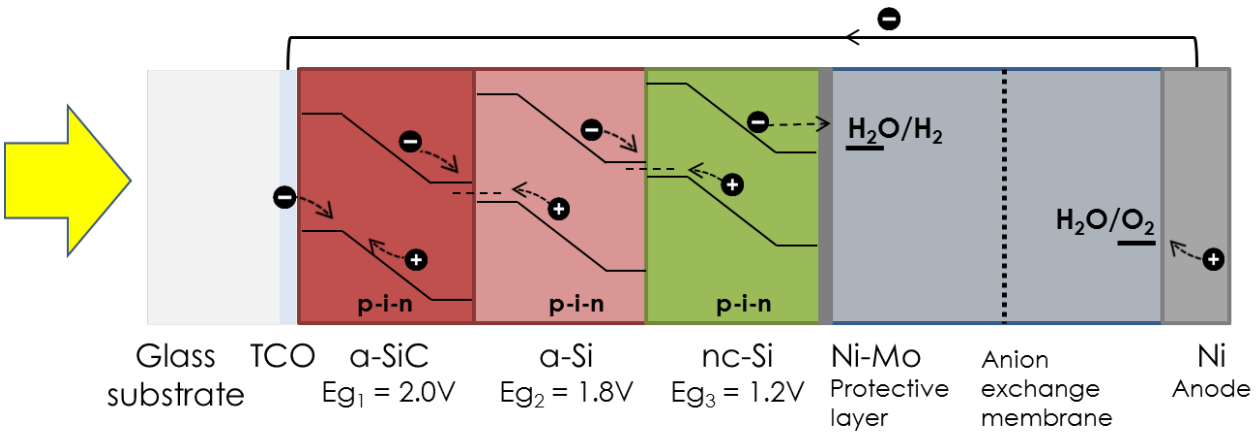

Figure 26. Possible structure of a triple junction Si-based photocathode device

5.4 Manufacturing of the device designed

The manufacturing of the selected device involves four different steps, as presented in Figure 27. The cathode, anode and membrane must be manufactured separately. These three components will be assembled together in a posterior step, ensuring that the two electrodes are electrically connected via external wires.

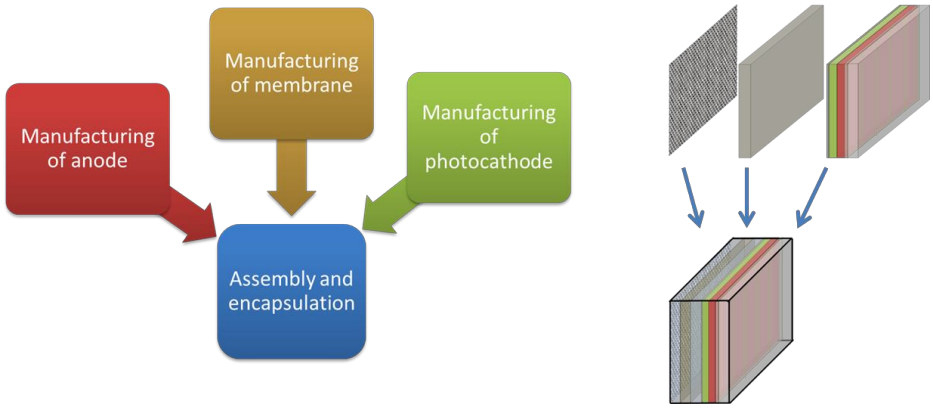

Figure 27. Main manufacturing steps of the PEC device

Anode

The anode is envisioned as a nickel mesh that provides high surface area for oxygen production. This micro-mesh can be directly purchased from many different suppliers, such as DeXmet Corporation (http://www.dexmet.com/). If it is desired, the anode could be manufactured in-house by perforating a sheet of nickel. This can be done with automated machines, such as the one provided by Benmetal® (http://www.benmetal.com/)

Membrane

Similarly to the anode, the membrane can be provided by an external supplier. A list of suppliers of commercial anionic exchange membranes can be found in (Guillet, 2015). Among the different options, Tokuyama Corporation (http://www.tokuyama.co.jp) offers reliable membranes, with the commercial name of Nosepta® with low resistivity (~0.2 Ωcm^{-2}).

Photocathode

This is a critical part of the device manufacturing, since the performance of semiconductor thin films is highly influenced by the crystalline structure, which at the same time depends on the deposition process (Luque & Hegedus, 2011). Ideally, the multilayers that compose the tandem photoanode could be deposited consequently in the same equipment to allow for fast manufacturing, avoiding transferring times and risks of contamination.

As mentioned earlier, the photocathode must be manufactured in a superstrate configuration, since light enters through the substrate side of the thin films stack. The glass substrate of the photoanode is the same one used for encapsulation of the device. On the glass substrate, thin metal contacts spatially separated about 2 cm are deposited in first place by vacuum evaporation. These metal contacts will allow the transport of electrons from the anode.

After the metal contacts are placed on the glass substrate, the TCO layer is deposited, ensuring that the edges of the metal contacts are not covered so they can be electrically connected to the cathode. The deposition technique used will influence both the optical and electrical properties of the TCO film (Liu, 2010). Sputtering is a popular technique for the deposition of these thin films, since large production rates can be obtained at a

low cost. However, the final properties of the film are poorer when compared to other techniques such as chemical vapour deposition (CVD) or pulsed laser deposition (PLD) (Delahoy, 2011). For superstrate a-Si solar cells, low pressure CVD (LPCVD) is commonly used since this process offers good quality of the TCO film while keeping the substrate at low temperatures (<150^{o}C), thus the front metal contacts are not damaged (Delahoy, 2011). Moreover, this deposition process results in a textured layer that enhances the light trapping of the photoelectrode (Addonizio, 2008). Therefore, it is suggested to deposit the TCO film by LPCVD.

On top of the textured TCO layer, the light absorbing semiconductors are deposited. The deposition technique will depend on the materials selected. For the envisioned triple junction a-Si thin films, plasma enhanced chemical vapour deposition (PECVD) is the most widely used technique (Schiff, 2011). A detailed description of the deposition of the different layers that compose an a-Si/µc-Si cell can be found in (Urbain, 2014).

Lastly, the protection layer that acts as catalyst for hydrogen evolution reaction must be deposited on the back of the multi-junction a-Si cell. NiMo was proposed for this protection layer, and can be applied by magnetron sputtering (Pletcher, 2012) A thin intermediate TCO layer can be deposited by LPCVD between the nc-Si layer and the back contact/protective layer to avoid contamination of the semiconductor film (Schiff, 2011).

Assembly and encapsulation

All the components must be assembled together to provide a working and safe device. The encapsulation of the device will be done with several components. First, an endplate (also called clamp plate) is needed at the back of the counter electrode. This plate has two holes, allowing for the input of electrolyte and the output of electrolyte with dissolved hydrogen. Several materials are used for this type of plates, being a common one a garolite sheet (Godula-Jopek, 2015). Garolite is made of glass cloth that has been impregnated with an epoxy resin under pressure and heat, and it has a low cost. Moreover, sealing gaskets will be needed to avoid leakage of the evolved gases as well as the electrolyte solution. The membrane need to be properly placed using a support frame.

As it has been pointed out in Chapter 4, the distance at which the two electrodes are placed has an impact on the transport losses: the longer the ionic path (i.e. distance between electrodes), the larger the Ohmic losses. This effect has been evaluated for different electrolyte conductivity, distance between electrodes and thickness of the membrane (Appendix N). A distance of 2.5 mm between electrodes is suggested for the PEC device, accommodating a 500 µm membrane in the middle. This distance would provide an Ohmic loss lower than 40 mV (Appendix N), considering a conductivity of the solution of 14 S/m (2.6 wt% NaOH). These losses are much lower than the criterion set for this type of resistances (< 200 mV).

It should also be considered that if the distance between the two electrodes is too low, the volume fraction of hydrogen and oxygen bubbles will increase. The increment in void fraction results in larger electric resistance in the electrolyte. Nagai *et al.* (2003) studied this relation of the distance between the electrodes and the efficiency of the water electrolysis process, for a range of spacing between electrodes from 1 to 20 mm, and current densities from 0.1 to 0.9 A/cm^2. It was concluded that for low current densities (0.1 A/cm^2), spacing between electrodes of 1 mm was optimum. Since our device works at current densities one order of magnitude lower than those considered by Nagai *et al.* (2003), it is foreseen that the void fraction would be even lower and thus the electric resistance of the electrolyte will not play an important role. Indeed, using the equation given in the cited article, it was calculated that the void fraction in the PEC water splitting device with a current density of 122 A/m^2 (current density for a device with 15% STH efficiency under 1 sun illumination) would be of about 1%.

Metal wires, which could be made of copper, are used to electrically connect the front metal of the tandem photocathode and the anode. The wires should be perfectly sealed to avoid their contact with the electrolyte

solution. At the periphery of all components the casing components, a sealant with good mechanical properties is needed to avoid water and gas leaks and to facilitate the distribution of the compression forces. As a housing material, PVC could be used since it provides high chemical resistance (to H_2, O_2 and electrolyte solution) (IPEX, 2009), it offers good mechanical properties and low permeability to gases, and it is also a good insulator (Nass, 1992). However, PVC can be used only if the device is kept below 70 ^{o}C. Therefore, once the operating conditions are define, the housing material selection should be reconsidered.

5.5 Device operation

Figure 28 shows how a hydrogen production plant based on PEC devices could be operated. It should be noted that it is out of the scope of this *conceptual design* to size the auxiliary equipment (compressors, storage tanks, etc.)

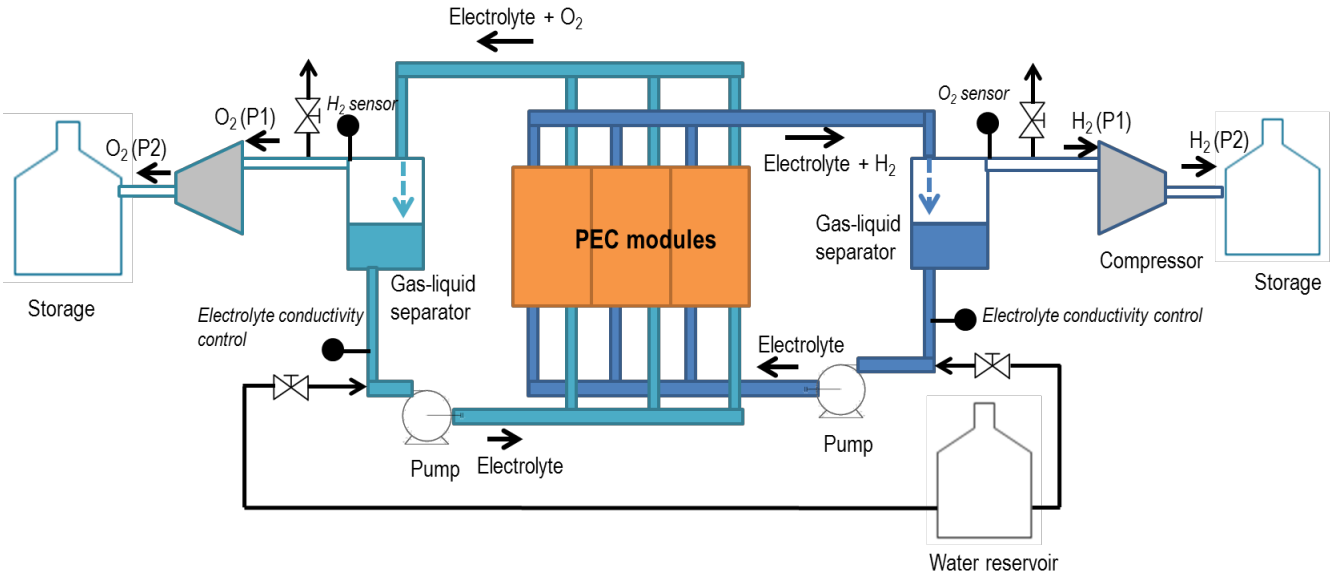

Figure 28. Sketch of the operation of a hydrogen production plant based on PEC water-splitting

An external pump should be used to induce the flow of the electrolyte solution. This will have several advantages: (a) enhancement of the collection of the gases, (b) minimization of transport losses due to coverage of the electrodes' surface by the bubbles and (c) cooling of the electrolyte to keep its temperature at moderates levels (< 80 ^{o}C) (d) pressurization of the gases (if the electrolyte feed is pressurized), decreasing the energy involved in the posterior gas compression step.

In the recirculation of the electrolyte, the gases will be separated by density difference in a gas-liquid separator tank. The gas output from these tanks should have a control on the purity of the gases. In case the oxygen level in the hydrogen stream (or vice versa) is too high, the gas mixture should be released. Since hydrogen has a very high volatility, it will disperse quickly without reaching explosive concentrations in air (see the safety section on chapter 7 for more details). The gases at low pressure would be directed to a compressor, where they would be pressurized before being stored in a gas compression tank.

Before the electrolyte enters again the PEC cell, the conductivity of the electrolyte will be controlled to adjust automatically the concentration of the solution by introducing more water. It is assumed here that the electrolyte will not be consumed in the process. However, a more detailed analysis should investigate the need of adding electrolyte.

One of the first assumptions for the selected device is that it would work “bias-free”, meaning that no external voltage is applied to the cell. Therefore, the only energy input for the operation of the device is solar energy. This is one on the main advantages of this device, i.e. the use of clean and renewable energy source. However, this also carries complexity on the design of its operation, since the amount of hydrogen produced will depend on the solar irradiation, which varies from location, time of the day and season and depends on unpredictable weather changes. The design of each plant based on PEC devices should thus should be done for each specific day and taking into account available data from weather conditions.

The flow management of the electrolyte inside the PEC device should be investigated in more detail. The flow should ensure the homogeneity of the electrolyte solution, avoiding pH gradients that could induce losses in the system (Singh, 2015).

6

Economic analysis

In this chapter an economic analysis of a hydrogen production plant based on the design selected is performed in order to understand its economic viability. First, the parameters that have been assumed to performed the analysis, such as the plant location and capacity, are presented. Thereafter, the capital investment of the plant is described, followed by the operating cost. The profitability of the plant is then shown by calculations of the net present value and the internal rate of return. Lastly, a sensitivity analysis is performed to show the effect of several parameters on the levelized cost of hydrogen.

It should be noted that an economic analysis performed at such early stage of the development of the artificial leaf design carries many uncertainties. Therefore, the accuracy of the estimations presented here will have a low accuracy level (± 50%).

6.1 Plant capacity and location

The location of the plant and its capacity have a large influence on the economic profitability, since they will influence the plant size, the area of land needed and its cost, the labour cost, etc. Therefore, these parameters must be established before proceeding with the analysis.

A daily production of **500 kg H_2/day** was chosen in order to be able to compare the results with the economic analysis performed by the *Department of Energy* of the US on the production of hydrogen by PEM electrolysis. In their "forecourt" scenario, for the first commercial plants, a 500 kg/day capacity was used (Ainscough, 2014). Assuming that the plant is closed 5 days a year to performed maintenance and repairs, the annual production is estimated as 180 tonne/year.

The location of the plant was chosen as New Mexico (US), which has an average daily irradiation of **6,5 kWh/m^2 day**. A more detailed analysis should consider the variation in sun irradiation throughout the year, as well as climate variations. For this first analysis, the daily irradiation is assumed constant and equal to the annual average.

6.2 Total capital investment

The capital investment is composed by the fixed capital investment (equipment and land cost) and start-up cost (Peters, 1968).

In order to estimate the cost of the reactor, the required area of panels with a Solar-to-Hydrogen efficiency of 15% was calculated for the given sun irradiation (6,5 kWh/m^2 day) and capacity (500 kg H_2/day), resulting in **17,092 m^2**. The price of the reactor was estimated by the price of its main components per m^2 and multiplied by the required area (Table 10).

Table 10. Fixed capital investment

Direct cost			
	Component	**$/unit**	**$**
PEC panel	**Photoelectrode**		
	• Front glass/TCO	11 $/m^2	
	• Front contacts	0.2 $/m^2	
	• Semiconductor (3-jn Si)	15 $/m^2	
	• Back metal	5 $/m^2	
	Total photoelectrode cost	31.20 $/m^2	533,280
	Membrane	18.18 $/m^2	310,738
	Counter electrode	0.10 $/m^2	1,709
	Housing and wiring	21.21 $/m^2	362,455
	Total PEC panel cost	70.69 $/m^2	**1,208,203**
Manifold, piping, and pump	(1% of total reactor assembly)	0.71 $/m^2	12,204
	Total reactor assembly	**71.40 $/m^2**	**1,220,386**
Land		540.00 $/acre	**4,242**
Gas processing	10% of direct cost – land	8.21 $/m^2	**140,274**
Controls	3% of direct cost - land	2.46 $/m^2	**42,082**
		Total direct cost	**1,406,985**
Indirect cost			
Engineering Construction general expenses Contractor's fee Contingency Up-front R&D Up-front License	20% of fixed capital investment		**351,746**
		Fixed capital investment	**1,758,731**

The core of the device is the photoelectrode, which is composed by a glass substrate coated with a TCO layer, front metal contacts, the semiconductor, and a back metal contact that act as protection layer as well as catalyst when in contact with the electrolyte. The cost of these components were estimated using values from the PV industry (Zweibel, 2000). For the estimation of the price of the semiconductor a thickness of 3 µm was assumed, and a cost of 5 $ for 1 µm/m^2 was taken from Zweibel *et al.* (2000). The cost of the photoelectrode resulted in 31.20 $/m^2. This value compares to current market price of thin film solar modules (0.45 $/Wp ≡ 45 $/m^2 of 10% efficiency module) if it is considered that the BOS accounts for 30% of the total module cost.

Another important component of the device is the ion exchange membrane. Its price was obtained from a study promoted by the DOE on the cost of PEM electrolysers, which showed a price of this component of 18.18 $/m^2 (James, 2012). Thirdly, the cost of the counter electrode was estimated by using the price of Nickel (http://www.metalprices.com) and assuming an electrode of 1 µm thickness.

For this preliminary analysis, it was assumed that the cost of the housing and wiring, accounts for 30% of the cost of the PEC panels. This assumption resulted in a cost of housing of 21.21$/m^2, which is indeed in the same order of the housing cost of PEM electrolysers, i.e. 20.36 $/m^2 for bipolar plates and gaskets (James, 2012). To finally estimate the total cost of the reactor assembly, some extra cost for manifolding, piping and pumping should be considered. The magnitude of this cost was taken from the analysis performed by the DOE, where it was estimated that this cost corresponds to 1% of the total reactor assembly (James, 2009). Considering the same cost weight of these components (1%) the total cost of the reactor assembly resulted in 1.22 M$.

The cost of the land was taken from the value given by the US government for New Mexico (USDA, 2014), which corresponds to 540 $ per acre. Assuming fixed panel arrays with a tilt angle of 30^o – optimum angle for a location with latitude 35^o, like Albuquerque (Luque and Hegedus, 2011) – each m^2 of panel occupies 0.86 m^2 of land. Assuming 1 m of distance between the panel arrays, the total land needed is 1.86 times the panel area, resulting in 7.86 acres, with a total cost of 4,240 $.

The cost of the auxiliary equipment for gas processing (compressor to 20 bar, intercooler unit and condenser, plus corresponding piping), and controls (remote monitoring, alarming, etc.) were taken from the DOE analysis. In this analysis it is shown that the cost of the gas processing equipment correspond to 10% of the total direct cost, and the controls to 3% (James, 2009). Assuming the same percentage, the cost of gas processing was estimated as 0.14 M$ and the cost of controls 42,082 $. Adding up the cost of the gas processing and control equipment to the reactor assembly and the land gives a total direct cost of 1.41 M$ (Table 10).

Indirect cost that arise from additional engineering and construction general expenses and contingency among others, has been assumed equal to 20% of the total fixed capital investment which is a common value in chemical engineering plants with high contingency due to novel technologies (Asselbergs, 2013). Indirect cost are then estimated to be 0.35 M$. All these cost are summarized in Table 10, and resulted in a fixed capital investment of 1.76 M$.

Finally, additional start-up cost due to modifications, loss in production and start-up labour, is estimated as 0,10 M$ under the assumption that it equals 5% of the total capital investment (Asselbergs, 2013). The **total capital investment results in 1,85 M$.** The cost breakdown is summarized in Figure 29.

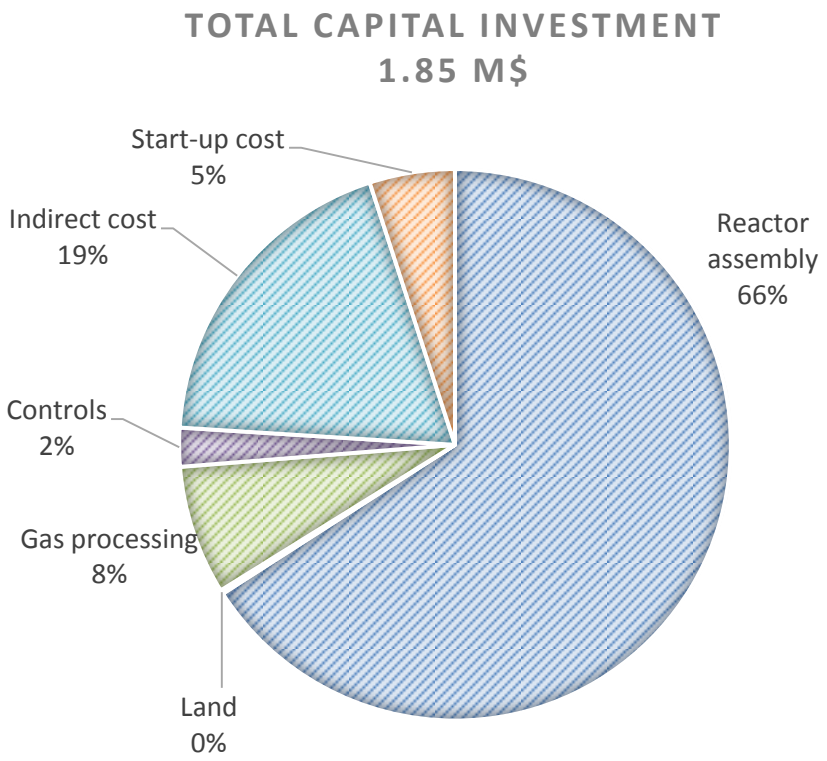

Figure 29. Cost breakdown of the capital investment of a plant of 500 kg/day

6.3 Operational expenditures

The raw materials, utilities, labour, and other indirect expenses compose the cost of operating the solar-driven hydrogen production plant. It is already foreseen that the cost of raw materials as well as electricity will be very low, since most energy comes directly from the sun and the main raw material is water.

In the production of 500 kg/day of H_2, 4.55 m^3 of water is consumed per day under the assumption that 1% is lost in the gases output streams (James, 2009). The price of demineralized water in US is 1.4 \$/m^3, and thus the yearly cost of water is about 2,300 \$. The price of the NaOH used to prepare the electrolytic solution is about 125 \$/tonne (The Glosten Associates, 2010). The amount of electrolyte needed is unclear, since it is only added at the beginning of the operation and it will not be consumed in the water-splitting reaction. If at the beginning of the operation the PEC panels are filled with the electrolytic solution, 17.1 m^3 of 1M NaOH solution (selected in Chapter 5) would be needed, since the space between electrodes will be of about 1 mm. Moreover, some additional solution is needed because the electrolyte will be pumped to facilitate the collection of the gases. If, for example, the amount of solution is doubled to account for the circulation, 1.06 tonne of NaOH are needed. This implies a cost of only 133 \$, and therefore it is neglected for this analysis. Nevertheless, once the systems in designed (including the recirculation), the amount of electrolyte could be calculated more precisely, and the need of replacement should be considered.

The electricity used in the plant to run the compressor, the cooling system, the pumps and the control system, was taken from the analysis performed by the DOE and adjusted to the capacity of our plant and results in 0.365 MWh/year. Taking the price of electricity of 7.01 c\$/kWh (IEA, 2015) the total expenditure in electricity is 25,600 \$/year.

The cost of labour has been estimated considering the number and type of personnel needed, and the salaries for each type of personnel for the state of New Mexico (U.S. Department of Labor, 2015). The values are represented in (Table 11), and the total cost of labour results in 0.48 M$/year. The total direct production cost (raw materials, utilities and labour) then results in 0.48 M$/year.

Table 11. Operational expenditures

Direct production cost			**511,220 $**
Raw materials	Water (1,638 m^3/year)	0,0014 $/l	2,291 $
	Electrolyte (NaOH)	125 $/ton	Neglected
	Total		**2,291 $**
Electricity		0,0701 $/kWh	**25,629 $**
Labour	• Operating Labour: 15 $/h	16 h/day	86,400 $
	• Panel Operator: 13 $/h	16 h/day	74,880 $
	• Security: 13 $/h	24 h/day	112,320 $
	• Supervision labour: 25 $/h	16 h/day	144,000 $
	• Lab analyst: 20 $/h	8 h/day	57,600 $
			475,200 $
Maintenance			**122,039 $**
Plant overhead			**36,774 $**
General expenses			**73,548 $**
TOTAL OPERATIONAL EXPENDITURES			**735,481 $**

An extra cost for maintenance and repairs has been estimated as 10% of the reactor assembly cost, resulting in 0.12 M$/year. To put this number in perspective, this cost would be equivalent to replacing all the membranes every 2.5 years.

Moreover, indirect cost will arise from general expenses (administrative cost, sales & marketing, engineering service and R&D) as well as from plant overhead (safety and protection, warehousing, quality controls, etc.) need to be considered. These have been assumed to account 15% of the total expenditures, which is within the typical range of these expenditures in chemical plants (Asselbergs, 2013).

Adding up the direct production cost to the maintenance, plant overhead and general expenses, the total operating cost results in **0.74 M$/year**. The cost breakdown of the OPEX is summarized in Figure 30.

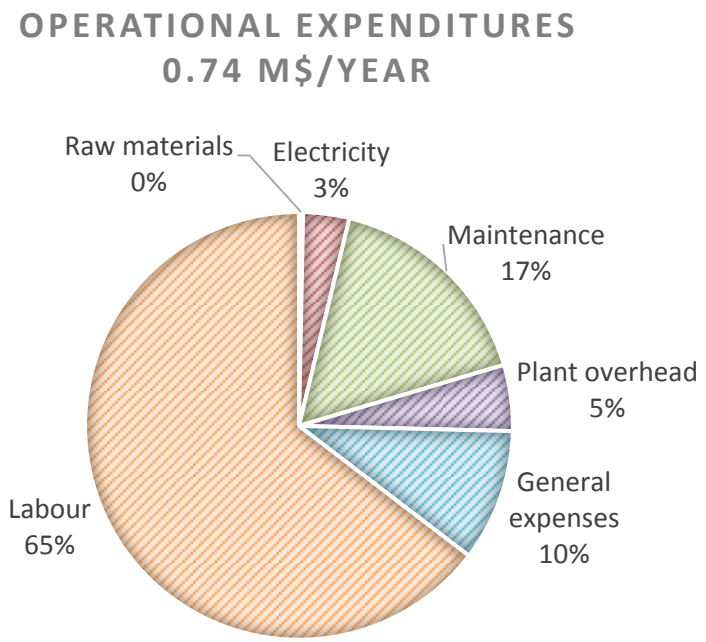

Figure 30. Cost breakdown of the operational expenditures

6.4 Profitability analysis

A cash flow analysis is performed to estimate the profitability of the plant. It is assumed that the plant has a lifetime of 20 years, and that the plant is built within one year (in the year 0). Initially, the selling price of hydrogen is considered 10 $/kg, which is about the same price at which it is currently being sold in the H_2 refuelling plants in Germany that use electrolysers. Later in this analysis the levelized cost of hydrogen will be calculated, since this is the common figure used for comparison of different hydrogen production technologies.

Another assumption done in this analysis is that all the hydrogen produced is sold. Due to the small capacity of the plant and the multiple applications of hydrogen, it is believed that it is very likely to sell all the hydrogen. This gives a yearly sales revenues of 1.8 M$.

A profit and loss (P&L) analysis is performed in order to calculate the net income (Table 12). First, the EBITDA (*Earnings before interest, taxes, depreciation, and amortization*) was calculated by subtracting the expenditures to the sales revenues. It should be noted that the maintenance cost has been removed from the expenditures, as this will be deducted over the course of several years as a depreciation expense. The EBITDA resulted in 1.19 M$. Using the equation below, the depreciation was calculated as 0.61 M$, leading to a EBIT (*Earnings before interest and taxes*) of 0.97 M$.

$$Depreciation = \frac{Total\ capital\ investment}{Plant\ lifetime} + Maintenance\ expenditures$$

In this analysis, it is assumed that the investment comes from an investor or venture capitalist, who will own equity from the company. Therefore, no interest are considered in the P&L analysis, thus the EBT (*Earnings before taxes*) is equal to the EBIT. Finally, a tax rate of 30% has been assumed resulting in 0.29 M$. The yearly net income is then estimated as 0.68 M$.

Table 12. Profit and loss analysis

Year	0	1	2	…	20
Investment ($)	1,851,295				
Sales revenues ($)		1,800,000	1,800,000	1,800,000	1,800,000
Expenditures ($)		613,442	613,442	613,442	613,442
EBITDA ($)		**1,186,558**	**1,186,558**	**1,186,558**	**1,186,558**
Depreciation ($)		214,603	214,603	214,603	214,603
EBIT ($)		**971,955**	**971,955**	**971,955**	**971,955**
Interest ($)		-	-	-	-
EBT ($)		**971,955**	**971,955**	**971,955**	**971,955**
Taxes ($)		291,586	291,586	291,586	291,586
Net income ($)	-1,851,295	**680,368**	**680,368**	**680,368**	**680,368**

The **cash flow analysis** was also performed to study the profitability of the plant. The free cash flow is calculated by subtracting the working capital, the maintenance expenses and the taxes from the EBITDA. The working capital is a payment that results from the offset between the payment to the providers of raw materials and utilities (assumed to be every 90 days), and the money received from the client (assumed every 30 days). In this case, since the expenses in utilities and raw materials are very small, this offset of capital is cleared up in the first year, and it does not affect the cash flow of the remaining years (Table 13).

Table 13. Calculation of the working capital

Year	0	1	2	…	20
Sales revenues		1,800,000	1,800,000	1,800,000	1,800,000
Utilities and raw materials		27,920	27,920	27,920	27,920
Payment from clients (every 30 days)		150,000	150,000	150,000	150,000
Payment to providers (every 90 days)		6,980	6,980	6,980	6,980
Need of financing		143,020	143,020	143,020	143,020
Working capital		143,020	-	-	-

Table 14 shows the results of the cash flow analysis. An internal rate of return (IRR) of 39% shows the high profitability of this plant. The IRR is the value of the cost of capital that would give a Net Present Value equal to 0.

Table 14. Cash flow analysis

Year	0	1	2	…	4
Investment	1.851.295				
EBITDA		**1,186,558**	**1,186,558**	**1,186,558**	**1,186,558**
WC		143,020	-	-	-
Maintenance		122,039	122,039	122,039	122,039
Taxes		291,586	291,586	291,586	291,586
Free cash flow	**-1.851.295**	**629,913**	**772,933**	**772,933**	**772,933**
IRR	**40%**				

The net present value (NPV) depends on the cost of capital set by the investor. For a cost of capital of 10%, the NPV results in 4.60 M$. Figure 31 shows the present value profile for each year, for a cost of capital of 10% as well as 5 and 15%.

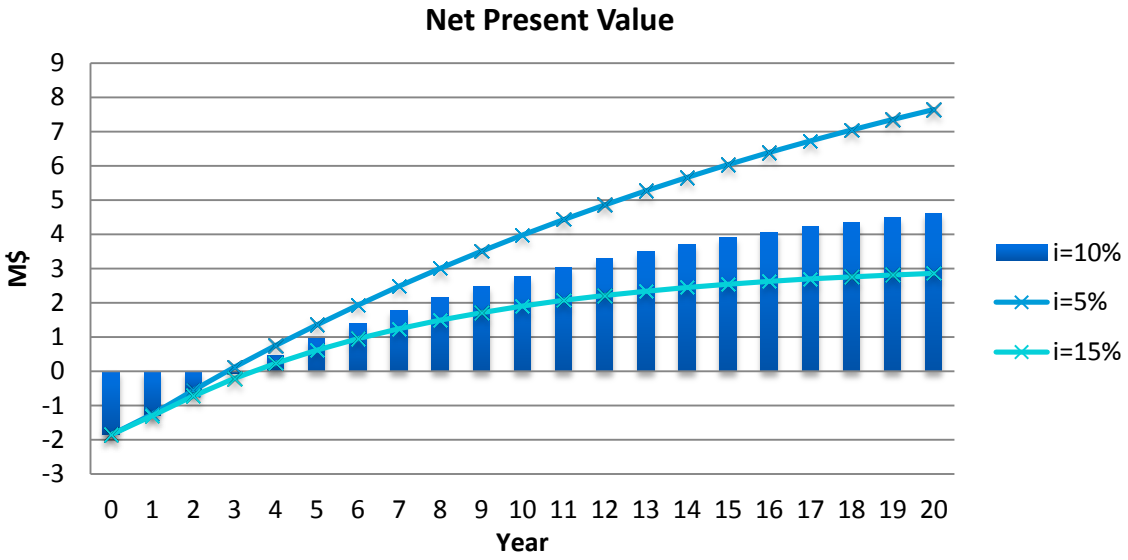

Figure 31. Net present value for different cost of capital

A widely used figure to compare the economic attractiveness of certain hydrogen production technologies is the levelized cost of hydrogen, in terms of $/kg. This value was calculated as the selling price of hydrogen that gives an IRR of 10%, as explained in the DOE analysis (James, 2009). This means the cost at which hydrogen can be sold in a project where the investor gets 10% of benefit on the investment, and giving a net present value of 0 at the end of year 20. This cost of hydrogen resulted in **5.66 $/kg of H_2**.

This preliminary economic analysis showed the potential profitability of a hydrogen production plant using the PEC device designed in this project. An investment of 1.85 M$ was estimated for a plant of 500 kg/day, which is for example 0.02‰ of the funding available at the Horizon 2020 European Research programme (http://ec.europa.eu/programmes/horizon2020/). This investment is not high and it could be recovered in 3 years if hydrogen is sold at 10 $/kg, providing 4.60 M$ by the end of the year 20. Moreover, the selling price of hydrogen could be as well as low as 5.66 $/kg of H_2 to breakeven at the end of year 20. This price is slightly lower than the cost of hydrogen from a plant of the same capacity (500 kg/day) based on PEM electrolysis, which was estimated as 5.79 $/kg by the DOE (DOE, 2014).

6.5 Sensitivity analysis

A sensitivity analysis was performed to understand the effect of some parameters on the economic viability of the plant. The levelized cost of hydrogen was used as figure of merit, as it allows comparison with other analysis for different hydrogen production technologies.

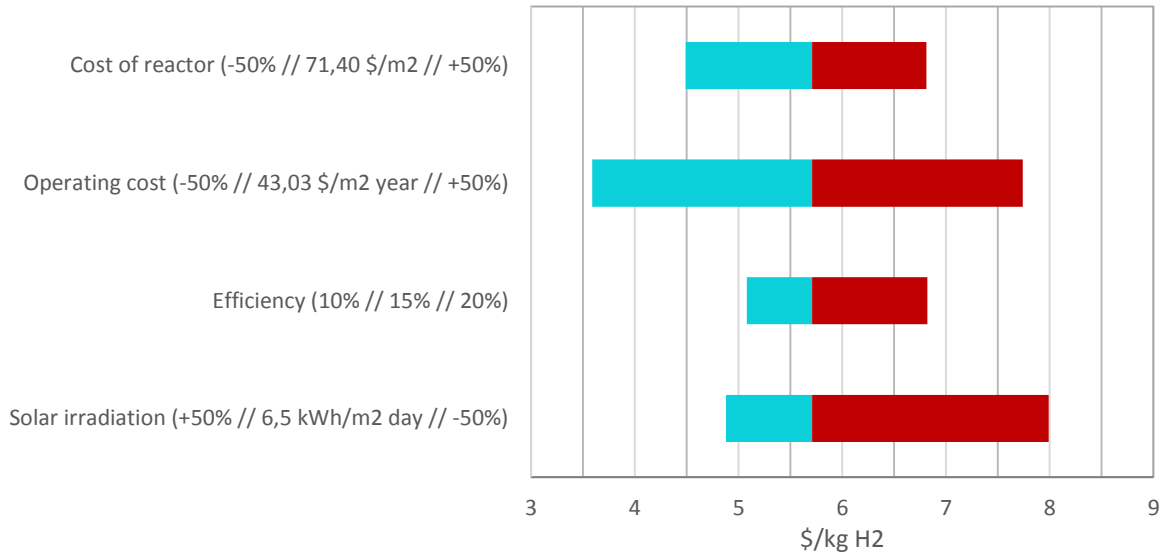

Figure 32. Sensitivity analysis of the levelized cost of hydrogen

Due to the high uncertainty in the estimations on the capital investment and the operating cost, these two parameters have been changed ± 50% to investigate their effect on the levelized cost of hydrogen. It can be seen in Figure 32 that the operating cost have a large impact on the cost of hydrogen, which could be as high as 7.8 $/kg if the OPEX were 50% higher than what it was estimated in this analysis (43.03 $/m^2). However, variations on the cost of the reactor did not influence much the price of hydrogen.

The efficiency of the large-scale modules is also unclear. Nevertheless, in can be concluded from Figure 32 that this parameter will not have a large influence on the cost of hydrogen. Although devices with 10% efficiency will not reach the cost target of 6 $/kg, in the short term they could provide hydrogen at a cost competitive to that of current hydrogen refuelling stations based on electrolysis.

The last parameter investigated was the solar irradiation, which will depend on the location of the plant. As shown in Figure 32 , this parameter greatly affects the final cost of hydrogen. Therefore it is recommended to place the PEC plants in areas with high insolation, and to consider the potential benefits of using solar concentrators in the areas with lower irradiation. The impact of the location on the cost of hydrogen is further represented in Figure 33. For the time being, the price of the land has been considered the same for the different locations. However, this can greatly vary for different locations and it should be considered when analysis the profitability of a plant in a new location.

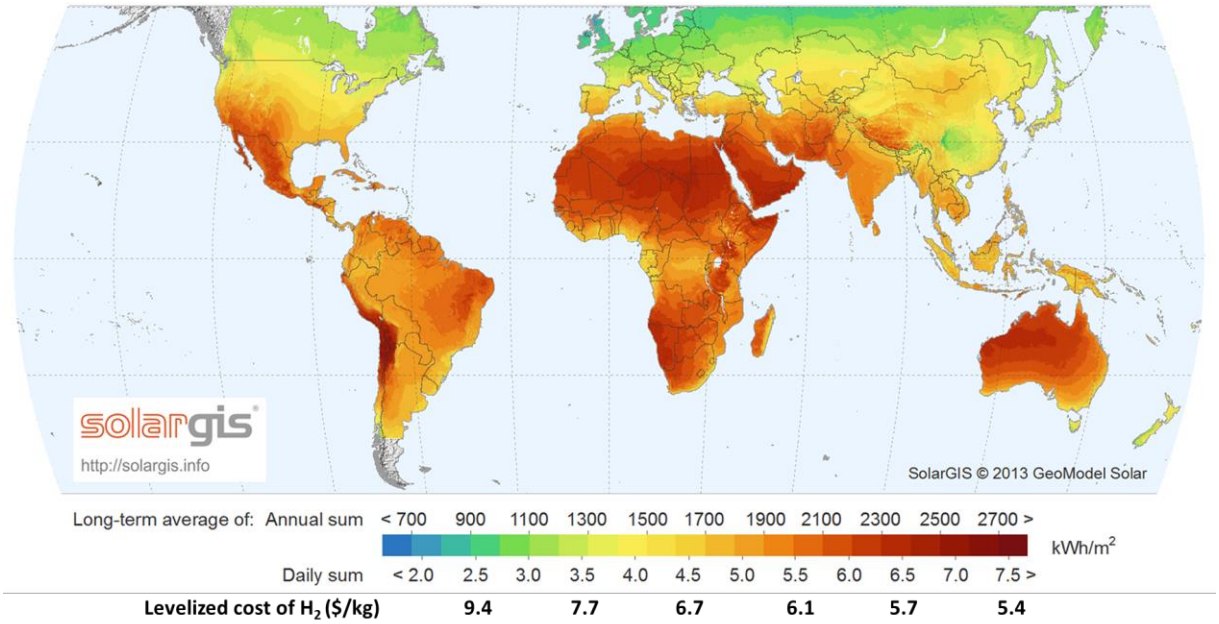

Figure 33. Levelized cost of hydrogen according to the solar irradiation

7

Social and environmental impact

This chapter contains an analysis of the potential environmental and societal impact of the device designed. It should be noticed that the lower the technology readiness level (TRL) of a technology, the more difficult is to perform an accurate life cycle assessment (LCA), due to the many uncertainties. However, at an early stage is when this analysis might be most useful, in order to identify early on the development potential risks and to orientate the technology in the responsible direction. For this reason, a sustainability LCA has been performed, leading to recommendations to reduce the environmental impact of the PEC water-splitting technology. Moreover, the safety of the device throughout its life cycle has been also analysed, and recommendations are provided to ensure a safe manufacturing and operation.

7.1 Social and ethical considerations

The biggest potential social impact of PEC water-splitting technology is related to the use of hydrogen as an energy carrier, which could bring a complete energy independency. The energy production can be done on a country/region level (i.e. large scale facilities that produce hydrogen and transport it to all the consumers), but can also be done on an individual/community level where each costumer could have his/her own "power plant". The first scenario would economically benefit many countries that currently depend on fossil fuels, which is provided by only a few other countries that decide their price. Producing your own fuel, could bring energy security and price stability. In the second scenario, the customer would have to deal with their own energy generation, which would increase the energy consumption awareness of the society and potentially it could lower the rapidly increasing consumption rates.

If the PEC device is not use for generating hydrogen as energy carrier, but rather as a chemical for other process (like ammonia production), the sustainability of the production chain of the end product would increase, if compared to the current H_2 production processes. Therefore, the widespread application of PEC devices could have a beneficial effect on the society.

A drawback of this technology is the large areas needed to deploy the solar-driven water-splitting panels, approximately 1 m^2 per kWh/day (assuming panels with 15% STH efficiency receiving a solar irradiation of 6.5 kWh/day/m^2). To reduce the social impact in this regard, the PEC panels should not be placed in crop fields or lands that could be used for food production. Instead, infertile grounds, roofs, paved roads, etc. should be used.

Moreover, since the technology highly depends on the amount of solar irradiation, the placement of a PEC plant in underdeveloped countries where large amount of solar energy is available (for example in central Africa) and the posterior transportation of the hydrogen to other wealthier, but less sunny locations might seem attractive. If this is done, it should be ensured that the consequences of the business actions contribute to the well-being of the society involved as well.

If this technology reaches low cost of hydrogen production, it would be suitable for power generation in underdeveloped countries. For example, sub-Saharan Africa countries, where over 75% of the population does

not have access to electricity (The World Bank, 2015), could benefit from this technology. To illustrate the potential benefit, let's consider Somalia as a case study. Somalia has a large solar irradiation (> 2.3 MWh/m^2 per year), and an energy consumption of 288 GWh/year produced 100% from fossil fuels, according to *The World Fact Book* (Central Intelligence Agency, 2015). However, as explained before, only 25% percent of Somalia's population has access to electricity. In order to provide electricity to the remaining population, it can be estimated that at least an additional 865 GWh/year would be needed. This energy could be supplied by 144 plants of the same capacity investigated before in the economic analysis (500 kg/day), which involved a capital investment of 1.85 M$ each. Therefore, the investment needed to provide electricity to all the population in Somalia that currently does not have access to it is in the order of 167 M$. This investment corresponds to about 11% of the GDP of Somalia, and 0.03% of the GDP of the Netherlands (Central Intelligence Agency, 2015). In terms of area, 2.46 km^2 would be needed (0.4 x 10^{-3} % of the land of Somalia). A logical question that might arise when considering the use of the PEC water-splitting technology in these underdeveloped countries is the availability of water resources. For the example of Somalia, 234,000 m^3 of water would be needed every year to produce the desired amount of energy. This volume of water corresponds to 0.13 x 10^{-3} % of the annual rainfall in Somalia, which is 180 x 10^9 m^3/year (Aquastat, 2015).

These numbers show the feasibility of employing the PEC water-splitting technology for energy generation in underdeveloped countries, if proper distribution and pricing systems are put in place to facilitate the implementation. Moreover, this technology would allow for the development of these countries in an environmental friendly way.

In conclusion, this technology has the potential to bring beneficial social impact, if used in an ethical and responsible way.

7.2 Environmental impact

7.2.1 Energy payback time

When designing an energy conversion technology, one fundamental environmental requirement is that the energy involved in manufacturing such a system is lower than the energy the system will produce during its lifetime. To investigate if the PEC water-splitting device meets this requirement, the primary energy required to manufacture was estimated.

A recent study by Zhai *et al.* (2013) analysed the primary energy consumed in the manufacturing of a PEC device with the layout shown in Figure 34. The similarities between this device and the one considered in our design allow us to use part of their results in our analysis. The main difference comes in the (photo)electrodes. Zhai *et al.* (2013) used two photoelectrodes with a catalytic layer (of platinum) on top. In our analysis we consider a 3-jn a-Si photoelectrode, and a nickel mesh as counter electrode.

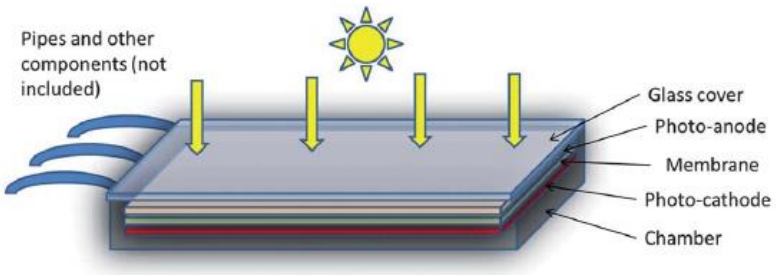

Figure 34. Structure of the PEC device studied by Zhai *et al.* (2013)

The energy involved in the procurement of materials as well as the fabrication of the components of the PEC device is shown in Table 15. The total energy involved in manufacturing the PEC device (cradle-to-gate) is 1.8 GJ/m^2.

Table 15. Primary energy requirement for manufacturing the PEC water-splitting device

Component	Energy (MJ/m^2)	Reference
Photocathode (3-jn Si cell)	• Materials*: 180 • Fabrication: 620	Kim (2011)
Anode (Ni mesh)	• Materials: 2 • Fabrication: 13	Idemat (2015) Zhai (2013)
Membrane	• Materials: 139 • Fabrication: 166	Zhai (2013)
Encapsulation material	420	Zhai (2013)
Ancillary processes**	256	Zhai (2013)
Total	**1,796 MJ/m^2**	

* *Includes the glass substrate*

** *Includes miscellaneous materials, water pumping, environmental control and cleaning.*

To estimate the energy payback time (EPBT), the energy produced by the PEC device should be considered. This energy production depends on the efficiency of the cell and the amount of solar irradiation. For the location selected previously in the economic analysis (New Mexico, US), with an annual insolation of 2.4 MWh/m^2 per year, the EPBT for different efficiencies is illustrated in Figure 35.

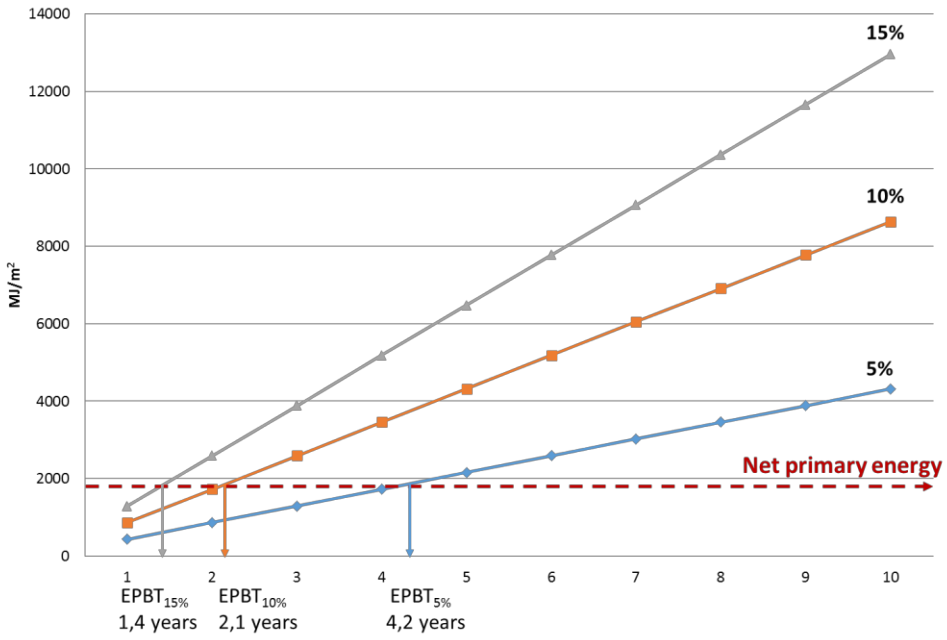

Figure 35. Accumulated energy generated vs time for different cell efficiencies. The net primary energy involved in the device manufacturing is also represented to illustrate the EPBT

For the location selected, the EPBT shows very promising numbers: from 1.4 to 4.2 years depending on the efficiency of the device. Figure 36 illustrates the influence of the location on the EPBT. The figure shows the EPBT for different locations assuming panels of 10% efficiency. It can be seen that for some northern areas, like the Netherlands, the EPBT would be of about 5.5 years.

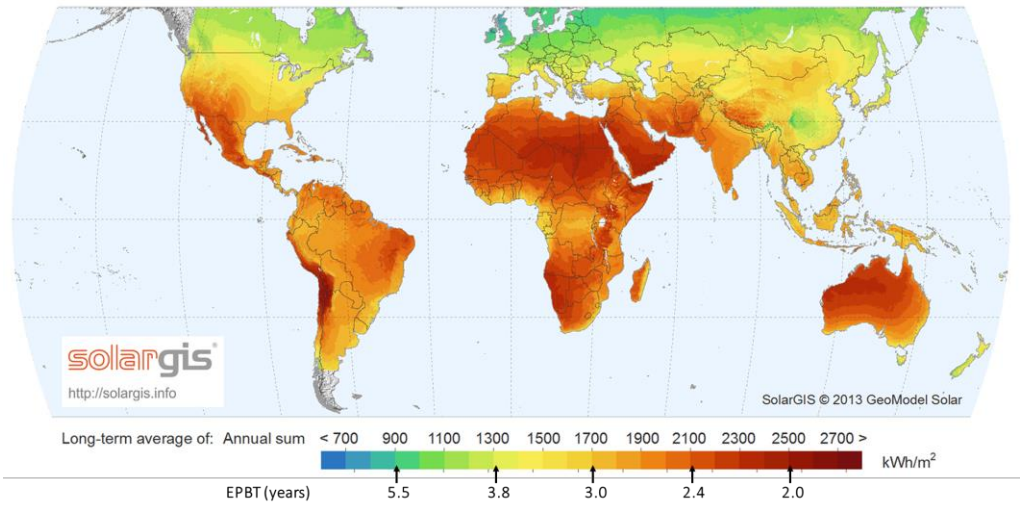

Figure 36. EPBT as function of the annual solar irradiation for PEC panels with 10 % efficiency

7.2.2 Sustainability Life Cycle Assessment

In the design of a new product, it is important to understand its effects towards the environment in all its life stages (Figure 37) in order to minimize the environmental impact. A cradle-to-grave life cycle assessment has been performed to study the CO_2 emissions in each life stage. As explained before, due to the uncertainties in the early stage of the development of this technology, the accuracy of this analysis is rather low. However, this primary analysis allows for the identification of the technological components that could provide the main environmental concerns.

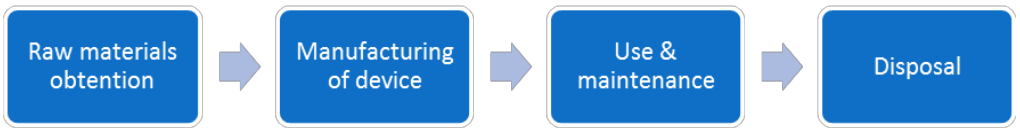

Figure 37. Cradle-to-grave life cycle stages of the artificial leaf device

Raw materials and manufacturing of the device

The energy spent in the obtainment of the raw materials and the production of the PEC device, was already estimated for the calculation of the EPBT. The total energy has been estimated as 1.8 GJ/m^2, which corresponds to 251 kg CO_2 eq. if the emissions per MJ are considered for the Western Europe energy mix (Idemat, 2015). The breakdown of the primary energy requirement is shown in Figure 38.

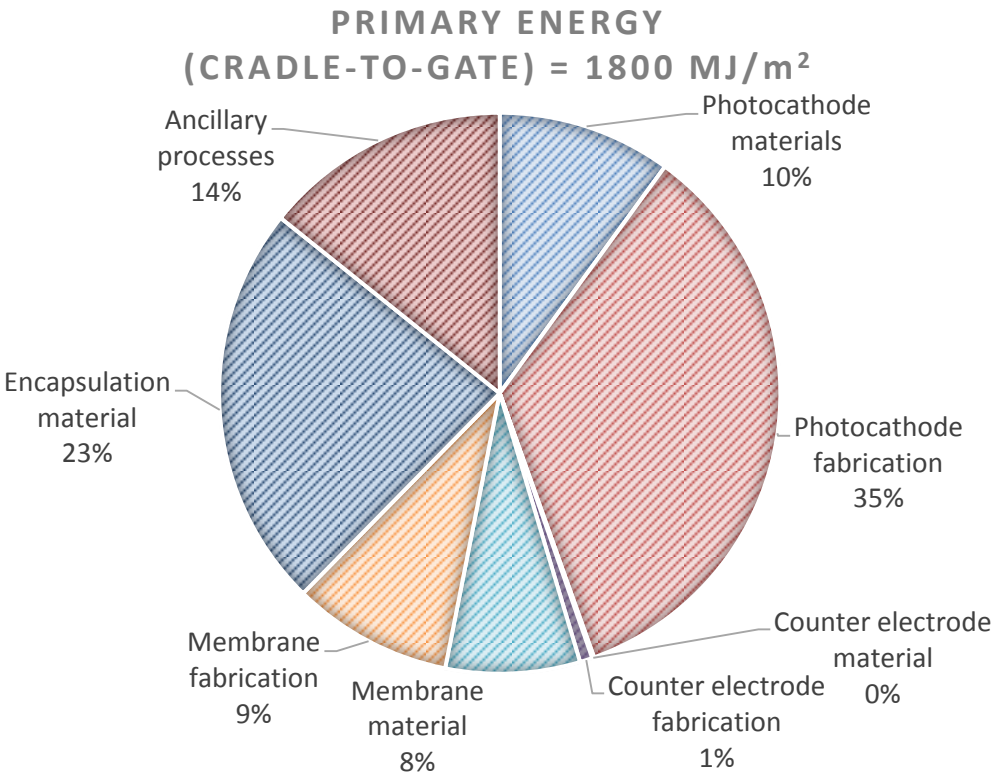

Figure 38. Breakdown of the total primary energy required for manufacturing 1 m^2 of PEC device

It should be noted that the semiconductor photoelectrode accounts for more than 40% of the total energy consumed. This energy is mainly due to the manufacturing process, which involves energy intense deposition methods such as chemical vapour deposition, with a slow deposition rate of less than 1 nm/s (Kim, 2011). The energy requirement could be greatly reduced if low energy processes are used (i.e. spray pyrolysis), or if the deposition rate was increased.

Use and maintenance of the device

The energy involved in operating the device comes mainly from the sun, and thus it does not produce any harm to the environment. Additional energy is needed to operate the plant for pumps and compressors. However, the LCA analysis is limited to the PEC device, and not to the complete plant. Therefore, only the energy used in pumping the electrolyte is considered here, which is about 0.65 MJ/m^2 per year, and thus it is considered neglectable since it is less than 0.05% of the energy content of the H_2 produced by the device.

In the operation of the device, water is also consumed. Per year, the CO_2 emissions related to the water consumed per m^2 of PEC device will be in the order of 43 g of CO_2 eq. (considering that the emissions associated with the consumption of deionized water are 0.45 kg CO_2 eq. per m^3 (AnglianWater, 2015). Moreover, the emissions involved with the use of electrolyte are minimal. In the case of using NaOH, its emissions are 1.24 kg CO_2 eq. per kg of NaOH (Idemat, 2015), and less than 100 g would be sufficient for 1 m^2 of device.

Besides the emissions of the materials and energy needed to run the device, the environmental impact of the products must be considered. Two products are obtained by operating the PEC device: hydrogen and oxygen. This first one is aimed to be stored and used, and thus it will not be released to the atmosphere. However, due to the small size of the H_2 molecule and its high volatility, the possibility of leakage should be considered. If leakage occurs, one should consider the environmental effects of H_2 in the atmosphere. Hydrogen does not

interact with solar radiation; therefore it is not a direct greenhouse gas (GHG). However, hydrogen is considered to be an indirect GHG. In the troposphere, hydrogen reacts with hydroxyl radicals, perturbing the distribution of methane and ozone, i.e. the second and third most important GHG after CO_2 (Derwent, 2006). The global warming potential (GWP) of hydrogen has been estimated as 5.8 over a 100-year time horizon (Derwent, 2006). The GWP is a relative measure of how much heat a greenhouse gas retains in the atmosphere, using CO_2 as a reference ($GWP_{CO2} = 1$).

To put the meaning of the GWP of hydrogen into perspective: 3,100 Tg of hydrogen per year would be needed for substituting the entire fossil fuel based energy demand of about 104 x 10^3 TWh in 2012 (IEA, 2014). If a leakage of 3 wt% is considered, 93 Tg of H_2 would be emitted per year, which would be equivalent to 539 Tg of CO_2 emissions per year. If it is considered that about 32,300 Tg of CO_2 were emitted in 2012 from the consumption of energy (IEA, 2014), the global effect of hydrogen would account for only 1.6 wt% of the current value. Although this represents a substantial reduction of the environmental impact, it will be important to ensure a low level of leakage of hydrogen during its production, storage and usage in order to minimize global warming.

The second gas produced, oxygen, might be stored and used for many different purposes, as suggested in the market analysis. However, it has been widely accepted that oxygen could be released to the atmosphere without any pernicious effect. This is indeed a plausible option, since oxygen molecule does not interact with the infrared radiation coming from the Earth and thus it does not contribute to the greenhouse effect.

Disposal

In this cradle-to-grave LCA it is assumed that the full device is disposed and sent to landfill. As a reference value, landfill has a CO_2 eq. emissions of 0.44 kg per kg of waste disposed. The weight of the device under consideration would in in the order of 10 kg/m^2 (1 kg of water, 2 kg of glass cover, and 7 kg for chamber and other materials). Therefore the emissions would be around 4.4 kg CO_2 eq. per m^2 of device.

Recyclability of the device

Ideally, all components of the PEC water-splitting device should be recyclable. The recycling process will start with the dismounting and separation of the components: semiconductor photoelectrode deposited on the glass, the housing and manifolding materials, the metal counter electrode, the membrane and the wiring components.

The main uncertainty in the recyclability of the PEC device is the semiconductor photoelectrode. However, learnings from PV industry could be taken in this respect. The semiconductor deposited on the glass could be recycled in the similar way as current PV panels are. First, the glass is crushed into small pieces, and the semiconductor films are removed by the addition of acid and peroxide in a rotating stainless steel drum, followed by solid-liquid separation processes that involve several precipitation steps (Krueger, 1999). This process, carried out for many years at *First Solar*, results in the recovery of more than 95% of the semiconductor material and 90% of the glass, to be used in new modules.

Another novel component whose recyclability is under question is the ion exchange membrane. It was found in literature that the membranes could be recycled by dissolution and recasting of the polymer (Xu, 2002). Although this should be tested at an industrial-scale and the performance of the recycled membrane, it is assumed here that this component is 100 % recyclable.

The counter electrode will be made of metal, such as Nickel. The recycling of metals is a well-known process, and high recycling efficiencies can be achieved (Graedel, 2011). Lastly, the housing material (PVC) can be

also recycled efficiently.

Table 16. Recyclability of the components of the PEC device

	Recyclable?	Recovery
Semiconductor	Yes	95%
Glass	Yes	90%
Membrane	Yes	> 95%
Counter electrode	Yes	> 95%
Housing	Yes	> 95%

The recycling of all these components into new PEC devices would save about 95% of the energy of obtaining new materials, ~700 MJ/m^2. However, this does not consider the energy spent into the recycling process. A cradle-to-cradle LCA analysis should be performed for a more detailed study of the benefits of recycling the materials.

Conclusions

Despite the large amount of uncertainties related to the manufacturing, use and disposal of this device, a preliminary cradle-to-grave LCA has been performed to identify environmental concerns. The energy used in the obtainment of the raw materials and the manufacturing of the device has been translates into CO_2 eq., and the emissions "saved" from using the PEC device have been estimated by the energy content of the hydrogen produced during its lifetime. Lastly, it was assumed that the full device was disposed by landfill and the CO_2 emissions were also estimated.

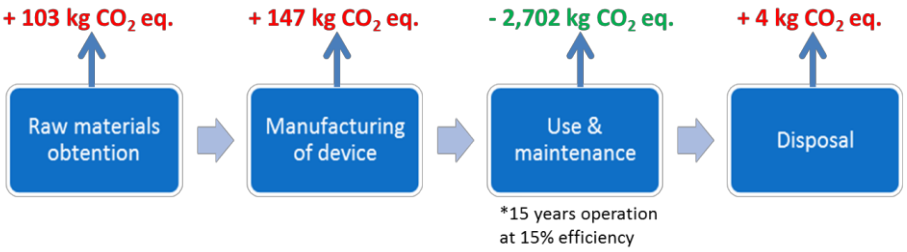

Figure 39. Estimated CO_2 emissions (or savings) in each life cycle stage of the PEC device

The following are some considerations to improve the sustainability of the device:

- The photoelectrode is the component that consumes the largest amount of energy in the manufacturing of the PEC device, due to the deposition of the thin films. Utilizing low energy deposition methods will improve the environmental friendliness of the PEC device.
- During the use of the device, it is important to ensure that hydrogen does not leak. The emissions of hydrogen have indirect greenhouse gas potential.
- The extension of the lifetime of the components of the PEC device will be crucial to reduce the amount of maintenance and replacement needed, which will in turn result in a lower environmental impact.
- For a deeper insight on the environmental impact of this technology, a LCA of the whole system, including hydrogen compression, storage and transportation, should be performed.

7.3 Safety in the life cycle

Safety is an important parameter to consider through the entire life cycle of the device, from its production to its disposal. In this analysis only the safety issues related to the PEC water-splitting device will be considered. Therefore, considerations on the storage, transportation of H_2 are out of the scope of this report. Standardised safety measures have been developed for hydrogen storage and transportation, such as NFPA 55.

Raw materials and manufacturing

It is necessary to ensure the safety of the raw materials and their handling. Among the components of the PEC device, the most challenging in terms of safety is the semiconductor photoelectrode, since in the manufacturing of a-Si thin films toxic gases (e.g. germane, phosphine, trimethylboron) are involved (Luque & Hegedus, 2011). It is thus recommended that safer production methods are explored. If CVD is to be used, one safety measure that should be taken is to install the gas cylinders of such gases in fireproof gas cabinets or even outside the building. Moreover, monitoring the level of toxic gases throughout the plant via sensors will be crucial, and operations shutdowns should be implemented. Although there are toxic gases employed in their manufacturing, the a-Si cells do not contain toxic elements.

Regarding the ion exchange membrane, it is recommended to wear protective gloves when handling it (Fumatech, 2015) since prolonged contact with the membrane, which can produce skin irritation. Besides risk of irritation, no other safety concern is related with this membranes (Membranes International, 2015). For Nafion ®, very low toxicity by oral intake has been reported (LD_{50} larger than 20,000 mg/kg of body weight).

When manufacturing the counter electrode, made of Nickel, respiratory and eye protection equipment should be worn when to avoid irritation of the eyes or inflammation of the lungs from nickel dusts (HSE, 2015).

Use and maintenance of the PEC device

The biggest safety concern in the use of the device is on the production of mixtures of hydrogen and oxygen due to gas crossover through the membrane. Concentrations from 4 to 75 vol% of H_2 in O_2 are flammable. This is a wider range of flammable concentrations in air than other fuels, and thus it can ignite much more easily (Table 17). Hence it is critical to ensure the separation of the gases. Therefore, the an appropriate membrane should be used, with minimal permeability to the dissolved gases. The membrane should be well sealed, to avoid crossover of electrolyte within the anode and the cathode chamber containing dissolved gases. The gas output stream from the anode chamber should feature a hydrogen sensor to control the safety level, and a shutdown mechanism should be implemented. Moreover, all the peripheral equipment should be grounded to avoid the formation of static electricity, which could ignite hydrogen. Common precautions in current gas stations such as no smoking or use of spark generation equipment should also be taken in the surroundings of the PEC equipment.

Nevertheless, since the device will be operated in open spaces, it is highly unlikely that the flammability limit in air will be reached if the device or the storage unit has a leak, because hydrogen gas is lighter than air and diffuses at a speed of 20 m/s (6 times faster than natural gas) (McCarty, 1981). For this reason, if released to the air hydrogen gas would rise and disperse quickly. The fact that the PEC cell has to be placed outdoors brings and intrinsically safe hydrogen production in case of leakage, supposing an advantage over an electrolysis system placed indoor.

Table 17. Properties of hydrogen and other fuels (Busby, 2005)

	Hydrogen	Natural gas	Propane	Gasoline vapour
Density relative to air	0.07	0.55	1.52	4.0
Density (kg/m^3)	0.084	0.651	1.87	4.4
Diffusion coefficient (cm^2/s)	0.61	0.16	0.12	0.05
Explosive energy (MJ/m^3)	9	32	93	407
Flammability range (vol%)	4 to 75	5 to 15	2 to 10	1 to 8
Detonation range (vol%)	18 to 59	6 to 14	3 to 7	1 to 3
Minimum ignition energy (mJ)	0.02	0.29	0.26	0.24
Autoignition T in air (^{o}C)	565-581	539	454-509	257
Flame speed (cm/s)	346	43	47	42

It can been concluded from Table 17, that ignited hydrogen produces very little radiant energy. The burning of hydrogen also produces neither poisonous emissions nor sooty particles (Busby, 2005). This suppose an advantage over other conventional fuels, such as gasoline, whose combustion by-products can be lethal, since the radiant heat, smoke and hot soot reach far beyond the flame. On the other hand, because hydrogen burns with an almost invisible blue flame, special flame detectors are needed. In conclusion, hydrogen can be as safe as other fuels used today with the proper handlings and controls.

Regarding safety standards, these are lacking for the device under consideration due to its low TRL. However, standards from the fuel cell industry could be adapted. More information about these standards can be found at http://www.fuelcellstandards.com, a continuously-updated website to track global codes and standards that apply to hydrogen safety.

Safety measures should also be taken in case of spill of the electrolyte solution, if highly acidic or basic solutions are used. Ensuring the proper sealing of the device would be crucial to avoid leakage of the solution. Moreover, spill containment equipment should be install to avoid the damage of the ground were the device is placed. Besides, the personnel handling the device should wear personal protective equipment.

Finally, it should be highlighted that ensuring the safety of the first commercial devices is of special importance, since any incident could harm the social acceptance of this technology. A catastrophic incident could mean an impediment for this technology to be successfully penetration of the market.

8

Discussion of results

This chapter provides a discussion on the way the selected design fulfils the established design criteria. Moreover, recommendations for further improvement of the device will be provided and parameters that still need more research are highlighted.

Technical criteria

The first and most important parameter that was set is the 15% **solar-to-hydrogen (STH) efficiency**. This efficiency has been reached in the laboratory scale (Khaselev, 2001; Licht, 2001), although expensive III-V semiconductor absorbers and noble metal catalysts were used. So far, efficiencies in the order of 5 – 10% have been reached using low cost and earth abundant materials and a lot of research effort has been focused on achieving even higher efficiencies (Han, 2014; Kelly, 2006; Urbain, 2014; Wang, 2013). It seems thus realistic that in the upcoming years 15% efficiency could be achieved using low cost and earth-abundant materials.

In this design project, multi-junction Si-based semiconductors have been selected as a promising option for a photo-electrode material. Current laboratory-scale devices based on Si photo-electrodes have reached STH efficiencies close to 10% (Urbain, 2014). The record efficiency of commercial PV modules using this type of thin films is 13.4% (Green, 2015). Therefore, 15% efficiency cannot be ensured yet, and further optimization of the multi-junction semiconductor should be done to improve its efficiency.

A **lifetime** of 15 years has been set as design criteria for a commercial device, which is the current lifetime of Polymer electrolyte membrane (PEM) electrolysers (Auprêtre, 2013). This is a very optimistic target for the first PEC devices, since laboratory-scale devices have proven a lifetime in the range of hours. However, it is important from the economical and sustainability point of view that the lifetime of the PEC devices is in this time range. The main reason for the short lifetime of current lab devices is the poor stability of catalysts or semiconductor materials in contact with the electrolytic solution. This is why the use of protective layers, such as metallic layer, was proposed for the final design. Even though the presence of a semiconductor-liquid junction has been the essence of PEC devices studied in many laboratories, having a “buried junction” seems the most plausible way to increase the stability of the device.

The stability tests performed in the laboratory usually consist of measuring the photocurrent generated under constant illumination (Ager, 2015). It is recommended that stability is also tested under variations of conditions such as light/dark cycles (simulating day/night), by measuring no only the photocurrent but also the hydrogen and oxygen generated.

Regarding the **operating conditions**, it has been assumed in this design project that the cell works under room temperature and atmospheric pressure. However, these parameters should be optimized to improve the efficiency of the device, and to reduce the energy consumed in a posterior compression step. PEM electrolysers work at about 15 bar, and 60 ^{o}C. Since this technology is already commercially available, and it has been investigated and optimized for many years, a good approach would be to investigate the performance

of the PEC cell under similar conditions.

The **hydrogen and oxygen evolution rates**, as well as the **water consumption rate**, depend on the photocurrent generated by the device. Since the efficiency of the device is still unknown, it is not straight forward to predict these values. An estimation of these criteria was done assuming 15% STH efficiency and 1 sun light intensity (1 kW/m^2). However, real light conditions will greatly differ from 1 sun. For a better understanding of the hydrogen and oxygen output from a PEC device, the actual concentration of evolved gases should be measured, together with the photocurrent density, for different light intensities, and preferably under real sunlight.

The maximum **allowable losses** on the system were estimated as 0.9 V, assuming that the device would produce about 2.2 V, while 1.23 V are needed for the water splitting reaction. If a higher voltage could be obtained, the allowable losses could be higher as well. The criteria for the different losses predicted in the PEC device have been achieved as follows:

a) The over-potentials at the electrodes surfaces depend on the catalyst material. The proposed materials are Ni-Mo for the hydrogen evolution catalyst with 0.1 V over-potential, and Ni for the oxygen evolution catalyst, with 0.4 V over-potential. These materials, in theory, should fulfil the requirement of 0.6 V. It should be noted that the over-potentials would depend on the current density and the operating conditions. Therefore, it is highly recommended to test the materials under real operating conditions.
b) The losses due to bubbles have not been quantified due to the lack of information. However, measures to minimize these losses have been proposed, knowingly, the flow of the electrolyte that enhances the removal of the bubbles from the system.
c) Positioning the electrodes facing each other, at a short distance, has minimized the Ohmic losses due to the transport of ions through the electrolyte and the membrane. If a distance of 2 mm is kept between the electrodes, and the thickness of the membrane is of 500 µm, the losses would be in the order of 35 mV. However, it should be considered that besides the path length, other parameters influence the magnitude of the Ohmic losses, such as the conductivity and the pH of the electrolytic solution, the conductivity and thickness of the membrane, and the generated current. For this preliminary analysis, the conductivity of the solution and the membrane was considered 14 S/m and 4.2 S/m respectively, and the photocurrent 122 A/m^2.
d) The main electric losses would come from the transport of electrons through the transparent conductive oxide. These losses has been minimized by the placement of a “grid” of metal contacts, separated 2 cm from each other, leading to losses of about 80 mV. It should be noted that these losses depend also on the current density and the thickness of the transparent conducting oxide TCO layer.

Regarding the **light losses**, a target of 10% was set, as 8% is already loss through the glass window. The goal was to eliminate any other component that could absorb or reflect light, reducing the transmittance towards the semiconductor photo-absorber. By selecting a device design that is based on a back-illuminated photo-electrode only losses from the glass cover and the front metal contacts are incurred. If the metal contacts are spaced 2 cm, and they are 1mm tick, 5% of the light would be lost. Together with the 8 % loss, due to the absorbance of the glass window, the total light losses result in 13%. This value could be reduced by, for example, using a thinner glass. However, this is not recommended because it would affect the mechanical stability of the window. Another way of reducing these losses would be by placing less and more separated front metal contacts, at expenses of higher losses due to sheet resistance.

A summary of the technical criteria discussed here is shown in the following table.

Table 18. Technical parameters established as design criteria

Design parameter	Value	Fulfilled?
η_{STH} (%)	15%	Expected from research
Lifetime	15 years	X ✓ (with protective layer)
Photocurrent density	122 A/m^2	Depending on irradiation and efficiency
Operating temperature	293 – 360 K	✓
Operating pressure	1 – 20 bar	✓
Solar irradiation	50 – 1000 W/m^2	Not studied
Hydrogen evolution rate	0.63 mmol/s m^2	Depending on irradiation
Oxygen evolution rate	0.32 mmol/s m^2	Depending on irradiation
Water consumption rate	0.63 mmol/s m^2	Depending on irradiation
R_{total}	< 0.9 V	✓
$R_{anode}+R_{cathode}$	< 0.6 V	✓
$R_{bubble,O2}+R_{bubble,H2}$	< 0.05 V	Achievable with flow
$R_{electrolyte}+R_{membrane}$	< 0.15 V	✓
$R_{electric}$	< 0.1 V	✓
Light losses	< 10 %	X (13%)

Economic criteria

The **capital cost** and the **operational expenditures** have been estimated for a plant with a capacity of 500 kg of H_2/day. The normalized capital cost was estimated as 71 \$/m^2, with **materials** (photo-electrode, membrane and counter electrode) accounting for 70% of the cost (i.e. 50 \$/m^2). Both values are therefore within the target set as criteria (Table 19). On the other hand, the operating cost estimation resulted in 43 \$/m^2. The cost of labour is that major contributor to the operating cost (about 65%). For smaller, localized facilities with no need for operating labour, security staff, panel control and laboratory analyst, the cost could be below 16 \$/m^2 per year.

The levelized **cost of hydrogen** was estimated as 5,66 \$/m^2, meeting the cost target of <6 \$/m^2. This cost represents the selling price of H_2 at which the net present value is 0 at the end of the plant lifetime with an interest rate of return of 10%. Therefore, the investor would get the investment back with additional 10%, while the plant will not give any profit. If hydrogen was sold for 10 \$/kg, as the current hydrogen refuelling stations in Germany (IPHE, 2013), the plant would be very profitable, with a **payback time** of 4 years and an internal rate of return of 40 %. However, if hydrogen was sold at 6 \$/kg, as the target set (Parkinson & Turner, 2013), the payback time would be of 13 years. The target payback time of 7 years could be achieved with prices of hydrogen below 7 \$/kg.

Table 19. Economic parameters established as design criteria

Design parameter	Value	Fulfilled?
Capital cost PEC cell	< 180 $/m^2	✓
Cost of materials	< 120 $/m^2	✓
Operating cost PEC cell	< 16 $/year/m^2	X With labour ✓ Without labour
Cost of hydrogen	< 6 $/kg	✓
Payback time	< 7 years	✓ If < 7 $/kg X If > 7 $/kg

This preliminary economic analysis showed that the selected design would be commercially viable and even has the potential of competing with PV + electrolysis as a solar-to-hydrogen technology. However, care should be taken regarding the results of this analysis due to the large amount of uncertainties at this stage of the technological development. Many assumptions have been made to come up with these numbers (see chapter 6). For example, it has been assumed that all the solar light can be converted into hydrogen with the same efficiency. This will not be true under actual working conditions, since it is possible that at low light intensity the device does not provide enough voltage to split water. The lower capacity of hydrogen production per m^2 per year would lead to larger areas needed, increasing the cost of the plant.

Moreover, the cost of storing hydrogen has not been considered. In a more in depth analysis, the variations on production throughout the year due to variation on solar irradiation, as well as the variation on demand, would allow for an estimation of the size of storage needed.

It should be pointed out that in the analysis it is assumed that oxygen will be released to the atmosphere. However, oxygen is a valuable product with many different applications (refer to Appendix D). Especially for the first commercial devices, it would be of interest to sell the generated oxygen as well. A study by Kato *et al.* (2005) showed the potential of selling oxygen, produced by electrolysis, for medical purposes in Japan. The price of oxygen in Japan widely varies, from 0.60 to 25 US$ per kg. Taking a price within this range, for example 5 $/kg, considering the plant studied with a capacity of 500 kg H_2/day, 4,000 kg of oxygen would be produced per day, potentially leading to a revenue of 7.2 M$/year from the oxygen sales. Certainly, selling oxygen for medical purposes could bring economic benefits, allowing for a lower selling price of hydrogen and thus promoting a *hydrogen economy*. A more detailed analysis should therefore consider as well as the cost of compressing, storing and transporting oxygen, to understand the potential benefit.

Furthermore, the implementation of a 1 axis solar tracking could lead to an increment of light harvesting of 40% (Luque and Hegedus, 2011). The impact of the capital and maintenance cost of such system should be also analysed.

Sustainability criteria

The **recyclability** of each of the separated components was studied, and it was concluded that it would be possible to meet the criteria of recycling 90% of the components. Moreover, all the proposed materials are **earth abundant**.

The energy consumed in manufacturing the PEC device was estimated, and the time that would take to recover that energy (**energy payback time**, EPBT) was calculated. A device with 15% STH efficiency placed in a location with high solar insolation (2.4 MWh/year) would have an estimated EPBT lower than 1.5 years. However, this could be as high as 5.5 years if the device has an efficiency of 10% and was located in an area

with an insolation of 900 MWh/m^2 per year (like the Netherlands).

If the energy of the compressor was also considered, the operating energy would be of 77 MJ/m^2 per year. Assuming a lifetime of 15 years, the total energy involved in operating the device is 1.2 GJ/m^2 (161 kg CO_2 eq.). This would affect the EPBT of devices with low efficiency (~5%), increasing this value in about 1-2 more years, but it would barely affect the EPBT of devices with higher efficiencies.

The **leakage of H_2** has not been estimated, as a more detailed design should be provided (including sealing materials) for this estimation. It is encouraged to measure this parameter when a prototype device is built, and to minimize the leakage of hydrogen due to it high global warming potential (GWP).

Table 20. Environmental parameters established as design criteria

Design parameter	Value	Fulfilled?
% of recyclable materials	> 90%	✓
Availability of materials	Earth abundant	✓
Energy payback time (EPBT)	< 2 years	Depends on location and efficiency
H_2 leakage	< 1 wt%	Not considered

Safety criteria

The main concern is the **gas crossover**, which can lead to the formation of flammable gas mixtures. The designed device includes an ion exchange membrane that would, in principle, avoid the gas crossover. Since current laboratory-scale devices do not have a membrane, the gas separation is an uncertain parameter. Nevertheless, from PEM electrolysis technology we can predict that it will be indeed possible to maintain the gas crossover within safe concentrations.

Table 21. Safety parameters established as design criteria

Design parameter	Value	Fulfilled?
% H_2 in O_2 stream	<< 4 vol.%	✓ (with use of membrane)
% O_2 in H_2 stream	<< 6 vol.%	✓ (with use of membrane)

9

Conclusions

This report described a *Conceptual Design of an Industrial-Scale Artificial Leaf Device*. The goal of the design project was to deliver a design of a PEC water-splitting device that could be manufactured at industrial-scale.

First of all, a market analysis was performed to understand the commercial opportunities for the artificial leaf technology (see chapter 3). Besides the large potential of this technology for producing fuel for a future hydrogen-based economy, many other market niches were identified that would allow for the commercialization of the early prototype-like devices. After evaluating the identified market opportunities with a SWOT analysis and evaluation matrix, it was concluded that the use of this technology in stand-alone power systems has the most potential for implementation in 2020. The main reason for this is that such off-grid power systems are employed in areas where electrification is very complex and expensive (such as islands or mountains). Therefore, the expected higher cost of hydrogen will not be a large impediment in this market segment. Moreover, most common stand-alone power systems rely on fossil fuels, and the artificial leaf could provide the advantage of complete energy autonomy. Another application for the stand-alone power systems based on the artificial leaf technology are Universities, due to their openness to innovation and their environmental awareness. Two case studies were developed to further investigate the two market opportunities in more detail, showing the feasibility of off-grid power generation plants composed by solar panels and PEC devices with reasonable use of land.

Once the market was analysed and it was clear that there would be many opportunities for the PEC devices to succeed in the market, the design of the device was made. For this purpose, it is important to understand the scientific background behind this technology (see chapter 1 for a detailed description). Understanding the technology helped identifying the main design challenges: (a) the need of finding efficient, durable, low-cost and earth-abundant semiconductors and catalysts, (b) the separation of the evolved gases in a reliable way to ensure the safety of the device, (c) the optimization of the components size and relative positioning to minimize internal losses and enhance light absorption, and (d) the optimum operating conditions. These challenges, described in chapter 4, were analysed in order to set the design criteria for a device that could be functional, economically attractive, sustainable and safe.

A literature search on available designs for large-scale PEC devices was performed and, together with individual and group creativity sessions, many design alternatives were created and identified. To facilitate the design selection, a step-wise methodology was applied consisting of different levels going from more general to more detailed characteristics of the design. Four design levels were completed, with increasing detail in the design:

- A first design level was used to identify the most promising type of reactor. A planar electrodes based reactor without solar concentrator was selected as the best reactor type due to the higher development of this type of devices and the possibility of implementing highly developed manufacturing technologies used in the photovoltaic industry.

- A second design stage aimed to select the configuration of such planar electrodes based reactor. Different relative positioning of electrodes were considered, and a faced electrodes configuration was selected. This configuration has the potential for providing very low Ohmic losses due to ion transport, easy manufacturing and high inherent safety.
- The third design stage went into more detailed design of the device, defining the position of the components with respect to the incoming light. The design selected was a back-illuminated photo-electrode with a metal counter electrode.
- The forth design stage was focused on defining materials that have the potential to provide a sustainable and economic device. It was concluded that amorphous Si-based is a promising low-cost and earth-abundant material that could make an efficient photocathode. The low stability in water of this material was solve by the use of a protection layer. The material proposed for this layer is Ni-Mo, as it can catalyse the hydrogen evolution reaction providing a low overpotential. Ni-based counter electrode was selected for oxygen evolution. This material selection would work under alkaline conditions. Nevertheless, the selected device offers flexibility in terms of materials selection, and thus new material developments could be easily implemented.

A possible manufacturing route for the envisioned device has been described, using well-developed techniques for the deposition of the multi-junction photoelectrode, namely sputtering and low pressure chemical vapour deposition. Other components such as the membrane and the counter electrode are commercially available and could be obtained from different providers. Moreover, a possible operation of a hydrogen production plant based on the designed PEC device has been proposed. A pump will be used to induce a flow of the electrolyte in the device in order to enhance the gas removal and reduce losses due to coverage of the electrodes' surface by the bubbles. The gases will be separated from the electrolyte by density difference in a gas-liquid separator tank, and they will be compressed to be stored is pressure.

An economic analysis was performed to estimate the profitability of a hydrogen production plant based on the PEC device designed. Although there are many uncertainties in the cost estimation of the PEC device due to the current low technology readiness level of the technology, this analysis allows to identify potential show-stoppers. A plant with a capacity of 500 kg H_2/day located in New Mexico (US), with a solar irradiation of 6.5 kWh/m^2/day, was used for the analysis. The analysis lead to a capital cost of a PEC reactor of about 70 \$/m^2 and a total investment cost of about 108 \$/m^2, taking into account land, gas conditioning and other indirect costs. The operating cost was estimated to be 43 \$/m^2, being the labour cost the highest expenditure (65%). With these values, a levelized cost of hydrogen was estimated as 5.66 \$/kg H_2, which falls within the cost target set as <6 \$/kg H_2. A sensitivity analysis showed that parameters such as the location of the plant and the efficiency of the cell could vary this cost. For example, if the plant was located in a place with a daily irradiation of 3.2 kWh/m^2, like the Netherlands, the cost of hydrogen would increase by 40%.

An important requirement for any energy conversion equipment is that the energy invested in the device manufacturing is recovered during its lifetime. It was estimated that the energy payback time of the device could range from 1.5 to 5.5 years, depending on the assumed efficiency and location, which is indeed lower than the expected lifetime of the device (15 years). Moreover, the environmental impact of the PEC device designed was also investigated by performing a cradle-to-grave life cycle assessment (LCA). It was concluded that the device would have a beneficial environmental impact, with savings of 2.5 ton CO_2 eq. emissions per m^2 of device during its full lifetime.

Lastly, the safety of the device has been analysed. For a safe operation of the PEC device, it should be ensured that hydrogen and oxygen are collected separately, without contamination of the other gas. In the designed device, an ion exchange membrane is used for this purpose. Moreover, proper sealing of the device is important to avoid leakage of hydrogen to the atmosphere. Nevertheless, since the device will be operated outdoors and hydrogen has a very high volatility, it is believed that potential leakage of the evolved gases does not constitute a major safety concern.

It is concluded that the *conceptual design* of a PEC water-splitting device presented in this design report has the potential of succeeding in the market, providing a safe and environmental friendly process for hydrogen production. A subsequent *detailed design* should be performed on the operating conditions and the flow management inside the device, since these will affect the performance of the device. A deeper study on the effect of temperature, pressure and sun intensity is needed to understand how the device would operate under real conditions. In the study of these parameters, not only the efficiency of the device should be considered, but also the gas crossover through the membrane, since safety should always be a priority when further designing the PEC water-splitting device. Later on, engineering design should be done on how to interconnect the modules (and the optimum size of these) to make a large-scale facility. With respect to laboratory research, this should focus on improvement of the materials stability, including semiconductors, catalysts and membranes, which currently constitute the biggest impediment for the commercial implementation of the artificial leaf technology.

References

Abdi, F. F., Han, L., Smets, A. H., Zeman, M., Dam, B., & van de Krol, R. (2013). Efficient solar water splitting by enhanced charge separation in a bismuth vanadate-silicon tandem photoelectrode. *Nature communications*, *4*.

Abdi, F. F. (2013) *Towards highly efficient bias-free solar water splitting* (Doctoral dissertation). Retrieved from Delft University of Technology repository. (ISBN 978-90-6464-693-5)

Addonizio, M. L., & Diletto, C. (2008). Doping influence on intrinsic stress and carrier mobility of LP-MOCVD-deposited ZnO: B thin films. *Solar Energy Materials and Solar Cells*, *92*(11), 1488-1494.

Ager, J. W., Shaner, M., Walczak, K., Sharp, I. D., & Ardo, S. (2015). Experimental Demonstrations of Spontaneous, Solar-Driven Photoelectrochemical Water Splitting. *Energy & Environmental Science*.

Ainscough C., Peterson D., Miller E. (2014) Hydrogen Production Cost From PEM Electrolysis. *DOE Hydrogen and Fuel Cells Program Record*. Retrieved from http://www.hydrogen.energy.gov/pdfs/14004_h2_production_cost_pem_electrolysis.pdf

AnglianWater (2011) Water efficiency self-assessment guide from anflianwater. Retrieved on July 23th 2015 from: http://www.anglianwater.co.uk/_assets/media/Water-Efficiency-Self-Assessment.pdf

Aquastat (2015) *Water resources sheet – Somalia*. Food and Agriculture Organization of the United Nations. Retrieved on 24th of July 2015 from: http://www.fao.org/nr/water/aquastat/data/wrs/readPdf.html?f=SOM-WRS_eng.pdf

Arkema Inc. (2000) *Plexiglass® Optical & Transmission Characteristics*. Retrieved from: http://www.plexiglas.com/export/sites/plexiglas/.content/medias/downloads/sheet-docs/plexiglas-optical-and-transmission-characteristics.pdf

Arges, C. G., Ramani, V., & Pintauro, P. N. (2010). Anion exchange membrane fuel cells. *Electrochemical Society Interface*, 31.

Aroutiounian, V. M., Arakelyan, V. M., & Shahnazaryan, G. E. (2005). Metal oxide photoelectrodes for hydrogen generation using solar radiation-driven water splitting. *Solar Energy*, *78*(5), 581-592.

Asselbergs, C.J., (2013) The Chemical Investment Decision. *28th Course in Techno-economic evaluation in the process industry at Delft University of Technology (Netherlands)*.

Auprêtre, F. (2013) *Technology roadmap and lifetime expectations in PEM electrolysis*. International workshop on durability and degradation issues in PEM electrolysis and its components. Freiburg, Germany. Retrieved from: http://www.sintef.no/globalassets/project/novel/pdf/1-4_ceth2_auprete_public.pdf

Ball, M., & Wietschel, M. (Eds.). (2009). *The hydrogen economy: opportunities and challenges*. Cambridge University Press.

Berger, A., Segalman, R. A., & Newman, J. (2014). Material requirements for membrane separators in a water-splitting photoelectrochemical cell. *Energy & Environmental Science*, *7*(4), 1468-1476.

Busby, R. L. (2005). *Hydrogen and fuel cells: a comprehensive guide*. PennWell Books.

Carmo, M., Fritz, D. L., Mergel, J., & Stolten, D. (2013). A comprehensive review on PEM water electrolysis. *International Journal of Hydrogen Energy*,*38*(12), 4901-4934.

Central Intelligence Agency (2015) *The World Fact Book*. Retrieved on 20th of July 2015 from: https://www.cia.gov/library/publications/the-world-factbook/

Chen, Z., Jaramillo, T. F., Deutsch, T. G., Kleiman-Shwarsctein, A., Forman, A. J., Gaillard, N., ... & Dinh, H. N. (2010). Accelerating materials development for photoelectrochemical hydrogen production: Standards for methods, definitions, and reporting protocols. *Journal of Materials Research*, *25*(01), 3-16.

Chen, Y., Xiang, C., Hu, S., & Lewis, N. S. (2014). Modeling the Performance of an Integrated Photoelectrolysis System with 10× Solar Concentrators.*Journal of The Electrochemical Society*, *161*(10), F1101-F1110.

Chen, Y., Hu, S., Xiang, C., & Lewis, N. (2014). A Sensitivity Analysis to Assess the Relative Importance of Improvements in Electrocatalysts, Light Absorbers, and System Geometry on the Efficiency of Solar-Fuels Generators. *Energy & Environmental Science*.

Chen, Y., Sun, K., Audesirk, H., Xiang, C., & Lewis, N. S. (2015). A quantitative analysis of the efficiency of solar-driven water-splitting device designs based on tandem photoabsorbers patterned with islands of metallic electrocatalysts. *Energy & Environmental Science*.

Corakci, B., Donato, N., Garcia, J.P., Nonclercq, A., Reddy, S., Victoria, M., (2014) *Conceptual Artificial Leaf Design*. Delft University of Technology, Delft, Netherlands.

Darling, H. E. (1964). Conductivity of Sulfuric Acid Solutions. *Journal of Chemical & Engineering Data*, *9*(3), 421-426.

Dawar, A. L., Jain, A. K., & Jagadish, C. (1995). *Semiconducting transparent thin films* (p. 181). Bristol, UK, Philadelphia, PA: Institute of Physics Pub..

Delahoy, A. E., Guo, S., (2011) *Transparent Conducting Oxides for Photovoltaics*. In A. Luque and S. Hegedus (Eds.) *Handbook of Photovoltaic Science and Engineering, Second Edition* (pp.716-796). John Wiley & Sons.

Deng, X., & Xu, L. (2010). *U.S. Patent No. 7,750,234*. Washington, DC: U.S. Patent and Trademark Office.

Deng, X., & Xu, L. (2005). *U.S. Patent Application 10/589,691*..

Derwent, R., Simmonds, P., O'Doherty, S., Manning, A., Collins, W., & Stevenson, D. (2006). Global environmental impacts of the hydrogen economy. *International Journal of Nuclear Hydrogen Production and Applications*, *1*(1), 57-67.

DOE (2014) *Hydrogen Production Cost from PEC Electrolysis*. DOE Hydrogen and Fuel Cells Program Record 14004. Retrieved from http://www.hydrogen.energy.gov/pdfs/14004_h2_production_cost_pem_electrolysis.pdf

EPA (1999). *Wastes from the Combustion of Fossil Fuels. Volume 2 – Methods, Findings and Recommendations*. United States Environmental Protection Agency. Washington, DC. Retrieved from http://www.epa.gov/osw/nonhaz/industrial/special/fossil/volume_2.pdf

European Commission (2006). *World Energy technology Outlook 2050 – WETO H2* (EUR Publication No. 22038). Luxembourg: Office for Official Publications of the European Communities. Retrieved from http://ec.europa.eu/research/energy/pdf/weto-h2_en.pdf

Fan, Q., Onischak, M., Liss, W. E., (2007). Solar Cell Electrolysis of Water to make Hydrogen and Oxygen. Patent US7241950 B2.

Faraj, M., Boccia, M., Miller, H., Martini, F., Borsacchi, S., Geppi, M., & Pucci, A. (2012). New LDPE based anion-exchange membranes for alkaline solid polymeric electrolyte water electrolysis. *international journal of hydrogen energy*, *37*(20), 14992-15002.

FAO (2015). *Water from the clouds*. Retrieved on 11th of March 2015 from: http://www.fao.org/nr/water/aquastat/infographics/Clouds_eng.pdf

Fraunhofer, I. S. E. (2013). Levelized Cost of Electricity-Renewable Energy Technologies. Retrieved from: http://www.ise.fraunhofer.de/en/publications/veroeffentlichungen-pdf-dateien-en/studien-und-konzeptpapiere/study-levelized-cost-of-electricity-renewable-energies.pdf

Fumatech (2015). *Technical Datasheet - Fumasep® FAA-3-PK-130*. Retrieved from: http://www.fumatech.com/NR/rdonlyres/54DEE07B-8674-49E4-BF70-709129051185/0/fumasepFAA3PK130.pdf

Godula-Jopek, A. (2015). *Hydrogen Production: By Electrolysis*. John Wiley & Sons.

Graedel, T. E., Allwood, J., Birat, J. P., Buchert, M., Hagelüken, C., Reck, B. K., ... & Sonnemann, G. (2011). What do we know about metal recycling rates?. *Journal of Industrial Ecology*, *15*(3), 355-366.

Green, M. A., Emery, K., Hishikawa, Y., Warta, W., & Dunlop, E. D. (2015). Solar cell efficiency tables (Version 45). *Progress in photovoltaics: research and applications*, *23*(1), 1-9.

Grievink, J., Swinkels, P.L.J. (2014). Chapter 4 in: *Delft template for Conceptual Design Process Plants*. Teaching document for Advanced Design course ST6064, at TU Delft.

Guillet, N., Millet, P., (2015). *Alkaline water electrolysis*. In A. Goula-Jopek, (Ed.), *Hydrogen production by electrolysis* (pp. 117-166).Wiley-VCH, Germany.

Han, L., Abdi, F. F., van de Krol, R., Liu, R., Huang, Z., Lewerenz, H. J., ... & Smets, A. H. (2014). Efficient Water-Splitting Device Based on a Bismuth Vanadate Photoanode and Thin-Film Silicon Solar Cells. *ChemSusChem*, *7*(10), 2832-2838.

Han, L., Digdaya, I. A., Buijs, T. W., Abdi, F. F., Huang, Z., Liu, R., ... & Smets, A. H. (2015). Gradient dopant profiling and spectral utilization of monolithic thin-film silicon photoelectrochemical tandem devices for solar water splitting. *Journal of Materials Chemistry A*, *3*(8), 4155-4162.

Haussener, S., Xiang, C., Spurgeon, J. M., Ardo, S., Lewis, N. S., & Weber, A. Z. (2012). Modeling, simulation, and design criteria for photoelectrochemical water-splitting systems. *Energy & Environmental Science*, *5*(12), 9922-9935.

Haussener, S., Hu, S., Xiang, C., Weber, A. Z., & Lewis, N. S. (2013). Simulations of the irradiation and temperature dependence of the efficiency of tandem photoelectrochemical water-splitting systems. *Energy & Environmental Science*, *6*(12), 3605-3618.

Hernández, S., Tortello, M., Sacco, A., Quaglio, M., Meyer, T., Bianco, S., ... & Tresso, E. (2014). New transparent laser-drilled fluorine-doped tin oxide covered quartz electrodes for photo-electrochemical water splitting. *Electrochimica Acta*, *131*, 184-194.

HSE (2015). *Nickel and you*. *Working with Nickel – are you at risk?*. Health and Safety Executive. Retrieved from: http://www.hse.gov.uk/pubns/indg351.pdf

HyWays (2008). *The European Hydrogen Energy Roadmap*. European Commission. Retrieved from http://www.hyways.de/docs/Brochures_and_Flyers/HyWays_Roadmap_FINAL_22FEB2008.pdf

Idemat (2015) Life Cycle Analysis inventory database. Retrieved from: http://www.ecocostsvalue.com/EVR/model/theory/5-data.html

IEA (2012). Total carbon dioxide emissions from the consumption of energy. Retrieved from http://www.eia.gov/cfapps/ipdbproject/iedindex3.cfm?tid=90&pid=44&aid=8&cid=ww,&syid=2008&eyid=2012&unit=MMTCD

IEA (2014). *Key World Energy Statistics*. International Energy Agency. Retrieved from http://www.iea.org/publications/freepublications/publication/KeyWorld2014.pdf

IEA (2015). Factors Affecting Electricity Prices. Retrieved July 20, 2015, from http://www.eia.gov/energyexplained/index.cfm?page=electricity_factors_affecting_prices

IPEX (2009) *PVC Chemical Resistance Guide*. IPEX. Ontario, Canada.

IPHE (2013). Workshop on commercial – ready hydrogen refuelling stations. Design and social acceptance. International Partnership for Hydrogen and Fuel Cells in the Economy. November 19, 2013. Retrieved from: http://www.a3ps.at/site/sites/default/files/newsletter/2014/no8/Workshop%20on%20Commercial-ReadyHRS%20Japan.pdf

Jacobsson, T. J., Fjällström, V., Sahlberg, M., Edoff, M., & Edvinsson, T. (2013). A monolithic device for solar water splitting based on series interconnected thin film absorbers reaching over 10% solar-to-hydrogen efficiency. *Energy & Environmental Science*, *6*(12), 3676-3683.

James, B. D., Baum, G. N., Perez, J., Baum, K. N., & Square, O. V. (2009). Technoeconomic analysis of photoelectrochemical (PEC) hydrogen production. *Directed Technologies Inc., Department of Energy contract GS-10F-009J technical report*. Retrieved from http://www1.eere.energy.gov/hydrogenandfuelcells/pdfs/pec_technoeconomic_analysis.pdf

James, B. D., & Spisak, A. B. (2012). Mass Production Cost Estimation of Direct H2 PEM Fuel Cell Systems for Transportation Applications: 2012 Update. *report by Strategic Analysis, Inc., under Award Number DEEE0005236 for the US Department of Energy*, *18*.

Jang, J. W., Du, C., Ye, Y., Lin, Y., Yao, X., Thorne, J., ... & Wang, D. (2015). Enabling unassisted solar water splitting by iron oxide and silicon. *Nature communications*, *6*.

Jeng, K. T., Liu, Y. C., Leu, Y. F., Zeng, Y. Z., Chung, J. C., & Wei, T. Y. (2010). Membrane electrode assembly-based photoelectrochemical cell for hydrogen generation. *international journal of hydrogen energy*, *35*(20), 10890-10897.

Kato, T., Kubota, M., Kobayashi, N., & Suzuoki, Y. (2005). Effective utilization of by-product oxygen from electrolysis hydrogen production. *Energy*, *30*(14), 2580-2595.

Keeping, S. (2012). Techniques to Limit Switching DC/DC Converter Inefficiency During Low Loads. Retrieved from http://www.digikey.com/en/articles/techzone/2012/jul/techniques-to-limit-switching-dcdc-converter-inefficiency-during-low-loads

Kelly, N. A., & Gibson, T. L. (2006). Design and characterization of a robust photoelectrochemical device to generate hydrogen using solar water splitting. *International Journal of hydrogen energy*, *31*(12), 1658-1673.

Khaselev, O., Bansal, A., & Turner, J. A. (2001). High-efficiency integrated multijunction photovoltaic/electrolysis systems for hydrogen production. *International Journal of Hydrogen Energy*, *26*(2), 127-132.

Kim, H. C., & Fthenakis, V. M. (2011). Comparative life-cycle energy payback analysis of multi-junction a-SiGe and nanocrystalline/a-Si modules. *Progress in Photovoltaics: Research and Applications*, *19*(2), 228-239.

Krueger, L. (1999). *Overview of First Solar's Module Collection and Recycling Program*. Retrieved on 21st of July from: https://www.bnl.gov/pv/files/PRS_Agenda/2_Krueger_IEEE-Presentation-Final.pdf

Larminie, J., Dicks, A., & McDonald, M. S. (2003). *Fuel cell systems explained*(Vol. 2). New York: Wiley.

Lewerenz, H.J. ; Peter, L. (2013). *Photoelectrochemical Water Splitting : Materials, Processes and Architectures*. Royal Society of Chemistry. Retrieved from http://www.eblib.com

Licht, S., Wang, B., Mukerji, S., Soga, T., Umeno, M., & Tributsch, H. (2001). Over 18% solar energy conversion to generation of hydrogen fuel; theory and experiment for efficient solar water splitting. *International Journal of Hydrogen Energy*, *26*(7), 653-659.

Lin, C. Y., Lai, Y. H., Mersch, D., & Reisner, E. (2012). Cu 2 O| NiO x nanocomposite as an inexpensive photocathode in photoelectrochemical water splitting. *Chemical Science*, *3*(12), 3482-3487.

Liu, H., Avrutin, V., Izyumskaya, N., Özgür, Ü., & Morkoç, H. (2010). Transparent conducting oxides for electrode applications in light emitting and absorbing devices. *Superlattices and Microstructures*, *48*(5), 458-484.

Liu, R., Zheng, Z., Spurgeon, J., & Yang, X. (2014). Enhanced photoelectrochemical water-splitting performance of semiconductors by surface passivation layers. *Energy & Environmental Science*, *7*(8), 2504-2517.

Lopes, T., Dias, P., Andrade, L., & Mendes, A. (2014). An innovative photoelectrochemical lab device for solar water splitting. *Solar Energy Materials and Solar Cells*, *128*, 399-410.

Luo, J., Im, J. H., Mayer, M. T., Schreier, M., Nazeeruddin, M. K., Park, N. G., ... & Grätzel, M. (2014). Water photolysis at 12.3% efficiency via perovskite photovoltaics and Earth-abundant catalysts. *Science*, *345*(6204), 1593-1596.

Luque, A., & Hegedus, S. (2011). *Handbook of photovoltaic science and engineering*. John Wiley & Sons.

Lymberopoulos, N., & Zoulias, E. (2008). *Hydrogen-based autonomous power systems: techno-economic*

analysis of the integration of hydrogen in autonomous power systems. Springer.

McCarty, R. D., Hord, J., & Roder, H. M. (1981). *Selected properties of hydrogen (engineering design data)* (No. NBS-Mono-168). National Engineering Lab. (NBS), Boulder, CO (USA).

McCrory, C., Jung, S., Peters, J., & Jaramillo, T. (2013). Benchmarking Heterogeneous Electrocatalysts for the Oxygen Evolution Reaction. *Journal of the American Chemical Society*, 16977-16987.

McCrory, C. C., Jung, S., Ferrer, I. M., Chatman, S. M., Peters, J. C., & Jaramillo, T. F. (2015). Benchmarking Hydrogen Evolving Reaction and Oxygen Evolving Reaction Electrocatalysts for Solar Water Splitting Devices. *Journal of the American Chemical Society*, *137*(13), 4347-4357.

McKone, J. R., Warren, E. L., Bierman, M. J., Boettcher, S. W., Brunschwig, B. S., Lewis, N. S., & Gray, H. B. (2011). Evaluation of Pt, Ni, and Ni–Mo electrocatalysts for hydrogen evolution on crystalline Si electrodes. *Energy & Environmental Science*, *4*(9), 3573-3583.

Membranes International Inc. (2015). *Material Safety Data Sheet AMI-7001S/AMI-7001CR Anion Exchange Membranes*. Retrieved from: http://www.membranesinternational.com/pdfs/tech-ami_msds.pdf

Merle, G., Wessling, M., & Nijmeijer, K. (2011). Anion exchange membranes for alkaline fuel cells: A review. *Journal of Membrane Science*, *377*(1), 1-35.

Miller, E. L., Rocheleau, R. E., & Deng, X. M. (2003). Design considerations for a hybrid amorphous silicon/photoelectrochemical multijunction cell for hydrogen production. *International Journal of Hydrogen Energy*, *28*(6), 615-623.

Modestino, M. A., Diaz-Botia, C. A., Haussener, S., Gomez-Sjoberg, R., Ager, J. W., & Segalman, R. A. (2013). Integrated microfluidic test-bed for energy conversion devices. *Physical Chemistry Chemical Physics*, *15*(19), 7050-7054.

Mueller-Langer, F., Tzimas, E., Kaltschmitt, M., & Peteves, S. (2007). Techno-economic assessment of hydrogen production processes for the hydrogen economy for the short and medium term. *International Journal of Hydrogen Energy*, *32*(16), 3797-3810.

Müller, J., Rech, B., Springer, J., & Vanecek, M. (2004). TCO and light trapping in silicon thin film solar cells. *Solar Energy*, *77*(6), 917-930.

Nagai, N., Takeuchi, M., Kimura, T., & Oka, T. (2003). Existence of optimum space between electrodes on hydrogen production by water electrolysis. *International journal of hydrogen energy*, *28*(1), 35-41.

Nass, L. I. (1992). *Encyclopedia of PVC: Compounding Processes, Product Design, and Specifications-Volume 3 of 4 (Print)* (Vol. 3). CRC Press.

NREL (2009) *Current State-of-the-Art Hydrogen Production Cost Estimate Using Water Electrolysis*. U.S. Department of Energy. Golden, Colorado.

Parkinson, B., Turner, J., (2013). The potential Contribution of Photoelectrochemistry in the Global Energy Future. In Lewerenz, H.J. & Peter, L. (Ed.), *Photoelectrochemical Water Splitting : Materials, Processes and Architectures* (pp.1-17)Royal Society of Chemistry. Retrieved from http://www.eblib.com

Peters, M. S., Timmerhaus, K. D., West, R. E., Timmerhaus, K., & West, R. (1968). *Plant design and*

economics for chemical engineers (Vol. 4). New York: McGraw-Hill.

Pinaud, B. A., Benck, J. D., Seitz, L. C., Forman, A. J., Chen, Z., Deutsch, T. G., ... & Jaramillo, T. F. (2013). Technical and economic feasibility of centralized facilities for solar hydrogen production via photocatalysis and photoelectrochemistry. *Energy & Environmental Science*, *6*(7), 1983-2002.

Pletcher, D., Li, X., & Wang, S. (2012). A comparison of cathodes for zero gap alkaline water electrolysers for hydrogen production. *international journal of hydrogen energy*, *37*(9), 7429-7435.

Reece, S. Y., Hamel, J. A., Sung, K., Jarvi, T. D., Esswein, A. J., Pijpers, J. J., & Nocera, D. G. (2011). Wireless solar water splitting using silicon-based semiconductors and earth-abundant catalysts. *Science*, *334*(6056), 645-648.

Santos, D. M., Sequeira, C. A., & Figueiredo, J. L. (2013). Hydrogen production by alkaline water electrolysis. *Química Nova*, *36*(8), 1176-1193.

Sasaki, Y., Kato, H., & Kudo, A. (2013). [Co (bpy) 3] 3+/2+ and [Co (phen) 3] 3+/2+ electron mediators for overall water splitting under sunlight irradiation using Z-scheme photocatalyst system. *Journal of the American Chemical Society*, *135*(14), 5441-5449.

Schiff, E. A., Hegedus, S., Deng, X., (2011). *Amorphous Silicon-based Solar Cells*. In A. Luque and S. Hegedus (Eds.) *Handbook of Photovoltaic Science and Engineering*, *Second Edition* (pp.716-796). John Wiley & Sons.

Seger, B., Castelli, I. E., Vesborg, P. C., Jacobsen, K. W., Hansen, O., & Chorkendorff, I. (2014). 2-Photon tandem device for water splitting: comparing photocathode first versus photoanode first designs. *Energy & Environmental Science*, *7*(8), 2397-2413.

Shockley, W., & Queisser, H. J. (1961). Detailed balance limit of efficiency of p-n junction solar cells. *Journal of applied physics*, *32*(3), 510-519.

Singh, M. R., Papadantonakis, K., Xiang, C., & Lewis, N. S. (2015). An electrochemical engineering assessment of the operational conditions and constraints for solar-driven water-splitting systems at near-neutral pH. *Energy & Environmental Science*.

Smith, D. L. (1995). *Thin-film deposition: principles and practice* (Vol. 108). New York etc: McGraw-hill.

Sørensen, B. (2012). *Hydrogen and fuel cells: emerging technologies and applications*. Academic Press.

Tassoul, M. (2009). *Creative facilitation* (3rd ed.). Delft, Netherlands: VSSD.

The Glosten Associates, (2010). *Sodium Hydroxide (NaOH) Practicality Study*. Seattle, Washington. Retrieved from http://yosemite.epa.gov/sab/sabproduct.nsf/953CCBEB820F047085257792007631 6D/$File/NaOH+Practicality+Study.pdf

The World Bank (2015). *Access to electricity (% of population)*. Retrieved on 20th of July 2015 from: http://data.worldbank.org/indicator/EG.ELC.ACCS.ZS

TU Delft Energy Monitor – Measures at the Sports Division (n.d.). Accessed 21 of December 2014. Retrieved from http://www.energymonitor.tudelft.nl/Building/Details?objectCode=37__GM_TOT

Urbain, F., Smirnov, V., Becker, J. P., Rau, U., Finger, F., Ziegler, J., ... & Jaegermann, W. (2014). a-Si: H/μc-Si: H tandem junction based photocathodes with high open-circuit voltage for efficient hydrogen production. *Journal of materials research*, *29*(22), 2605-2614.

USDA (2014). Land values 2014 summary. *USDA, National Agricultural Statistics Service*. *Retrieved from http://www.nass.usda.gov/Publications/Todays_Reports/reports/land0814.pdf*

U.S. Department of Labor (2015). *May 2014 National Occupational Employment and Wage Estimates*. Retrieved July 20, 2015, from http://www.bls.gov/oes/current/oes_nat.htm

van de Krol, R., & Grätzel, M. (2011). *Photoelectrochemical hydrogen production* (Vol. 102). Springer.

Walter, M. G., Warren, E. L., McKone, J. R., Boettcher, S. W., Mi, Q., Santori, E. A., & Lewis, N. S. (2010). Solar water splitting cells. *Chemical reviews*,*110*(11), 6446-6473.

Wang, X., Peng, K. Q., Hu, Y., Zhang, F. Q., Hu, B., Li, L., ... & Lee, S. T. (2013). Silicon/Hematite core/shell nanowire array decorated with gold nanoparticles for unbiased solar water oxidation. *Nano letters*, *14*(1), 18-23.

Webb, A. (2015). *German Wind-to-Hydrogen Plant Takes Car-Fuel Battle to Tesla*.

WHO (2005) *Climate and health*. *Fact sheet*. World Health Organization. Retrieved from http://www.who.int/globalchange/news/fsclimandhealth/en/index.html

Xing, Z., Zong, X., Pan, J., & Wang, L. (2013). On the engineering part of solar hydrogen production from water splitting: photoreactor design. *Chemical Engineering Science*, *104*, 125-146.

Xu, H. F., Wang, X., Shao, Z. G., & Hsing, I. M. (2002). Recycling and regeneration of used perfluorosulfonic membranes for polymer electrolyte fuel cells. *Journal of applied electrochemistry*, *32*(12), 1337-1340.

Xu, L. (2014) *Critical Research for Cost-Effective Photoelectrochemical Production of Hydrogen*. Retrieved from http://www.hydrogen.energy.gov/pdfs/review14/pd056_xu_2014_p.pdf

Zoulias, E. I., & Lymberopoulos, N. (2007). Techno-economic analysis of the integration of hydrogen energy technologies in renewable energy-based stand-alone power systems. *Renewable Energy*, *32*(4), 680-696.

Zweibel, K. (2000). Thin film PV manufacturing: Materials costs and their optimization. *Solar energy materials and solar cells*, *63*(4), 375-386.

APPENDICES

Appendix A – Scientific background

Electrolysis is a process of dissociating water (H_2O) into hydrogen (H_2) and oxygen (O_2) gas. Such process occurs in an electrochemical cell, where two electrodes are placed in an electrolyte solution. In the cell, reduction and oxidation reactions simultaneously take place, forming H_2 at the cathode and O_2 at the anode. The electrolyte is a solution that behaves as an electrically conductive medium. *Photoelectrolysis* is a type of electrolysis, which is carried out by the direct use of light. A photoelectrochemical (PEC) cell is used to perform this process. The cell is comprised of a semiconductor that absorbs solar energy and generates the necessary voltage to split water molecules. Photoelectrolysis integrates solar energy utilization and water electrolysis into a single photoelectrode and is considered a promising renewable method of hydrogen production.

A scheme of a photo-electrochemical (PEC) cell is shown in Figure 40. The cell shown in this figure is composed by a single photoanode and a metal counter electrode. More complicated configurations that involve various semiconductors have been also developed (Haussener, 2012; Khaselev, 2001; Lopes, 2014).

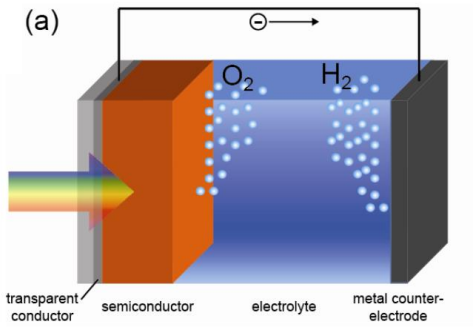

Figure 40. Illustration of photoelectrolysis (Abdi, 2013)

The main component of a PEC cell is the semiconductor, whose function is to convert incident photons into electron-hole pairs. These electrons and holes are then spatially separated from each other due to the presence of an electric field inside the semiconductor. The photogenerated holes travel toward the semiconductor/electrolyte interface, where they oxidize water to form oxygen gas. At the same time, the electrons move towards the back contact and are transported via a wire to the metal counter-electrode where they reduce water to form hydrogen. Gas evolution occurs based on the following half reactions at the surface of photoanode and cathode (van de Krol & Grätzel, 2011):

(In an acidic electrolyte)

$4h^+ + 2\,H_2O \rightarrow O_2 + 4H^+ \quad [E^0_{ox} = -1.229\,V]$ Reaction at the anode

$4e^- + 4H^+ \rightarrow 2H_2 \quad [E^0_{red} = +0.000\,V]$ Reaction at the cathode

(In an alkaline electrolyte)

$4e^- + 4\,H_2O \rightarrow 2H_2 + 4OH^- \quad [E^0_{red} = -0.828\,V]$ Reaction at the cathode

$4h^+ + 4OH^- \rightarrow O_2 + 2H_2O \quad [E^0_{ox} = -0.401\,V]$ Reaction at the anode

Therefore, the net reaction is:

$2H_2O \rightarrow 2H_2 + O_2$

At a neutral pH, all reactions above occur and contribute to the water-splitting. The ions generated at one electrode need to travel to the counter electrode to complete the overall reaction. The resistivity of the medium will affect the ion transport. Since water has a very low conductivity, an electrolyte is needed to facilitate the transport of the ions.

The simplified energy diagram of the described PEC cell is shown in Figure 41.

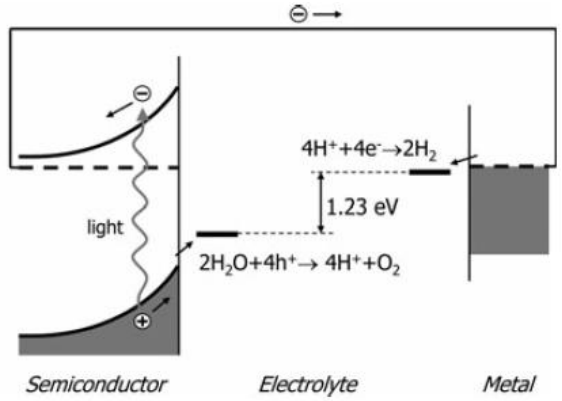

Figure 41. Energy diagram of a PEC cell consisting of a semiconducting photoanode and a metal cathode (van de Krol & Grätzel, 2011)

Appendix B – SWOT analysis

Appendix C – Mindmap of the artificial leaf

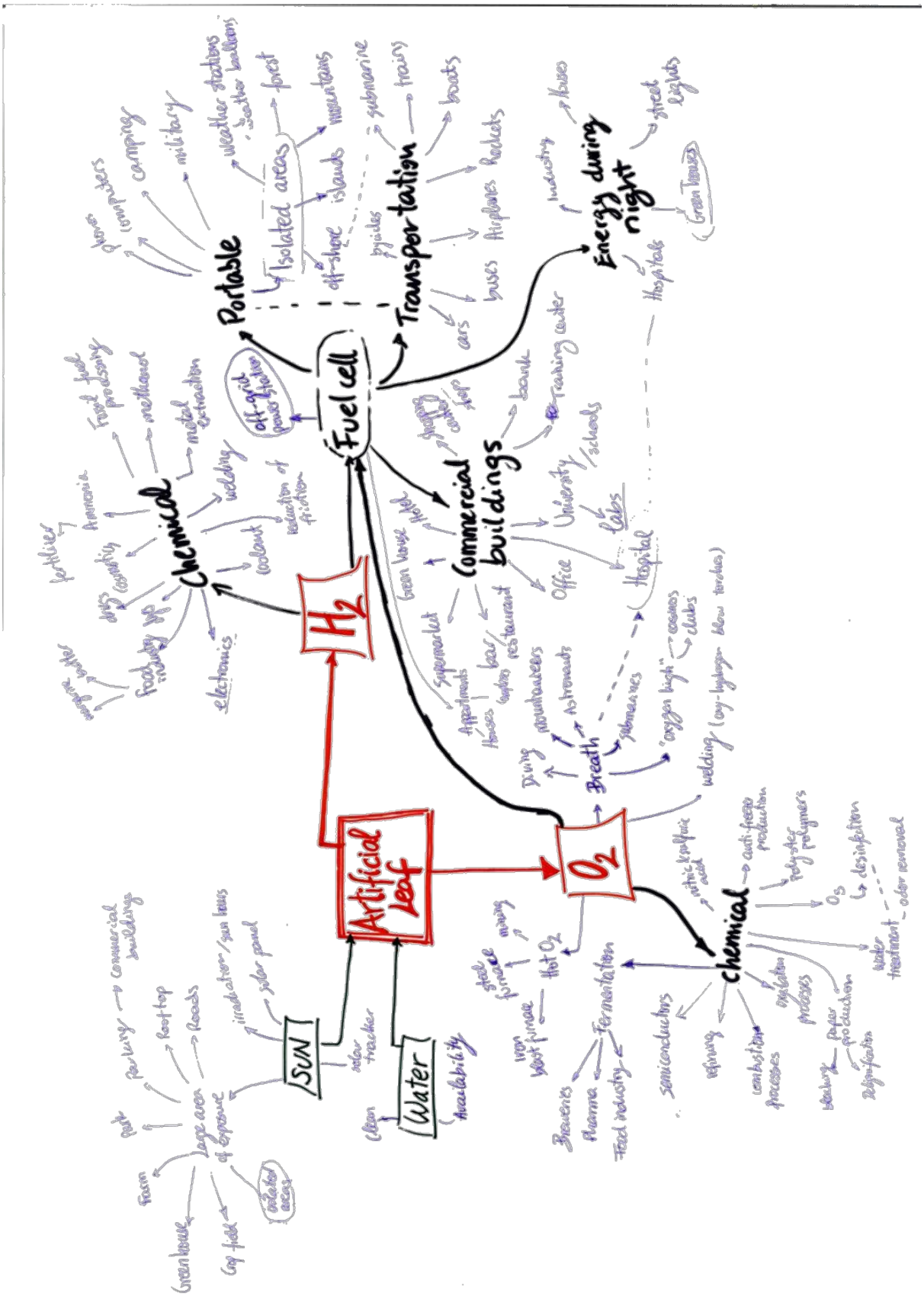

Appendix D – Ideas generated at the brainstorming session on market opportunities

Table 22. Ideas generated at the brainwriting session

H_2 as an energy carrier	H_2 use (no energy-related)
For transportation	For water purification
On the roof of a car	To inflate a balloon
On a parking (hospitals, offices…)	On a zeppelin
On a fuelling station	H2-zepelling to pull cargo boats
On a boat	For industrial hydrogenation reactions
On an offshore fuelling station for boats	In a farm, to produce ammonia (fertilizer)
On a harbour for fuelling boats	For CO2 decomposition
On a submarine	For welding
On a train	To cool down your drink on the beach
On a tram	H2+CH4 solar gas
On a helicopter	O_2 use
On a bike	For fermentation processes
For residential and commercial buildings	Wastewater treatment
On the roof of a house - Using water from rain - Using water from AC system	To produce O3 for water purification
On the roof of a commercial building	For medical purposes - On a hospital - In an ambulance - In elderly houses - For baby incubation
On a university	In a submarine (breathing)
On a sports stadium	For industrial oxidation processes
On a greenhouse	For mountaineering (breathing)
Other uses	On airplanes (breathing)
On a beach	H_2 and O_2 use
On the mountain	For diving (O_2 for breathing and H_2 for powering light)
On the desert (using condensed water)	For climbing (O_2 for breathing and H_2 for powering light)
At remote African villages	To explode mines
At the Antarctica stations	In concert halls (O_2 to the environment and H_2 for power)
On a back pack	To produce water
For camping	For desalination
For energy efficient cooking plates	For biofuels production
In the bottom of a cup of coffee	In a submarine (O_2 for breathing and H_2 for powering light)
Power supply for LEDs	For laboratories
Nearby hydroelectrical power stations	Algae production (O_2) and energy (H_2)
On the street lights	For burning (sewage, garbage, industrial waste)

On the side of the road, to power road lighting	To produce H_2O_2 - For bleaching - For rocket fuel
On an industrial site	To produce heat and warm up environments
On a large field (centralize facility)	Others
To power low power, long lasting devices (like clocks)	In vineyards
To charge a phone	In the curtains of offices and houses
As a back-up laptop battery	For terraforming
In an aquarium	For water removal
In a wind turbine (on the pole)	On mars
In a space station	On the moon
On the Dutch canals	

Appendix E – Stand-alone power systems based on PV and PEC panels – Case studies

1. Kythnos island case study

As mentioned previously, the artificial leaf technology could find a niche market as part of stand-alone power systems on an island. One of the main reasons is the difficult electrification of these locations, making the local electricity prices very high. Moreover, many islands are protected areas where diesel-based power generators are unwanted as they provide the potential to damage the ecosystem.

Zoulias *et al.* (2007) analysed the integration of hydrogen energy technologies (i.e. electrolysers and fuel cells) in a stand-alone power system for the Greek island of Kythnos (Figure 42), where currently there is an AC mini-grid composed of PV modules (8.8 kW ≡ 73 m^2), a battery bank and a small diesel generator (8 kW).

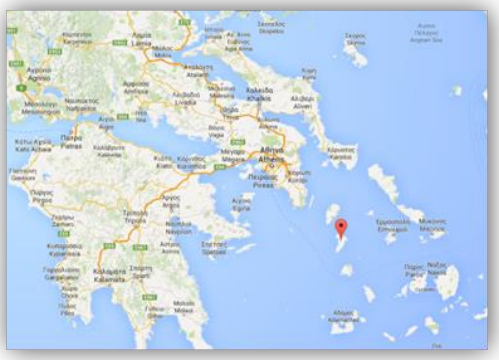

Figure 42. Location of Kythnos island, Greece (Google Maps)

This system powers a small community of 10 houses that are only populated during summertime. The problem with the current system is that during peak periods (summertime), the energy provided by the panels and the battery is not sufficient and the diesel generator is operated frequently (Figure 43). Here it is studied the possibility of replacing the diesel generator by PEC water-splitting devices that produce hydrogen and fuel cells that use this hydrogen to produce electricity.

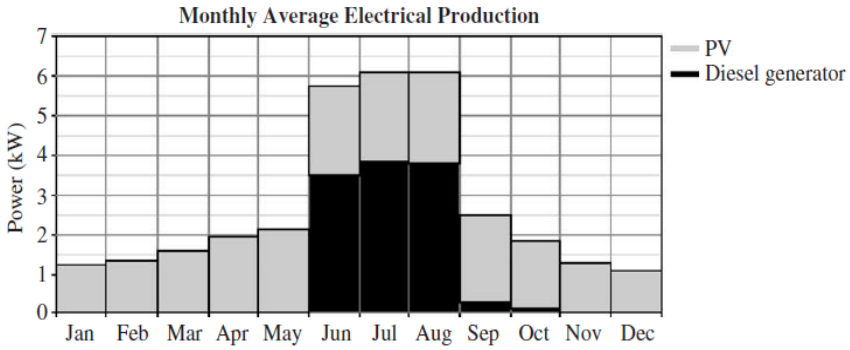

Figure 43. Monthly average production of electricity in the PV-diesel system at the Kythnos island (Zoulias, 2007)

For a first estimation, it was studied how much area of PEC panels should be installed to produce sufficient hydrogen to substitute the diesel generator. According to the study performed by Zoulias (2007), the diesel generator produces 8.6 MWh annually. Considering the efficiency of the compression and storage of hydrogen (85%), of the decompression (90%) and of the fuel cell (60%), the PEC panels should produce 18.6

MWh annually to supply the same electricity to the customers as the diesel generator. Using the data of the sun irradiation provided in Zoulias' study, it has been estimated that one m^2 of PEC panel with a STH efficiency of 15% would generate 263 kWh in a year (Table 23). Therefore, 71 m^2 of PEC panels could substitute the diesel generator.

Table 23. Energy production by the PEC cells

Solar resource		PEC		
Month	kWh/m^2day (*)	$E_{PEC\ (15\%\ eff)}$ (kWh/day)	E_{PEC} (kWh/m^2 month)	E_{PEC} 71m^2 (kWh/month)
Jan	2.2	0.33	10.23	726.33
Feb	2.7	0.41	11.34	805.14
Mar	4	0.60	18.60	1320.60
Apr	5.7	0.86	25.65	1821.15
May	6.7	1.01	31.16	2212.01
Jun	7.9	1.19	35.55	2524.05
Jul	7.7	1.16	35.81	2542.16
Aug	7	1.05	32.55	2311.05
Sep	5.5	0.83	24.75	1757.25
Oct	3.6	0.54	16.74	1188.54
Nov	2.5	0.38	11.25	798.75
Dec	2	0.30	9.30	660.30
		TOTAL	**262.92**	**18667.32**

(*) Zoulias, 2007

The storage capacity has been estimated according to the following formula:

$$E_{storage}(month_n) = E_{storage}(month_{n-1}) + E_{PEC}(month_n) - E_{Load}(month_n)$$

where

- $E_{storage}(month_n)$ is the energy (in kWh) available in the storage tank at the end of month *n*
- $E_{storage}(month_{n-1})$ is the energy (in kWh) available in the storage tank at the beginning of the month *n*, i.e. the energy at the storage tank at the end of the month *n-1*
- $E_{PEC}(month_n)$ is the energy (in kWh) produced during month *n*
- $E_{Load}(month_n)$ is the energy (in kWh) consumed during month *n*

Table 24. Calculation of the volume needed for hydrogen storage

	$E_{storage}(month_n)$ (kWh)	Kg of H_2	Moles of H_2	Volume of H_2 at 140bar and 21°C (m^3)
Oct	1188.54	36.02	36016.36	6.29
Nov	1987.29	60.22	60220.91	10.51
Dec	2647.59	80.23	80230.00	14.00
Jan	3373.92	102.24	102240.00	17.84
Feb	4179.06	126.64	126638.18	22.10
Mar	5499.66	166.66	166656.36	29.08
Apr	7320.81	221.84	221842.73	38.71
May	9532.82	288.87	288873.18	50.41
Jun	6476.87	196.27	196268.64	34.25
Jul	3439.02	104.21	104212.73	18.19
Aug	170.07	5.15	5153.64	0.90
Sept	67.32	2.04	2040.00	0.36

Assuming that the storage is empty at the beginning of October, the variation on the storage through the year was estimated (Figure 44). For these calculations it was assumed that 30% of the total 18.6 MWh that the PEC cells need to provide is consumed in each of the months June, July and August. The remaining 10% is consumed during September. This rough estimation is in accordance with the data provided in Figure 43.

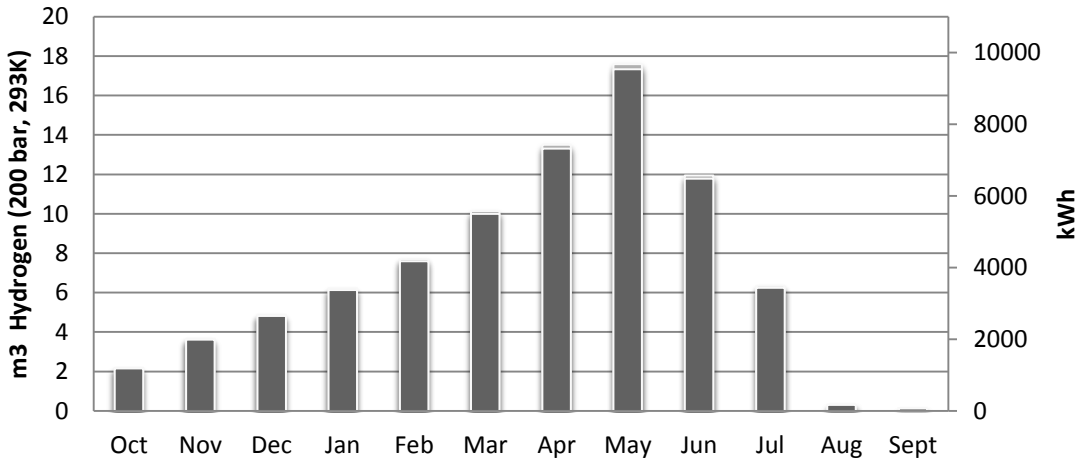

Figure 44. Energy available in the hydrogen storage tanks every month

It can be observed in Figure 44 that the hydrogen storage will be at its maximum level at the end of the month of May, previous to the summertime when the consumption will start. The capacity of the storage tank should have at least the size equivalent to this maximum level achieved in May. If compressed at 200 bars the maximum volume of hydrogen would be about 18 m^3.

In conclusion, this small community at the Greek island of Kythnos could be powered by a stand-alone power system that relies solely in the solar energy, by using a combination of 73 m^2 of solar panels and 71 m^2 of PEC modules.

2. TU Delft Sports Centre case study

Among the different buildings that compose the TU Delft campus, the sports division of the Sports & Cultural Centre is considered the best option for this case study. This building has been selected because, contrary to other faculty buildings, it is expected that a large portion of the electricity is consumed during the evening, when the outdoor fields have to be illuminated, and sun is not available for common solar panels to provide electricity. Moreover, this facility has a large surface area available for placing the PEC panels (see Figure 47).

The average daily electricity consumption at the Sports Centre for each month of 2014 was obtained from the *TU Delft energy monitor* website (http://www.energymonitor.tudelft.nl) (Table 25). Moreover, it is assumed in this case study that the electricity consumption will be decreased 30% by 2020 as demanded by University policy. These savings could be realised by the implementation of measures that include motion sensors in the sports halls and individuation of lighting of different outdoor courts (TU Delft Energy Monitor, 2014). With this assumption, the expected daily electricity consumption at the Sports Centre in 2020 is depicted in Figure 45. In the same graph, the daily radiation, obtained from the database of the Joint Research Centre of the European Commission (http://re.jrc.ec.europa.eu/pvgis/apps4/pvest.php) (Table 25), is also plotted. It can be observed that the months with higher radiation are also the ones with lower electricity consumption. This fact points out the convenience of storing solar energy, to use it in the months with lower radiation but higher electricity demand.

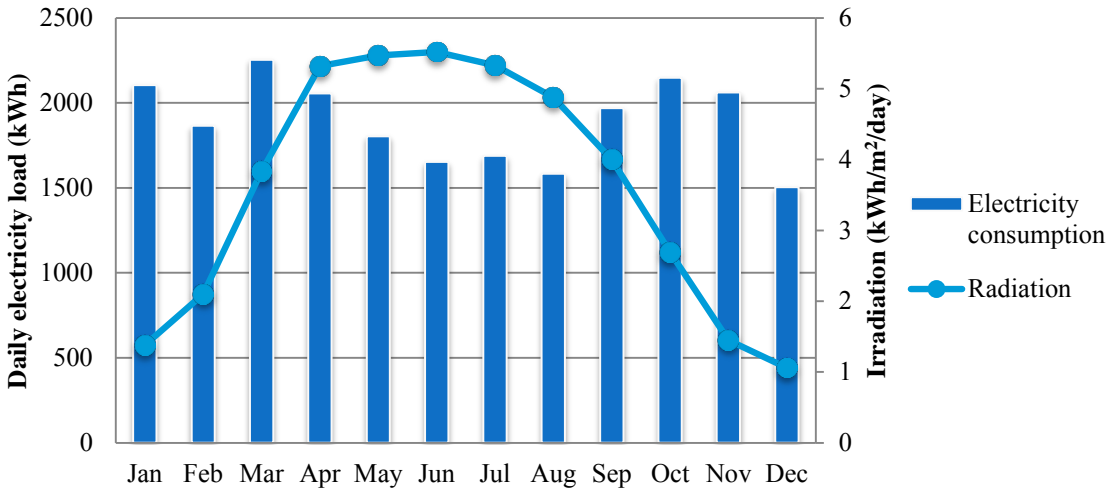

Figure 45. Average daily electricity consumption at the Sports Centre of TU Delft, assuming 30% reduction by 2020 (http://www.energymonitor.tudelft.nl/) and average daily irradiation in Delft (http://re.jrc.ec.europa.eu/pvgis/apps4/pvest.php)

Table 25. Irradiance and electricity consumption at the TU Delft sports centre in 2014, and the assumed consumption during day and night

Month	Irradiance* (Wh/m^2/day)	Electricity consumption** (MWh/month)	Daily average (kWh/day)	$E_{DemandDay}$ (kWh)	$E_{DemandNight}$ (kWh)
Jan	1.38	93.20	2104.61	841.84	1262.76
Feb	2.10	82.57	1864.49	745.80	1118.69
Mar	3.83	99.76	2252.75	1126.38	1126.38
Apr	5.32	91.04	2055.76	1027.88	1027.88
May	5.47	79.87	1803.52	901.76	901.76
Jun	5.52	73.18	1652.52	1322.01	330.50
Jul	5.33	74.72	1687.16	1518.44	168.72
Aug	4.88	70.05	1581.71	1423.54	158.17
Sep	4.00	87.20	1968.96	1575.17	393.79
Oct	2.69	95.06	2146.52	1073.26	1073.26
Nov	1.45	91.26	2060.64	1030.32	1030.32
Dec	1.06	66.54	1502.59	601.04	901.56

* From http://re.jrc.ec.europa.eu/pvgis/apps4/pvest.php

** From http://www.energymonitor.tudelft.nl

In order to find the best combination of PV and PEC panels, the amount of electricity consumed during sunlight hours and the one consumed during dark hours should be known. Since this information is not available in the website of the TU Delft Energy Monitor, an estimation was done according to the amount of hours of sun in the different months of year. For summer time, it was assumed that 80-90 % of the electricity is used while there is sunlight; for wintertime, it was assumed that only 40 % is consumed during the time that sun is available. The estimated demand during sunlight and dark hours for each month is shown in Table 25, and plotted in Figure 46. It should be noted that these rough estimations were necessary in order to understand the feasibility of powering the Sports Centre with a stand-alone power system that relies solely on the sun. For a more accurate system design, data of the electricity load and irradiation in an hourly basis should be used.

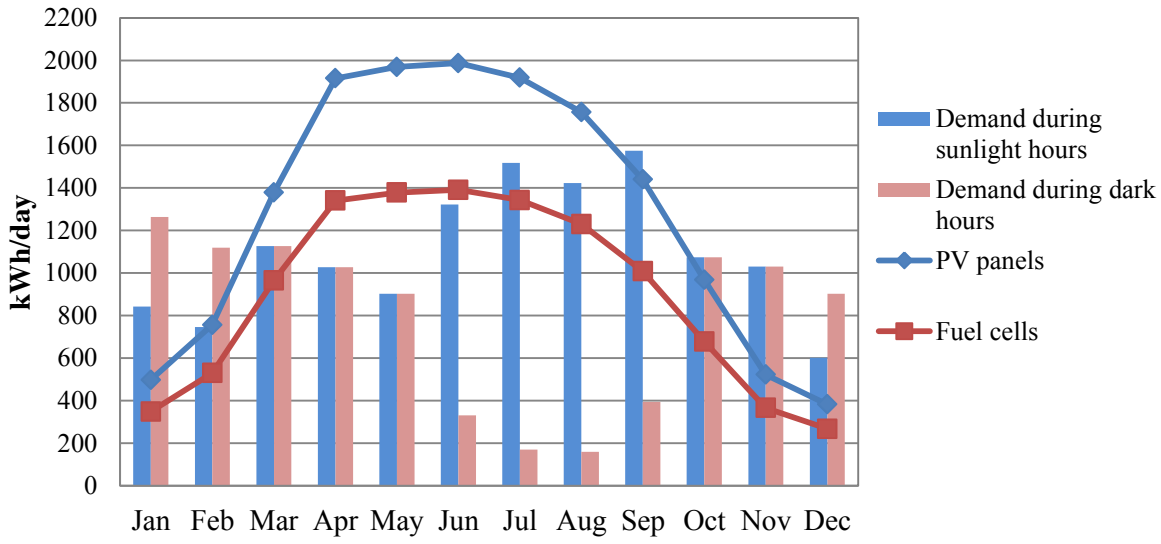

Figure 46. Electricity demand at the sports centre and supply provided by the PV panels and the fuel cells

Spreadsheet calculations (Table 26 and Table 27) showed that an area of PEC panels of 2,800 m^2 and 1,800 m^2 of PV panels would be needed to supply the electricity consumed in this building. Figure 46 shows the

electricity provided by the combination of PV panels, and PEC panels with fuel cells.

Table 26. Electricity provided by 1800m^2 the solar panels, used during sunlight hours

	E_{PV} [20% eff] (kWh/m2/day)	E_{PV} total [1800m^2] (kWh/day)	E_{PV} - $E_{DemandDay}$ (kWh/day)	Energy deficiency (kWh/month)
Jan	0.276	496.80	-345.04	-10696.32
Feb	0.420	756.00	10.20	-
Mar	0.766	1378.80	252.42	-
Apr	1.064	1915.20	887.32	-
May	1.094	1969.20	1067.44	-
Jun	1.104	1987.20	665.19	-
Jul	1.066	1918.80	400.36	-
Aug	0.976	1756.80	333.26	-
Sep	0.800	1440.00	-135.17	-4055.15
Oct	0.538	968.40	-104.86	-3250.60
Nov	0.290	522.00	-508.32	-15249.63
Dec	0.212	381.60	-219.44	-6802.55
Annual electricity total deficiency				**-40054.25**

Table 27. Electricity provided by the fuel cells, making use of the hydrogen produced by 2800m^2 of PEC modules

Month	E_{PEC} [15% eff] (kWh/m^2/day)	E_{PEC} total [2800m^2] (kWh/day)	E_{FC} [60% eff] (kWh/day)	E_{FC} - $E_{DemandNight}$ (kWh/day)	Energy deficiency/excess (kWh/month)
Jan	0.207	579.60	347.76	-915.00	-28365.12
Feb	0.315	882.00	529.20	-589.49	-16505.80
Mar	0.575	1608.60	965.16	-161.22	-4997.72
Apr	0.798	2234.40	1340.64	312.76	9382.73
May	0.821	2297.40	1378.44	476.68	14777.11
Jun	0.828	2318.40	1391.04	1060.54	31816.10
Jul	0.800	2238.60	1343.16	1174.44	36407.76
Aug	0.732	2049.60	1229.76	1071.59	33219.27
Sep	0.600	1680.00	1008.00	614.21	18426.21
Oct	0.404	1129.80	677.88	-395.38	-12256.72
Nov	0.218	609.00	365.40	-664.92	-19947.63
Dec	0.159	445.20	267.12	-634.44	-19667.51
Annual excess total electricity					**42288.68**

From February until September, the electricity provided by the solar panels covers the demand during the day. During the months from April until September, the PEC panels produce more hydrogen than the one used by the fuel cell to supply the demand of electricity during the night. The excess hydrogen will be stored and used when the PV and PEC panels cannot supply enough energy. Calculations showed that the annual deficiency of electricity supply by the PV panels (~40MWh) (Table 26), could be covered by the excess hydrogen produced (~42MWh) (Table 27).

Furthermore, it is necessary to look if the area needed for placing the PV and PEC modules (1,800 and 2,800 m^2, respectively) is available at the Sports Centre. Looking at the top view of the Sports Centre facilities, obtained in Google Maps®, an estimation of the surface area available for placing the panels was performed (Figure 47). In this figure, it can be observed that the 2,800 m^2 of PEC panels can be accommodated in the

areas marked in yellow. Notice that one of the areas is placed in the ground. This area could serve as a "showroom" to display this novel technology to the public, for education purposes and to attract attention of possible investors. On the other hand, the green areas in Figure 47 represent where the PV panels could be placed. Therefore, the area needed for placing the panels is indeed available in the building.

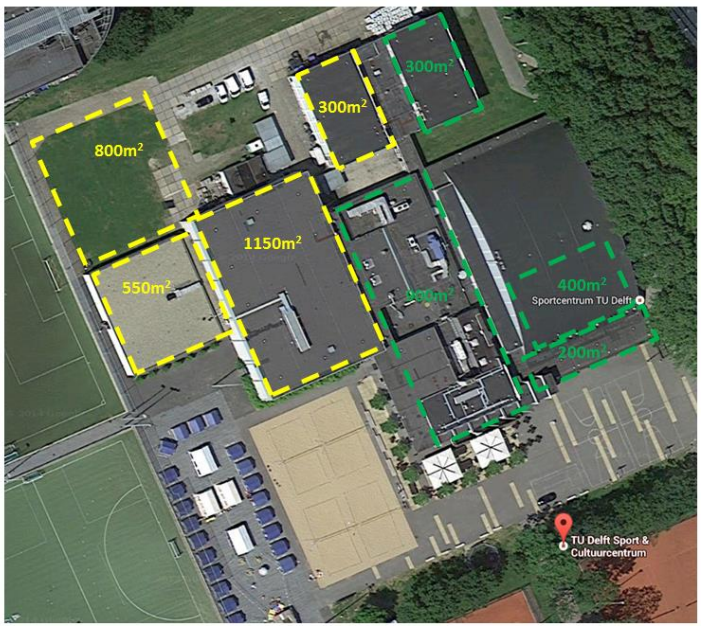

Figure 47. View of the sports centre from the top (Google Maps). In yellow, the area of the buildings envisioned to be covered by PEC cells. In green, the area envisioned to be covered by PV panels.

Appendix F – Hydrogen production technologies

Steam reforming of natural gas

More than half of the world hydrogen production is done using steam reforming of natural gas (Mueller-Langer, 2007). The basis of this process is the reaction of methane with steam at high temperature (700-1000°C) in the presence of a catalyst, which produces a mixture of H_2, CO and CO_2 and unreacted CH_4. In a following step, CO reacts with more steam producing additional hydrogen and CO_2 (this is the so-called *water gas shift reaction*). In a subsequent separation step, the CO_2 is removed from the shifted gas via chemical absorption, producing a hydrogen-rich gas which is further purified via pressure swing adsorption (PSA).

To avoid poisoning of the reforming catalyst, the small amounts of sulphur compounds that are present in the natural gas are previously removed by absorption on zinc oxide. The heat required for the steam reforming reaction is generated by the combustion of some natural gas and the *tail gas* (i.e. process waste gas) from the hydrogen purification step. A scheme of this process can be found in Figure 48.

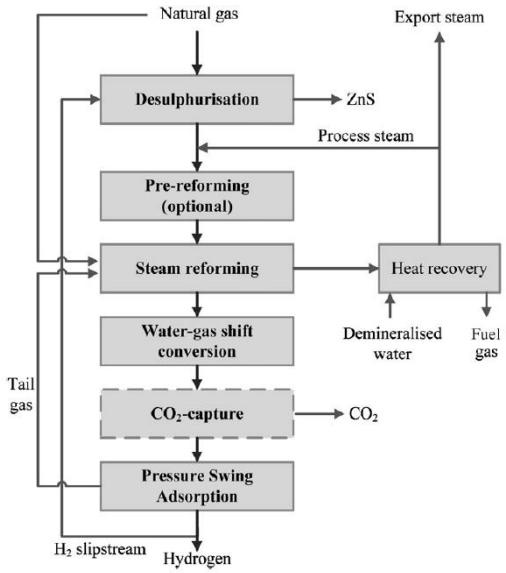

Figure 48. System components of steam reforming of natural gas (Mueller-Langer, 2007)

Large steam reforming plants have a capacity between 20,000 Nm^3/h and 350,000 Nm^3/h (approximately 1,800 kg/h and 31,500 kg/h, respectively), with fuel-to-hydrogen efficiencies in the range of 70-80 % (LHV). In the last years, progress has been made in developing cost-competitive small-scale steam reformers, which could be placed in refuelling stations (European Commission, 2007). Currently, small plants with capacity of 100-700 Nm^3/h are commercially available. However, these are purpose-designed plants and series production has not yet been established (European Commission, 2007). It should be noted that the CO_2 capture and storage from small-scale plants is not an economically viable option (Mueller-Langer, 2007), and therefore the CO_2 emissions from these small-scale plants will be difficult to avoid.

Coal gasification

Gasification of coal, also called partial oxidation, is a commercial technology for hydrogen production successfully implemented in regions with no access to natural gas. The process takes place in a gasifier, where pulverised coal reacts with steam at high temperature and pressure with controlled amounts of oxygen or air.

The products of this reaction are H_2 and CO along with CO_2, some CH_4 and residual steam. Moreover, impurities such as H_2S and carbonyl sulphide (COS) are present in the raw gas. The raw gas is then treated similarly to the steam reforming plant. Hydrogen-rich gas is produced by the water-shift reaction and it is further purified via pressure swing adsorption (PSA). Usually the waste gases from the PSA are used for power generation, to mitigate the heave electricity requirements of the plant.

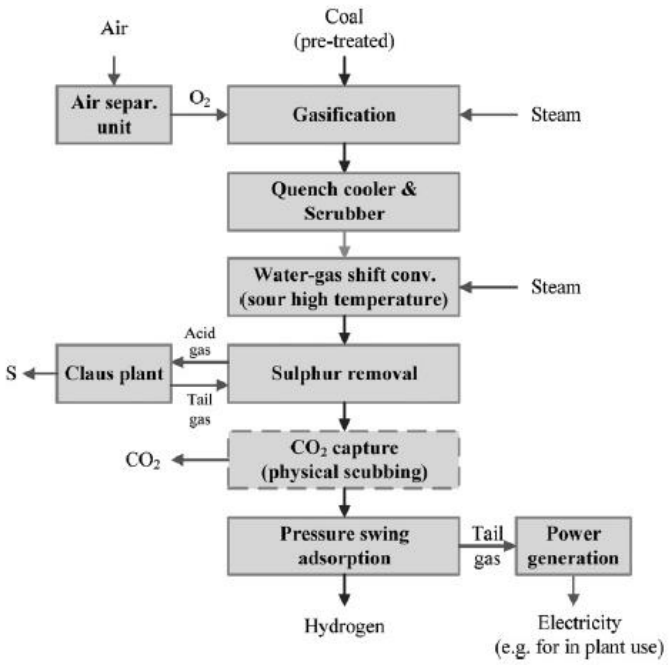

Figure 49. System components of gasification of coal (Mueller-Lange, 2007)

The large feedstock pre-treatment needed, the use of an air separation unit and the extensive multi-stage cleaning of raw syngas, make the hydrogen production process from coal gasification more complex when compared to steam reforming (Mueller-Lange, 2007). Because of this complexity, small-scale plants for hydrogen production are unattractive both economically and environmentally. Typical gasifier capacities are within the range of 20,000 and 100,000 Nm^3/h. Fuel-to-hydrogen efficiencies of this process are of the order of 55% (LHV) (Mueller-Lange, 2007).

Biomass gasification

Biomass can be gasified the same way as coal. However, biomass is a more complex and variable feedstock and therefore the process needs to be adapted accordingly (Figure 50). An advantage of the system is that a wide variety of biomass sources could be used, such as wood, straw and municipality solid waste. The use of the available feedstock in each region would avoid the long-distance transport of biomass, reducing the environmental impact and increasing the energy security of this process. However, the variety of biomass source also imposes a challenge: the adjustment of the process to the chemical and physical properties of the feedstock. Current biomass gasification systems are designed to produced raw gas for heat and power production, and no system is commercially available in Europe for hydrogen production (European Commission, 2007). Moreover, there is an ongoing debate regarding the reduction of land available for food production, due to land use for biomass grow for energy production. In Europe, biomass utilization for energy is currently focused on waste biomass and crops that can grow in locations on which food corps do not grow well.

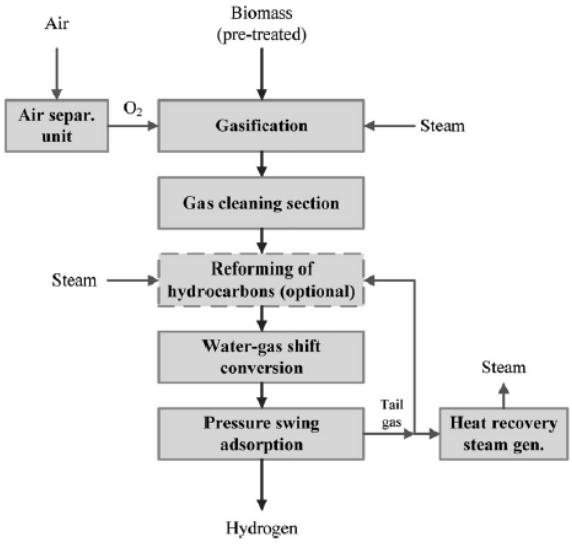

Figure 50. System components of biomass gasification (Mueller-Langer, 2007)

The reactors for gasification and the hot gas cleaning, together with other elements of this system, are still under development (Mueller-Langer, 2007). Beyond 2020, overall efficiencies of 65 % could be expected (European Commission, 2007).

Electrolysis of water

Electrolysis is the process of splitting water into hydrogen and oxygen by the use of an electric current. Two electrodes, namely cathode (where hydrogen is produced) and anode (where oxygen is produced), are the main component of the electrolysers. Electrolysis is easily scalable and the capacity of the commercially available units ranges from 250 Nm^3/h to 35,000 Nm^3/h (European Commission, 2007). Although electrolysis is a mature process, it only pays a minor role in Europe since the price of hydrogen is hampered by high electricity prices.

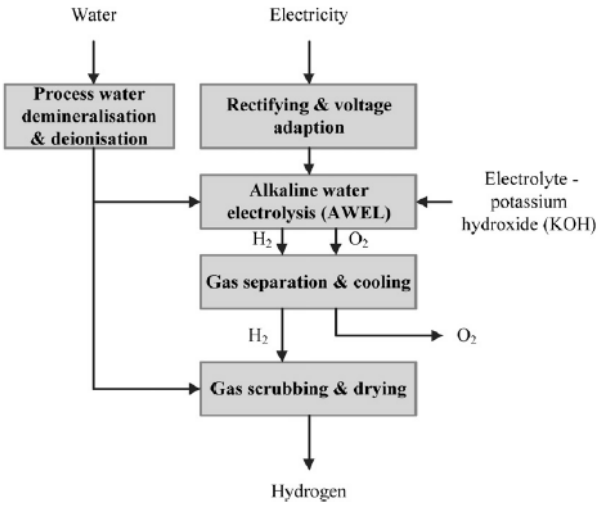

Figure 51. System components of alkaline water electrolysis (Mueller-Langer, 2007)

Appendix G – State-of-the-art electrolysers

In electrolysis, hydrogen is produced by passing a direct current through two electrodes immersed in water. Typical requirements for electrolysers include electricity to run the process and other peripheral equipment, cooling water for the hydrogen generation unit, pre-pressurization gas and inert gas (NREL, 2009). There are three types of low temperature industrial electrolysers: unipolar electrolyser, bipolar electrolyser, and polymer electrolyte electrolyser.

Alkaline electrolysers, the most common electrolysis units, can be either unipolar or bipolar. Alkaline electrolysers use an aqueous solution of 20-30% potassium hydroxide (KOH), which has a high conductivity and enhances the oxygen evolution reaction (Carmo, 2013).

A unipolar or *tank-type* electrolyser (Figure 52.a) consists of alternate positive and negative electrodes held apart by porous separators or diaphragm. The diaphragm keeps the products gases apart for the sake of efficiency and safety, and it is permeable to hydroxide ions and water molecules. This electrolyser design is a high-current, low-voltage system with all the anodes coupled together in parallel, as are the cathodes. The whole assembly is immersed in a single electrolyte bath forming a unit cell. The industrial-scale electrolyser is built by connecting these units electrically in series.

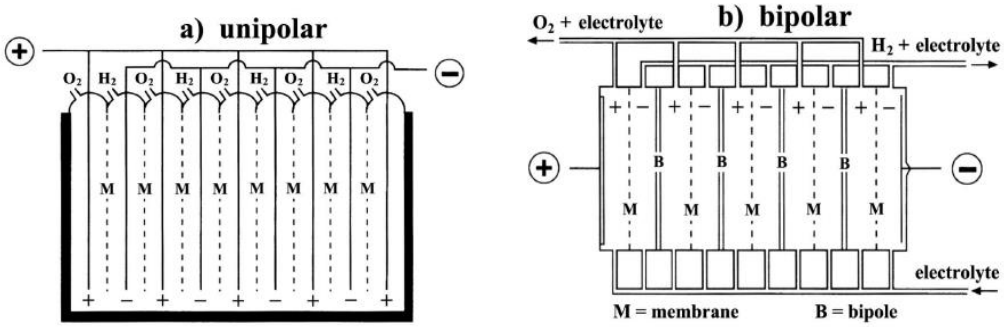

Figure 52. Electrolysis units with (a) unipolar and (b) bipolar cell configurations (Santos, 2013)

A bipolar electrolyser (Figure 52.b) consists of a metal sheet (or *bipole*) that connects electrically adjacent cells in series. In this electrolyser configuration the electrocatalyst for the cathode is coated on one face of the metal sheet and that for the anode of the adjacent cell is coated on the reverse face. A membrane is placed between the different electrodes to separate the gases. The biopolar electrolyser is a high-voltage, low current device. To build a large-scale electrolyser, the modules are connected in parallel in order to increase the current.

The unipolar configuration results in a simpler and easier to manufacture device. However, the higher electrical current at low voltages causes larger Ohmic losses (Santos, 2013). On the other hand, the bipolar configuration presents lower Ohmic losses. Nevertheless, its design and manufacturing requires more precision to prevent from electrolyte and gas leakage between cells. Most commercially available alkaline electrolysers use the bipolar design (NREL, 2009).

One issue associated with alkaline electrolysers is that the diaphragm does not completely prevent the product gases to cross-diffusing through it. This is particularly severe at low loads (<40%) (Carmo, 2013). The diffusion of oxygen into the cathode chamber reduces the efficiency of the electrolyser since oxygen can be catalysed back to water with the presence of hydrogen in the cathode side. Moreover, hydrogen could end in the oxygen output gas stream, reaching dangerous levels of gas mixture. Figure 53 shows the operating principle of an alkaline electrolyser.

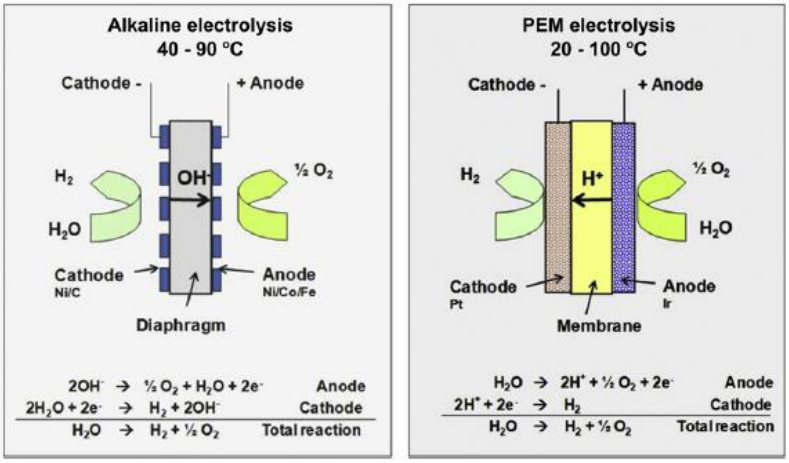

Figure 53. Operating principle of an alkaline and PEM water electrolysers (Carmo, 2013)

The gas crossover issue is solved in the third type of electrolysis units, namely *proton exchange membrane* or *polymer electrolyte membrane* (both with the acronym PEM) electrolyser, also referred to as *solid polymer electrolyte* (SPE) electrolyser (Figure 53). In this system, the electrolyte is a solid ion conductive membrane and the electrolyser is fed with pure water. Nafion® is the most commonly used membrane, and thus the PEM electrolysers work under acid environments. Therefore, significant precious metals loadings are used since they are the only practical option for stable catalysts in these environments (McCrory, 2015). PEM electrolysers are typically built in a bipolar configuration (Carmo, 2013). The state-of-the-art specifications of alkaline and PEM electrolysers are collected in Table 28.

Table 28. Specifications of state-of-the-art alkaline and PEM electrolysers (Carmo, 2013)

	Alkaline electrolyser	PEM electrolyser
Cell Temperature (°C)	60-80	50-80
Cell pressure (bar)	<30	<30
Current density (mA/cm^2)	0.2-0.4	0.6-2.0
Cell voltage (V)	1.8-2.4	1.8-2.2
Power density (mW/cm^2)	<1	<4.4
Voltage efficiency HHV (%)	62-82	67-82
Specific energy consumption: Stack (kWh/ Nm^3)	4.2-5.9	4.2-5.6
Specific energy consumption: System (kWh/ Nm^3)	4.5-7.0	4.5-7.5
Lower partial load rage (%)	20-40	0-10
Cell area (m^2)	>4	<0.03
H_2 production rate: Stack-System (Nm^3/h)	<760	<10
Lifetime stack (h)	<90,000	<20,000
Lifetime system (y)	20-30	10-20
Degradation rate (µV/h)	<3	<14

Appendix H – Design challenges for a commercial-scale artificial leaf

Photoelectrode Material

One challenge for the design of a large-scale PEC water-splitting device is that the suitable photoelectrode materials have yet to be found. Much research has been focused on finding a good semiconductor material that meets demanding requirements (van de Krol & Grätzel, 2011). First, the semiconductor material must absorb light efficiently and generate enough voltage to split water, and thus the charge transport within the semiconductor must be efficient. At the same time, the semiconductor interface must be favourable to sustain the hydrogen and oxygen evolution reactions. Moreover, the material needs to remain stable in solution, in order to provide a long lifetime of the device. Lastly, the material should be inexpensive so the device could be economically attractive for the market.

Despite recent advances in the field, researchers have not been able to find a single material that meets all these requirements. For example, devices based on III-V semiconductors have shown high conversion efficiencies (Khaselev, 2001; Licht, 2001). However, this class of semiconductors lacks stability and the cost of these materials is prohibitively expensive. Currently, multi-junction approaches seem to offer the best hope for achieving a photoelectrode with the desired properties. However, the use of photoelectrodes composed by multi-junctions of different semiconductors brings a challenge for manufacturing. If several materials are used to compose an efficient photoelectrode, they should preferably allow for a similar deposition process, so all the materials can be deposited in the same equipment; and each material should be stable at the deposition conditions of the subsequent materials. In this way, the complexity and cost of the photoelectrode manufacturing will be reduced.

Separation of Gasses

Another challenge is the separation of the gases evolved from the system. Since ions need to travel from one electrode to the other, it is not possible to use a fully impermeable barrier to avoid the gas crossover. For that reason, ion exchange membranes are a good candidate for gas separation, because they allow the transport of ions within the electrodes while keeping the gases apart. However, these membranes should also meet demanding requirements: (a) stability in the electrolyte; (b) high conductivity for the pertinent ions; (c) low permeability to gases; (d) good mechanical properties; (e) low cost; and, for some device configurations, (f) transparency. To date, no membrane is commercially available that meets all these requirements (Berger, 2014). The most developed and widely used ion exchange membrane is Nafion®, however, it is expensive and it is designed for acidic environments.

Bubble Removal

The gases evolved at the electrode surfaces form small bubbles that (a) grow, (b) detach from the surface and (c) rise to the top of the device where they are collected. Up to what extent the bubble accumulation at the electrode's surface affects the performance of the device is still unclear. In most experiments that are performed at laboratory-scale, a magnetic stirrer is used to promote the removal of the gases and therefore this effect is not as relevant as it could be at commercial-scale. Hence, it remains a challenge for the design to promote the removal of the bubbles from the electrode's surfaces in an efficient and economical way.

Spacing

The design should optimize the spacing between components. Especially the distance between the cathode and anode plays an important role in the performance of the system (Chen, 2014). The relation between distance and performance will be addressed by initial estimations shown in section 4.3. Moreover, the placement of the system components should maximize the light capturing by the photoelectrode. The final device should be such that it minimizes all the internal energy losses.

Operating Conditions

Furthermore, the optimum operating conditions of the large-scale device remain uncertain. On one hand, the operation conditions should favour the kinetics for the hydrogen and oxygen production reactions without affecting the performance of the semiconductor materials. Other factors such as the cost of heating up or pressurizing the system should be taken into account. In the laboratory-scale, most research is performed under room temperature and atmospheric pressure. However, working at higher pressure could have the benefit of lower cost of posterior hydrogen compression. The influence of the temperature on the performance of the device has also received limited research effort. In section 4.3, considerations on the effect of temperature and pressure on the device performance will be provided.

Durability

The lifetime of the system is another important challenge, as making the device durable is crucial not only for cost but also for sustainability. Currently, the main constraint on the durability of the device is the semiconductor and the catalytic material. State-of-the-art materials have a proven lifetime in the range of hours (Ager, 2015), whereas for the commercial-scale device it should be in the order of years. Also the durability of the membrane has not been investigated extensively.

Environmental Impact

Another challenge on the design of a commercial-scale artificial leaf is to minimize its environmental impact during the whole lifecycle of the product. This include the selection of environmental friendly raw materials that can be obtained without producing large amount of pollution, and that can be recycled or reused at the end of the life of the device. Furthermore, using manufacturing processes with low footprint is challenging, because current deposition processes for the semiconductor materials are very energy intense (Smith, 1995).

Safety

The safety of the device is also challenging, as hydrogen and oxygen are produced within the same piece of equipment, and they can create explosive gas mixtures. Therefore, the device should ensure the complete separation of the gases. Moreover, the design should account for safe storage of hydrogen and safety controllers that allow the detection of gas leakage, since hydrogen and air can produce explosive mixtures.

Social issues

There are also several societal challenges that need to be considered when designing the device. The first one is the safety on the production and usage of hydrogen as a fuel. Moreover, earth abundant materials should be use to ensure the availability of raw material for the construction of the device.

Appendix I – Losses through TCO layer

In the PEC device, as well as in PV panels, a transparent conductive oxide layer (TCO) needs to carry current laterally (in the plane of the film), as shown in Figure 54.

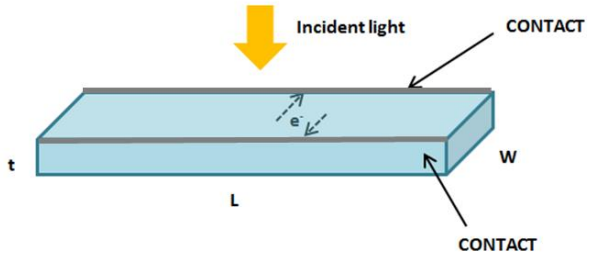

Figure 54. Sketch of the transport of electrons through the TCO layer towards the metal contacts

The resistivity of the film leads to the dissipation of power creating ohmic losses. The sheet resistance of the TCO films depends on their resistivity (ρ) and their geometric parameters - thickness (t), width (W), and length (L) - according to the following equation:

$$R_{TCO} = \rho \frac{W}{t\,L}$$

The resistivity of the TCO is dependent on the material. Commonly used materials are SnO_2:F and ZnO:Al, with resistivity in the range of 10^{-4} Ω cm (Delahoy, 2011). After the material selection, the optimization of a TCO is a complex issue involving choice of deposition method and deposition parameters, choice of doping concentration, and choice of thickness (Dawar, 1995). Given a resistivity, the sheet resistance of the TCO film can be reduced by increasing the thickness. However, thicker films will lead to an increase of the optical absorption of the film, according to the Lambert-Beer equation:

$$I(\lambda) = I_0(\lambda)\exp(-\alpha \cdot d)$$

where $I(\lambda)$ and $I_0(\lambda)$ are the transmitted and the incident light intensity, respectively, at a certain wavelength, α is the light absorption coefficient of the material and d is the thickness of the film. The optimal film thickness required to minimize the losses thus depends on the integrated optical absorption across the wavelength range of interest and the distance over which current has to travel in the TCO. For thin film silicon solar cells, typical thickness is in the range of 550 – 900 nm (Luque & Hegedus, 2011).

The longer the distance between the different metal contacts, the longer the path the electrons need to travel and thus the higher the losses. However, due to the reflectivity of the metal contacts, the minimum area as possible should be used of such materials, since they will carry light losses. This trade-off should be looked over and optimized for the industrial scale artificial leaf. Figure 55 shows an estimation of sheet resistance losses for different distance between the metal contacts (i.e. distance that the electrons have to travel). Different thicknesses have been considered to show how increasing the thickness of the film leads to lower losses.

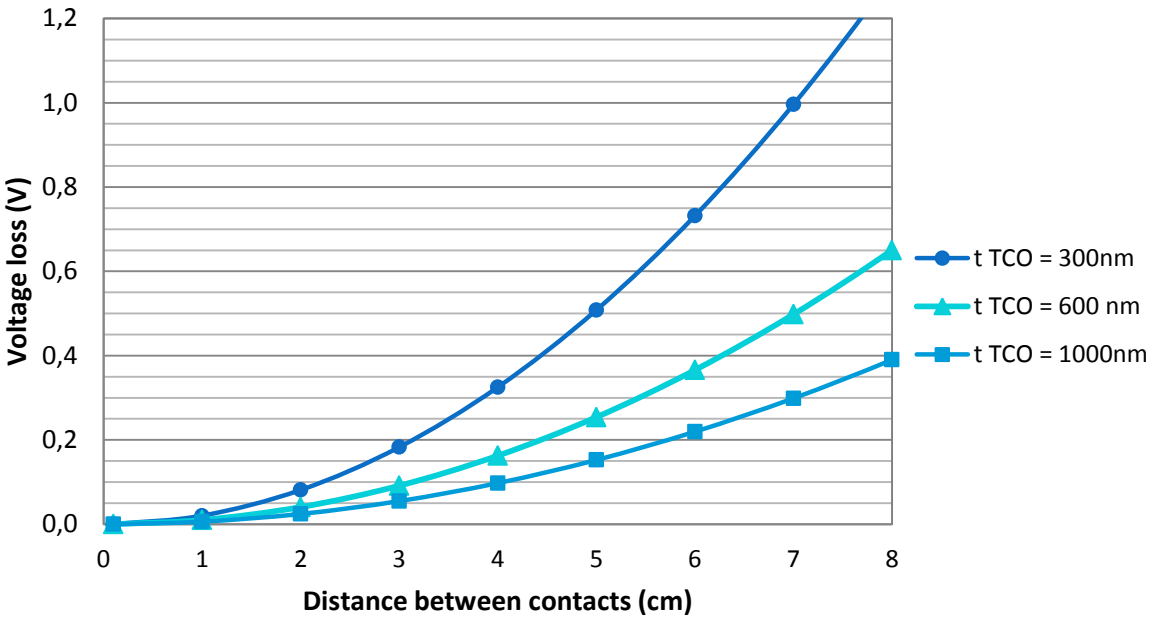

Figure 55. Voltage loss due to sheet resistance at the TCO layer for different travel lengths and film thicknesses

Placing the contacts 1 to 2 cm apart, similarly to the separation in commercial thin film solar cells (Luque & Hegedus, 2011), leads to losses below 40 mV for TCOs with thickness of about 600 nm (Figure 55).

Appendix J – Effect of temperature on PEC performance

On one hand, the increase in temperature increase in the radiative recombination, according to the following equation (Shockley & Queisser, 1961):

$$J_{rad} = \frac{e\,(n_{top}^2 + n_{bottom}^2)}{4\pi^2 c^2} \int_{E_g/\hbar}^{\infty} \omega^2 \exp\left(\frac{e\,V - \hbar\omega}{k\,T}\right) d\omega$$

where e is the unsigned charge on an electron, n_{top} and n_{bottom} are the refractive indexes of the media on the top and at the bottom of the cell, respectively, c is the speed of light, E_g is the bandgap of the photo-absorber, $\hbar$ is an abbreviation for $h/2\pi$ with h being Planck's constant, ω is the frequency of the incident light, V is the operating voltage, T is the absolute temperature, and k is Boltzmann's constant.

The radiative recombination negatively affects the performance of the cell. The operating current density (J) is equal to the current density produced by the solar radiation (J_{ph}) and the thermal radiation (J_{th}) minus the current density from radiative emission:

$$J = J_{ph} + J_{th} - J_{rad}$$

The analytical expressions for J_{ph} and J_{th} can be found in literature (Shockley & Queisser, 1961).

On the other hand, the overpotential for electrocatalysis decrease and the ion transport is enhanced at higher temperatures (Chen, 2014). The dependence of the overpotential for the oxygen evolution reaction (OER) with temperature is expressed as follows (Chen, 2014):

$$i_{T,OER} = i_{Tref,OER} \exp\left(\frac{E_{a,OER}}{R\,T_{ref}}\right) \exp\left(-\frac{E_{a,OER}}{R\,T}\right)$$

where $i_{T,OER}$ and $i_{Tref,OER}$ represent the current density at temperature T and at the reference temperature (T_{ref}), respectively and $E_{a,OER}$ is the activation energy for the oxygen evolution reaction. The same expression can be built for the current density of the hydrogen evolution reaction.

The improvement in ion transport is related to the increase of the conductivity of the electrolyte (σ_T) with temperature, which is described by the following equation (Chen, 2014):

$$\sigma_T = \sigma_{Tref}(1 + \alpha(T - T_{ref}))$$

where σ_{Tref} is the conductivity at a reference temperature and the coefficient α depends on the electrolyte solution. For example, for a solution of 1 M sulphuric acid, the coefficient α is 0.019 K^{-1} (Darling, 1964).

Appendix K – Data from the economic analysis by the DOE

In the economic analysis performed by the DOE (James, 2009), the capital investment involved in the PEC reactor was estimated considering efficiencies of 5, 10 and 20%. Using these values, the cost of a PEC panel with 15% efficiency, which is the target efficiency set in this project, was estimated as 180 $/m^2 (Figure 56).

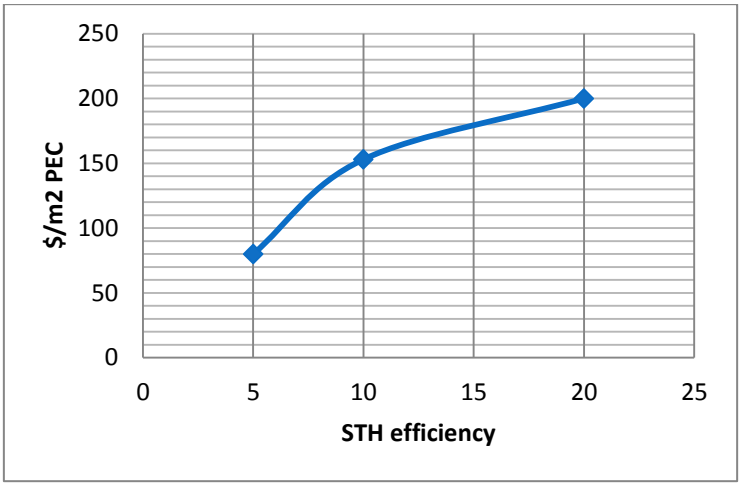

Figure 56. Cost of the PEC module as a function of its efficiency (James, 2009)

The breakdown of the cost of the PEC reactor was investigated according to the data provided by James *et al.* (2009) for a PEC panel of 5 % efficiency. It is of our interest to understand if the components will play an important role in the cost of the device. It can be observed in Figure 57 that 65 % of the total cost of the panel corresponds to the materials. Therefore, keeping the cost of materials as low as possible will be of great importance for the commercial viability of the device.

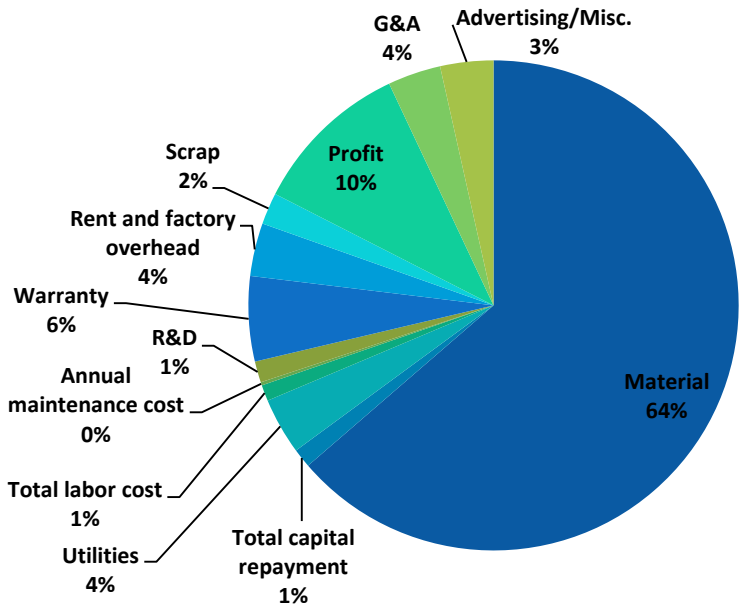

Figure 57. Cost breakdown of a PEC cell with planar configuration (James, 2009)

Looking at the breakdown of the cost of materials (Figure 58) the water cell hardware and the plexiglass windows have the largest weight in the cost (27 % and 23 %, respectively). The semiconductor material and the TCO-coated glass account for 10 % of the cost of the materials each. These estimated costs (TCO-coated

glass \$5/m^2 and semiconductor \$7/m^2) seem very optimistic. For this reason, these costs will be revised later on in this project.

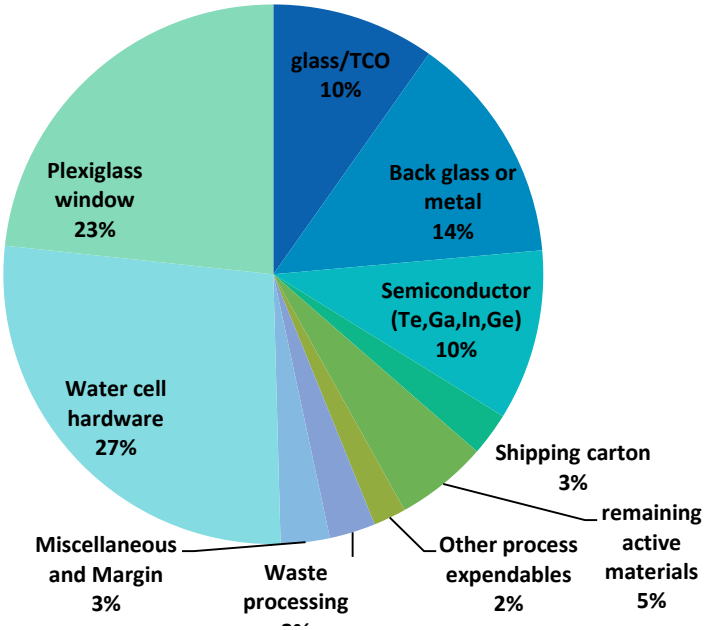

Figure 58. Materials cost breakdown (James, 2009)

It should be noticed that in the analysis performed by the DOE, the cost of the membrane was not considered, which can be as high as 250-500 \$/m^2 for Nafion®. This cost is too high, since the cost of the total device should be in the range of \$180 per m^2. Hence, a design alternative is to find a smart design is found were a very small area of membrane is needed, or a cheaper membrane needs to be employed. In the case that cheaper membranes are not transparent, a device configuration where the membrane is not placed in front of the photoelectrodes should be considered.

Knowing the capital cost of the device, the hydrogen output, and the selling price of hydrogen (6 \$/kg), a preliminary estimation of the operating cost can be done, for a target payback time (PBT). This target was set as 7 years, as explained in Chapter 4. To achieve this PBT, the operating expenditures should be in the order of 16 \$/m^2. The data and assumptions made for this calculation are presented in Table 29. The calculation of the Net Present Value, which was done assuming a cost of capital of 12%, is shown in Table 30, and represented in Figure 59.

Table 29. (left) Panel specifications for the economic analysis (right) Basic economic data to calculate the net present value

Panel specifications	
Area (m^2)	1
STH efficiency	15%
P light (kW/m^2)	1
Sun hours per day	6
G ($KJ/mol\ H_2$)	237
Production of H_2 ($g/s\ m^2$)	0.0013
Daily production (g/day)	27.30
Annual production (kg/year)	9.98
CAPEX ($)	**180.00**
OPEX ($/year)	**16.00**
SALES ($/year)	**59.88**
CASH FLOW ($/year)	**43.88**

Table 30. Calculation of the Net Present Value (NPV)

Year	Cash flow	Present value	NPV
0	-180,00	-180,00	-180,00
1	43,88	39,18	-140,82
2	43,88	34,98	-105,84
3	43,88	31,23	-74,61
4	43,88	27,89	-46,73
5	43,88	24,90	-21,83
6	43,88	22,23	0,40
7	43,88	19,85	20,25
8	43,88	17,72	37,97
9	43,88	15,82	53,80
10	43,88	14,13	67,92
11	43,88	12,61	80,54
12	43,88	11,26	91,80
13	43,88	10,06	101,86
14	43,88	8,98	110,83
15	43,88	8,02	118,85

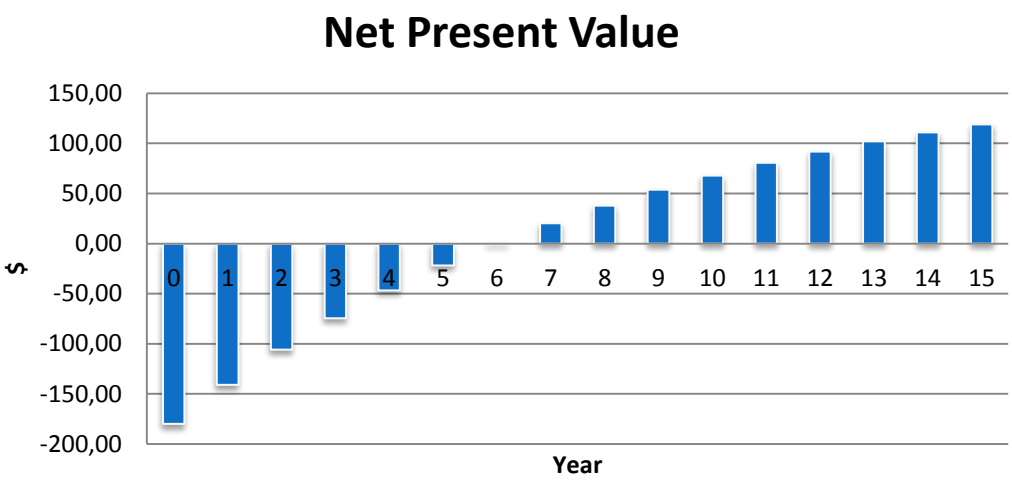

Figure 59. Net present value of the PEC cell in dollars over a period of 15 years

Appendix L – Design alternatives for an artificial leaf device

Some designs were found in literature, and the corresponding citation is given in the caption of the figure. The members of the Materials for Energy Conversion and Storage (MECS) group developed other designs during a small creativity session carried out on March 18th 2015. Those designs are cited as "MECS", and the caption collects the comments given (if any) by the person who made the design. The trainee developed the designs that have no sort of citation.

Particle-based reactors

Concept 1. Tubular particle reactor

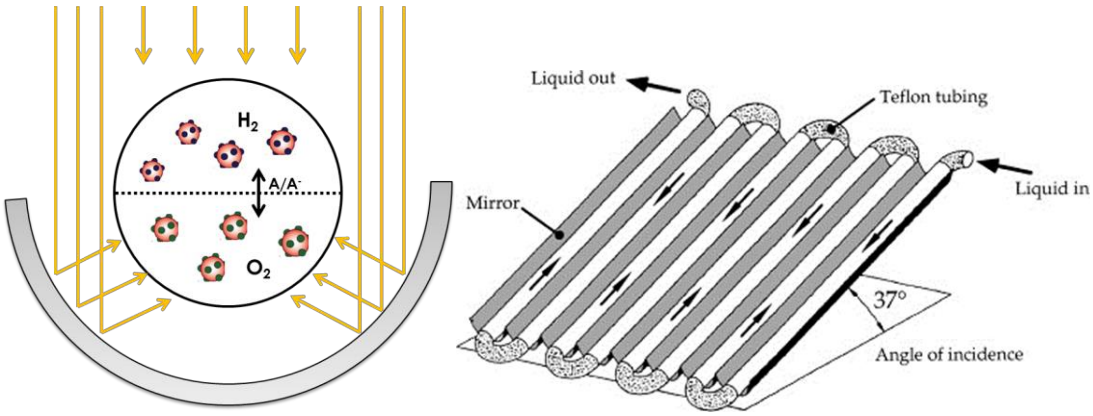

Figure 60. Schematic representation of the envisioned tubular particle-based reactor for solar water-splitting. A mirror is used for illumination of the backside of the tubes. H_2 and O_2 evolution sites separated via a membrane. Concept inspired by photocatalytic water treatment reactors, such as the one developed at the Plataforma Solar de Almeria (Spain) (left image) (http://www.psa.es/webeng/#)

Concept 2. Single chamber particle reactor

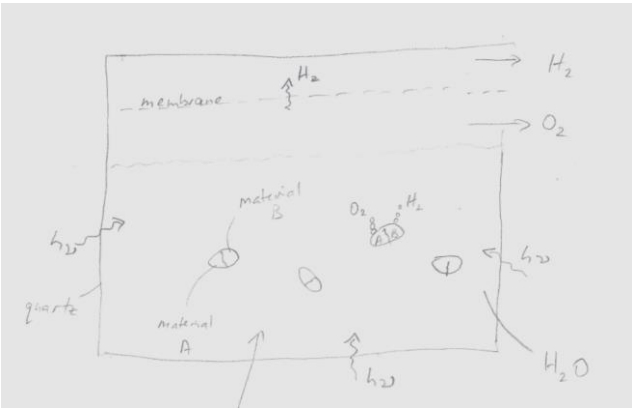

Figure 61. MECS - "Particles of at least two adequate materials suspended on a stable aqueous solution. It could also be a pond kept clean by fishes and snails". This configuration has been also reported in literature (Pinaud, 2013).

Concept 3. Dual chamber particle reactor

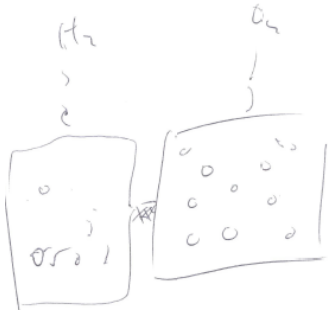

Figure 62. MECS - "Particles in a bag". This configuration has been also reported in literature (Pinaud, 2013).

Planar electrodes

Concept 4. Back-to-back photoelectrodes separated by a horizontal membrane

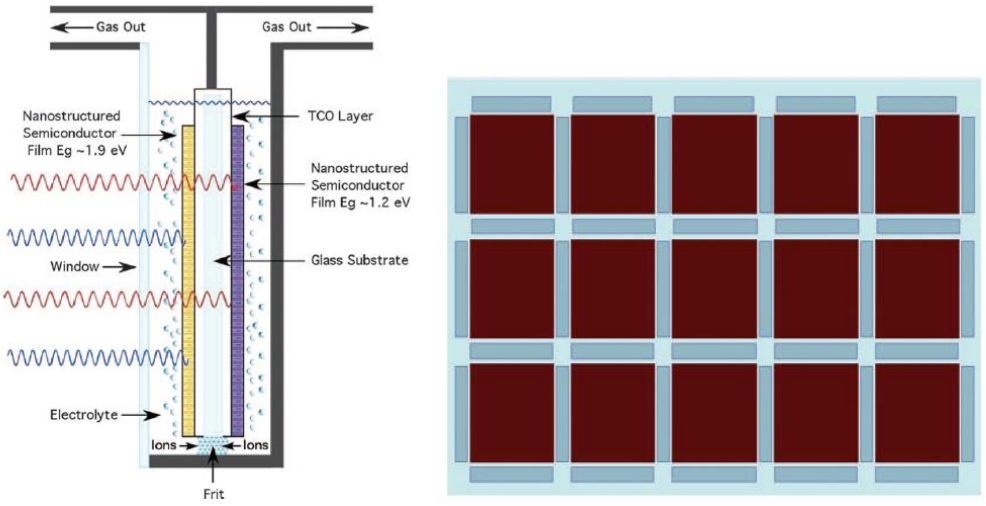

Figure 63. a) Side view of a tandem PEC water-splitting system. b) Front view of a tandem PEC water-splitting system. Maroon squares correspond to the nanostructured semiconducting thin film on a conducting glass substrate; while blue rectangles represent the area where a frit or membrane would be placed (Lewerenz, 2013)

Concept 5. Back-to-back photoelectrodes separated by a perpendicular membrane

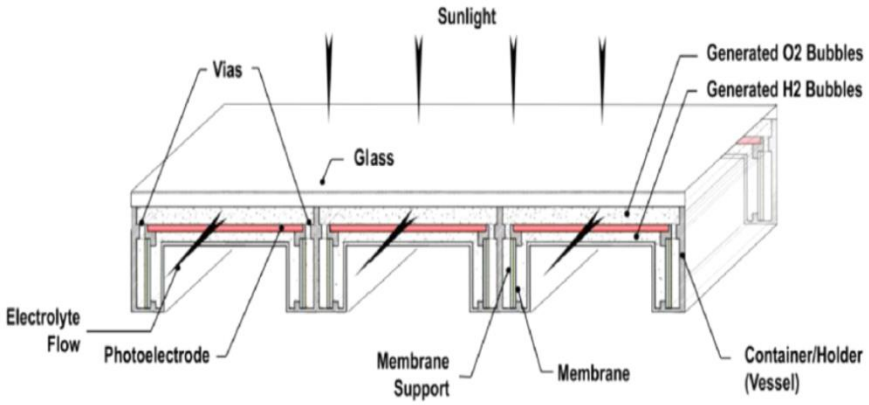

Figure 64. PEC cell configuration suggested by Deng and Xu (2010) *(Image obtained from (Xing, 2013))*

Concept 6. Back-illuminated photoanode+ cathode

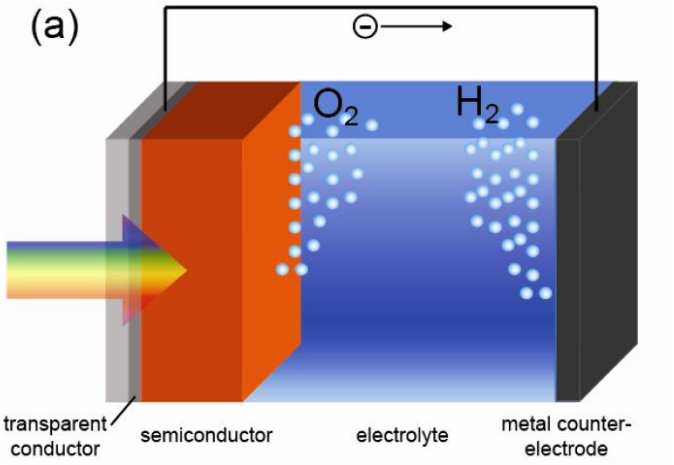

Figure 65. Faced electrodes, with a back-illuminated photoelectrode and a metal counter electrode (van de Krol, 2011)

Concept 7. PV (isolated) + two faced electrodes

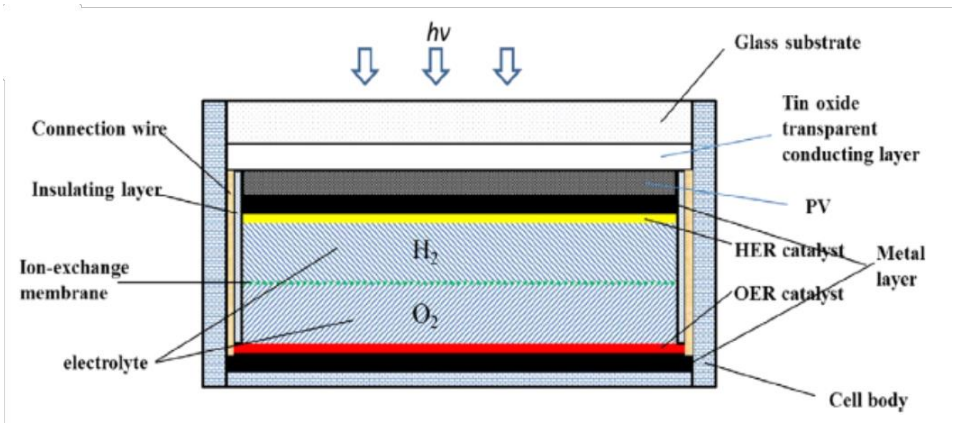

Figure 66. PEC cell configuration suggested by Deng and Xu (2005) *(Image obtained from (Xing, 2013))*

Concept 8. Side-by-side electrodes with perpendicular membrane

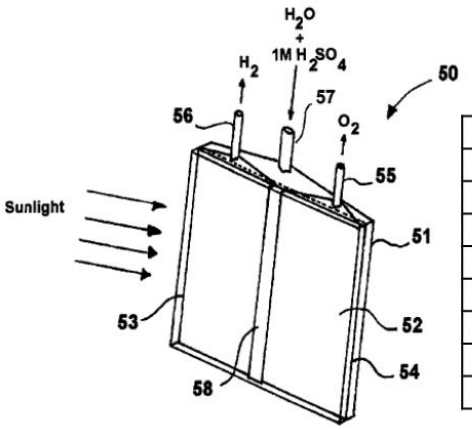

50	Dual flat-face half-cell
51	Housing or enclosure
52	Light transmissive wall
53	Photocathodes
54	Photoanodes
55	Oxygen outlet
56	Hydrogen outlet
57	Electrolyte inlet opening
58	Separator

Figure 67. PEC cell configuration suggested by Fan *et al.* (2007)

Concept 9. Side-by-side electrodes with cylindrical mirrors for light concentration

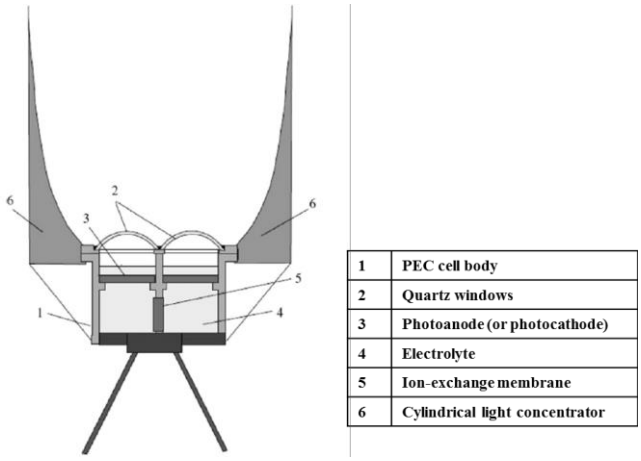

1	PEC cell body
2	Quartz windows
3	Photoanode (or photocathode)
4	Electrolyte
5	Ion-exchange membrane
6	Cylindrical light concentrator

Figure 68. PEC cell design (Aroutiounian, 2005)

Concept 10. Side-by-side photoanodes, with perpendicular cathode

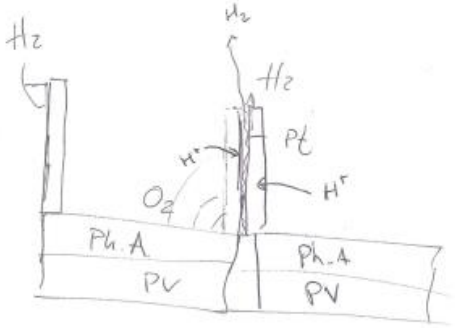

Figure 69. Side-by-side photoanodes, with a perpendicular cathode "sandwiched" between a proton exchange membranes

Concept 11. Alternating back-to-back electrodes with perpendicular membrane

In acidic conditions:

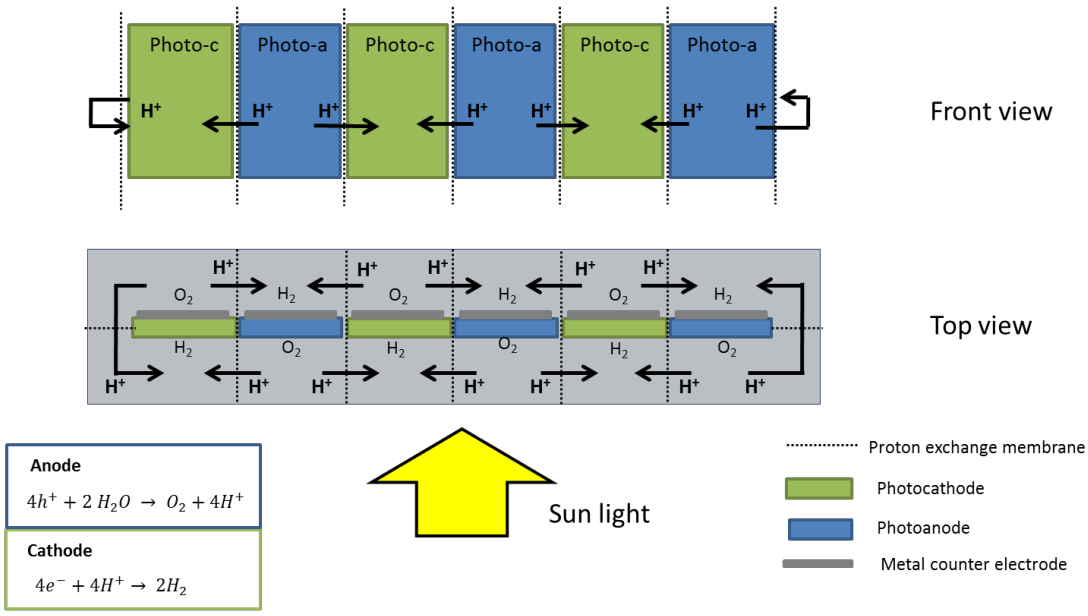

In near-neutral conditions:

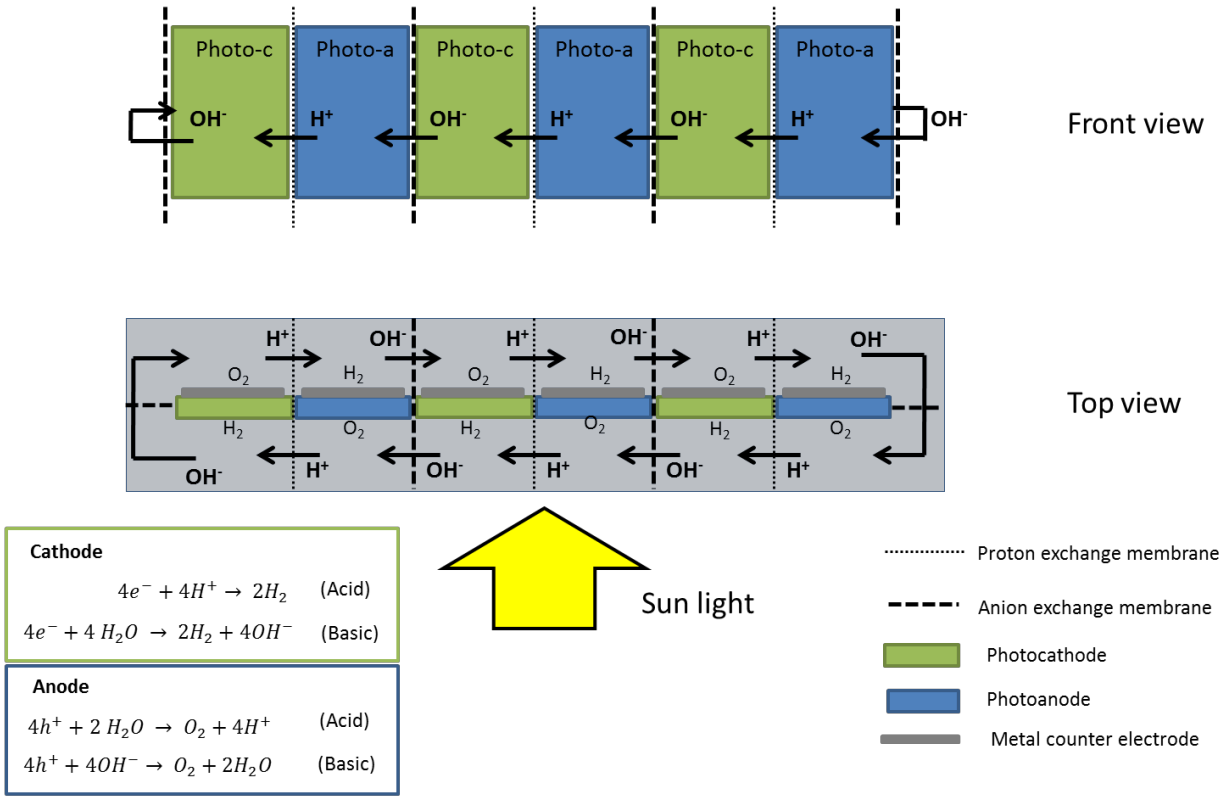

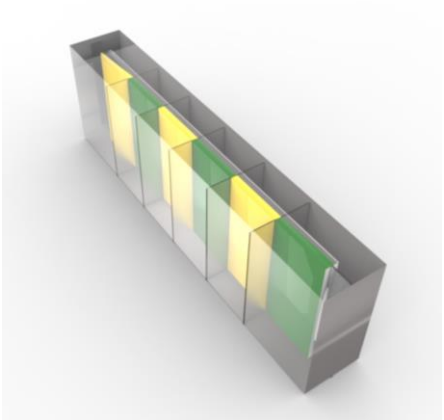

Figure 70. Photoanodes and photocathodes are placed side-by-side, but electrically connected to a counter electrode placed on the back

Concept 12. Faced electrodes mirrors at both sides for light concentration

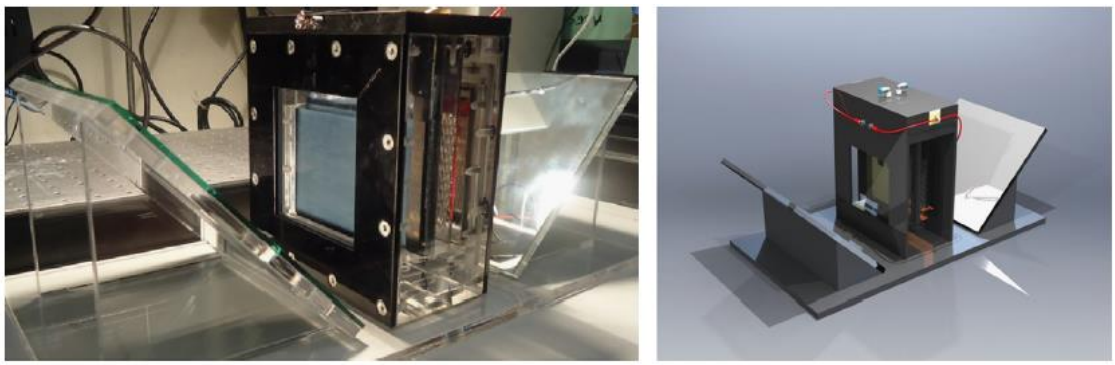

Figure 71. 10 x 10 cm prototype of a PEC cell with a mirror system to redirect the light beam (Lopes, 2014)

Concept 13. Faced electrodes with mirror for illumination from both sides of the cell

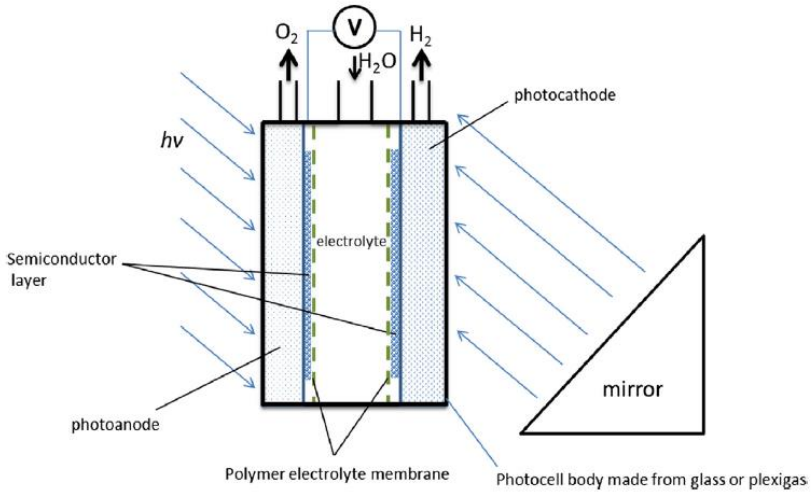

Figure 72. Patent US7241950 B2 (Fan, 2007) *(Image obtained from (Xing, 2013))*

Concept 14. Micro-reactor with side-by-side electrodes

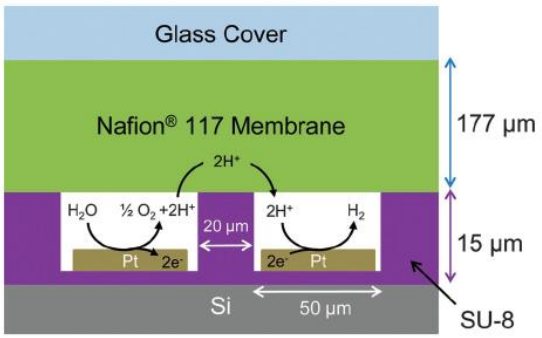

Figure 73. Schematic diagram of a microfluidic electrolyser (Modestino, 2013)

Concept 15. Front illuminated faced electrodes, with a "frame" counter electrode

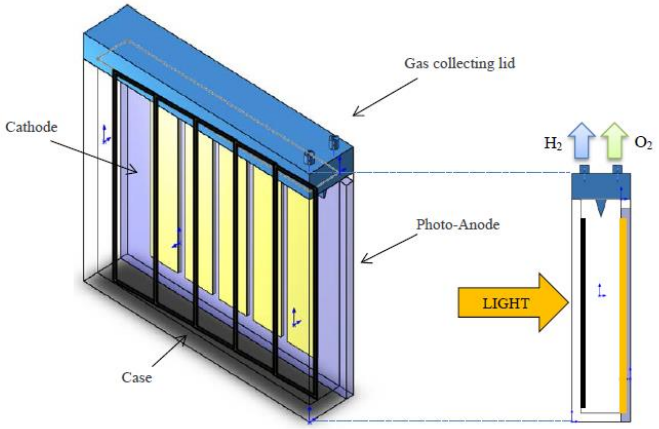

Figure 74. Prototype for a PEC water-splitting device (Corakci, 2014)

Concept 16. Front illuminated faced electrodes, with a "transparent" counter electrode

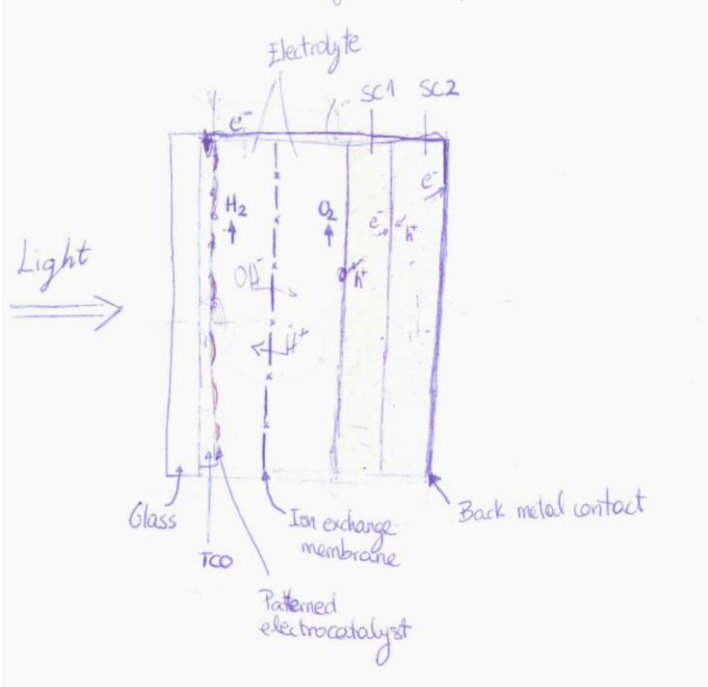

Figure 75. Faced electrodes, with front-illuminated photoelectrode and transparent counter electrode

Concept 17. Back illuminated photoanode + front illuminated photocathode

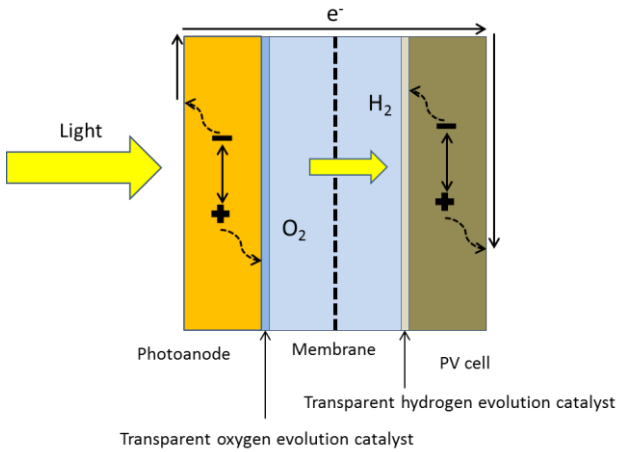

Figure 76. Faced electrodes, with back-illuminated photoanode and front illuminated photocathode

Concept 18. Back-to-back "hollow" photoelectrodes

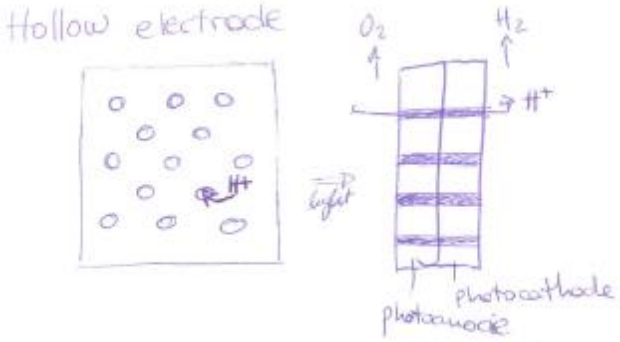

Figure 77. The two photoelectrodes are placed back-to-back, holes are performed to allow the transport of ions prom one side to the other.

Concept 19. Back-to-back "stairs" photoelectrodes

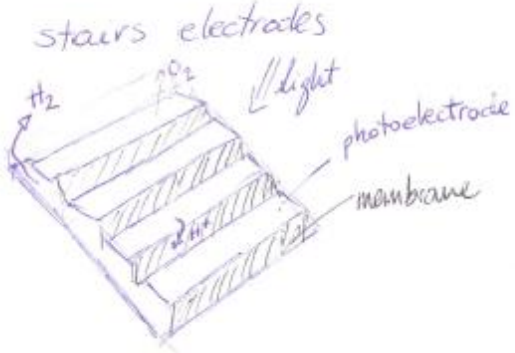

Figure 78. The two photoelectrodes are placed back-to-back, placed similarly to steps of a stair. A membrane is located in the space between the "steps" to avoid the crossover of gases.

Concept 20. Tubular PEC reactor with flexible electrodes

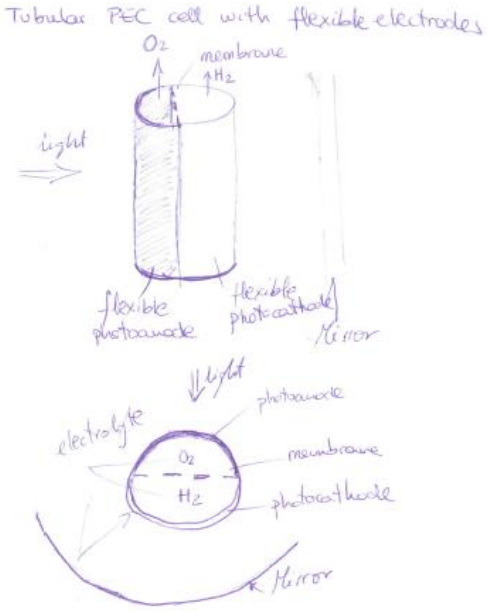

Figure 79. Flexible electrodes are placed in the shape of a tube, holding the electrolyte inside. A membrane is used to separate the oxygen and hydrogen evolution chambers. A mirror is used to allow for illumination of the backside of the tube

Concept 21. Hexagonal reactor

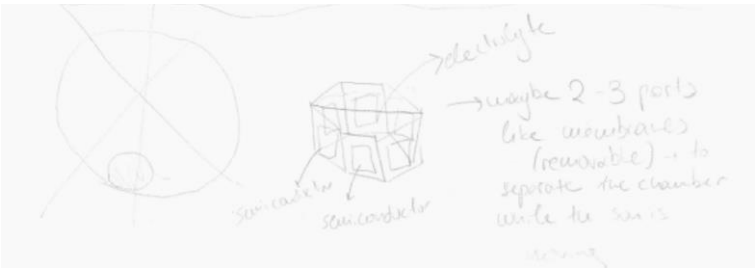

Figure 80. MECS - Photoelectrodes are placed next to each other forming an hexagon.

Concept 22. Multilayer back-to-back electrodes

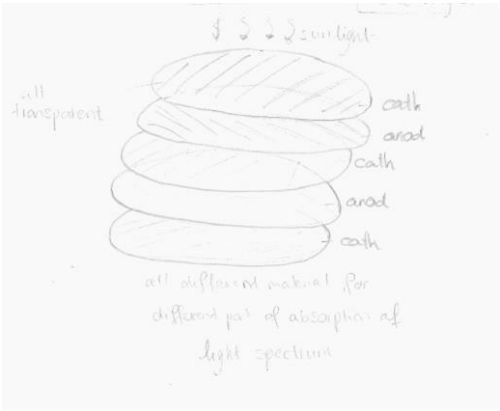

Figure 81. MECS - Cathodic and anodic layers with different absorption spectrum are placed back to back

Concept 23. "Multi-square" configuration

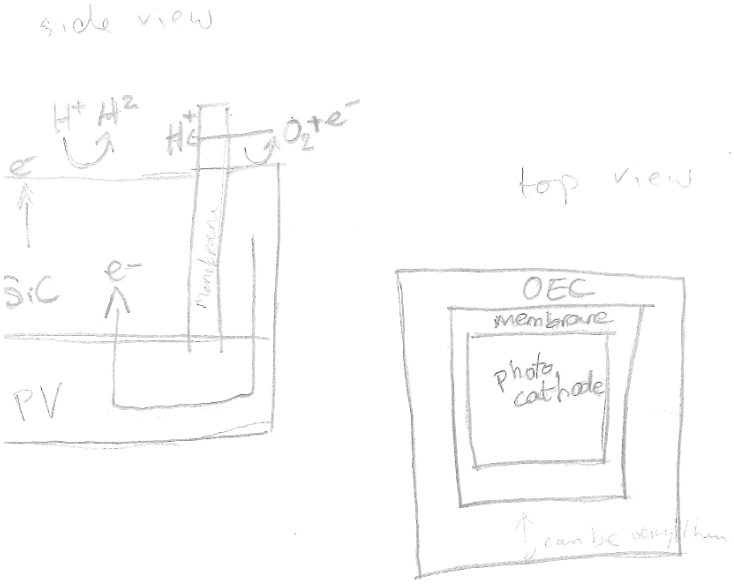

Figure 82. MECS - Photocathode inside a photoanode frame, separated by a perpendicular membrane

Concept 24. Concentrated faced photoelectrodes with bipolar membrane

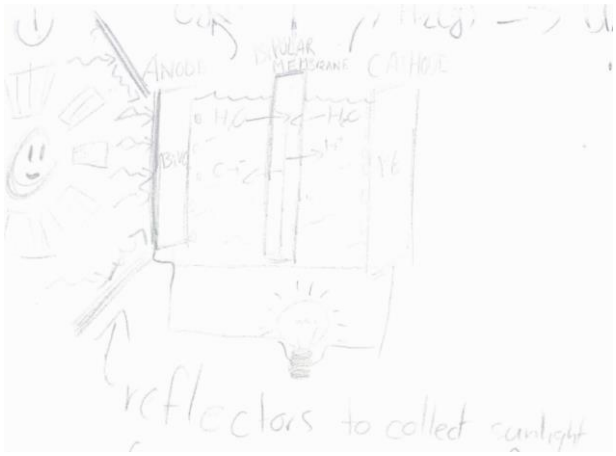

Figure 83. MECS - Faced electrodes with a bipolar membrane and reflectors to concentrate light

Concept 25. Back-illuminated photoanode with HEC deposited on membrane

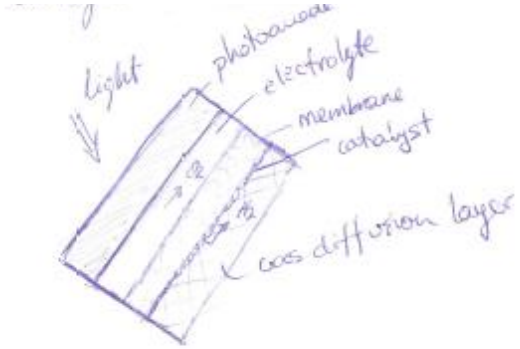

Figure 84. Faced electrodes, with a back-illuminated photoanode. The hydrogen evolution catalyst (HEC) is directly deposited onto the proton exchange membrane

Concept 26. Curved back-to-back photoelectrodes

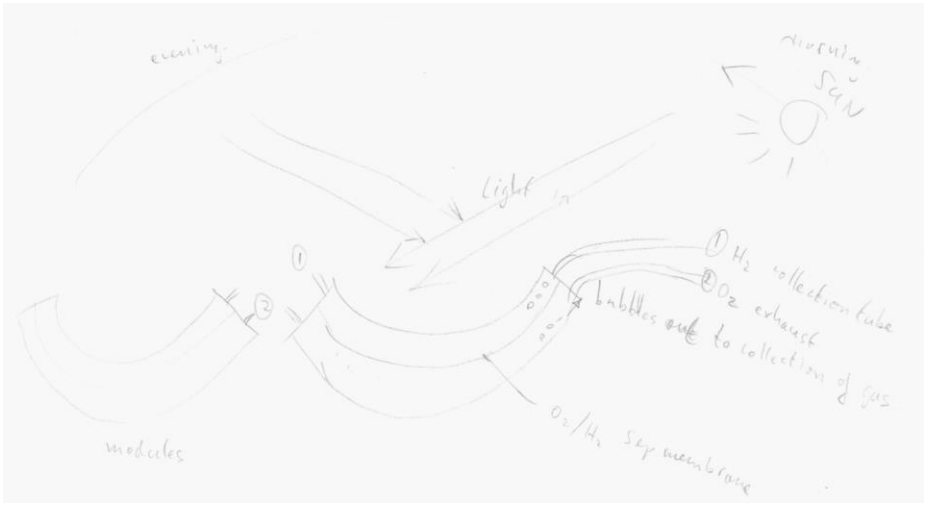

Figure 85. MECS - Flexible back-to-back electrodes

Concept 27. MEA PEC device using carbon cloth

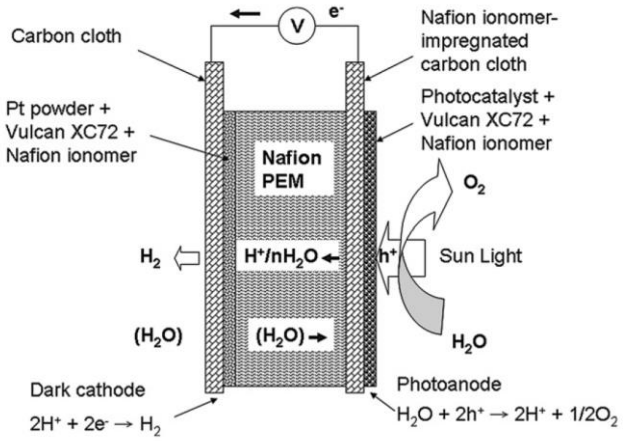

Figure 86. Membrane electrode assembly photoelectrochemical cell (Jeng, 2010)

Concept 28. MEA PEC device with transparent drilled electrodes

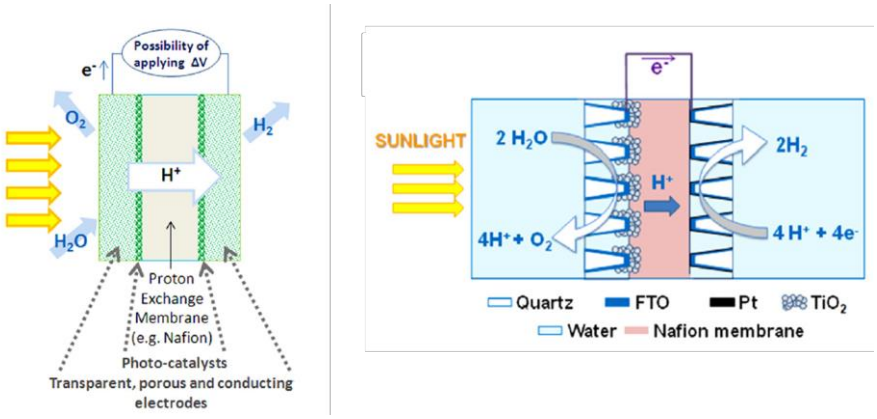

Figure 87. MEA photoelectrochemical cell using transparent drilled electrodes (Hernandez, 2014)

Concept 29. PV + perpendicular metallic electrodes

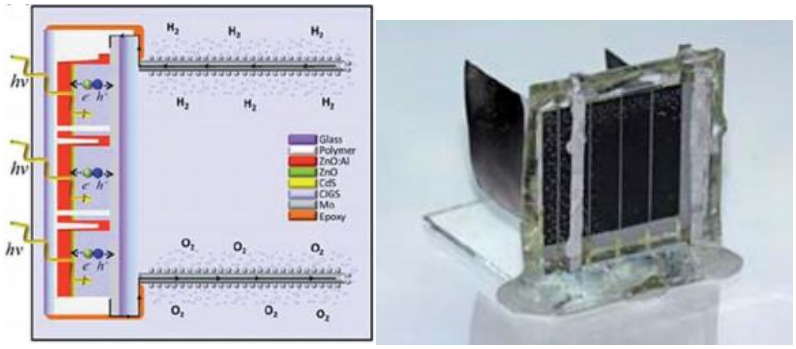

Figure 88. Device composed by a semiconductor photo-absorber and two perpendicular metallic electrodes(Jacobsson, 2013)

Appendix M – Light losses in a device based with a front illuminated photoelectrode

Fresnel losses

Fresnel losses can be calculated as follows if an angle of incidence of 0 degrees is assumed:

$$T = \frac{4^m \cdot n_1 \cdot (\prod_{j=2}^{m} n_j^2) \cdot n_{m+1}}{\prod_{j=2}^{m} (n_j + n_{j+1})^2}$$

where T is the light transmitted through m optical boundaries with refractive index n.

Figure 89 shows the reference materials used for a first estimation of the Fresnel losses in a front illuminated photoelectrode device. For the front panel PMMA is used as reference, the TCO material selected is In_2O_3, the membrane the commonly used Nafion®, and the refractive index of the electrolyte solution is assumed the same as that of water. The refractive index of the semiconductor material has been selected according to the study by Kumar *et al.* (2010), who modelled how to calculate the refractive index of materials according to their bandgap. In this review, it can be seen that materials a refractive index of 2.5 corresponds to band gaps of around 2.20 eV.

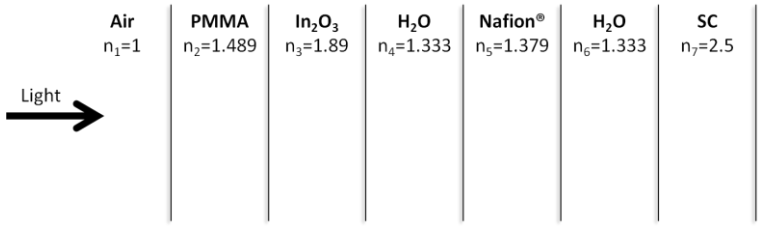

Figure 89. Sketch of the optical boundaries that light crosses in order to reach the semiconductor (SC) in a device based on a front illuminated tandem photoelectrode.

Using this combination of refractive indexes, the calculated Fresnel losses resulted in a transmission value of 83.3%.

A sensitivity analysis to the change in refractive index of the different materials with respect to the transmission has been performed (Figure 90). As it can be seen in Figure 90, the values selected for the front panel and the membrane are close to the optimum. However, a significant improvement of the light transmitted could be obtained if a TCO material with lower refractive index (1.3-1.5) is selected.

It can be observed as well in Figure 90 that using a semiconductor material with lower refractive index (<2) would increase the light transmission. However, it should be noticed that a refractive index lower than 2.0 corresponds to bandgaps larger than 3 eV (Kumar, 2010). This approach is therefore discarded, since materials with bandgaps that large will lower the efficiency of the system (Doscher, 2014). A possible approach to reduce the losses in the boundary of water and semiconductor would be to use an intermediate conductive layer with a refractive index lower than 2.5, for example an ITO layer.

It should be pointed out that the graph above corresponds to the sensitivity of the overall transmission to the change of one of the materials. If more than one material is changed compared to the ones used as reference (Figure 89), the value of transmission should be recalculated.

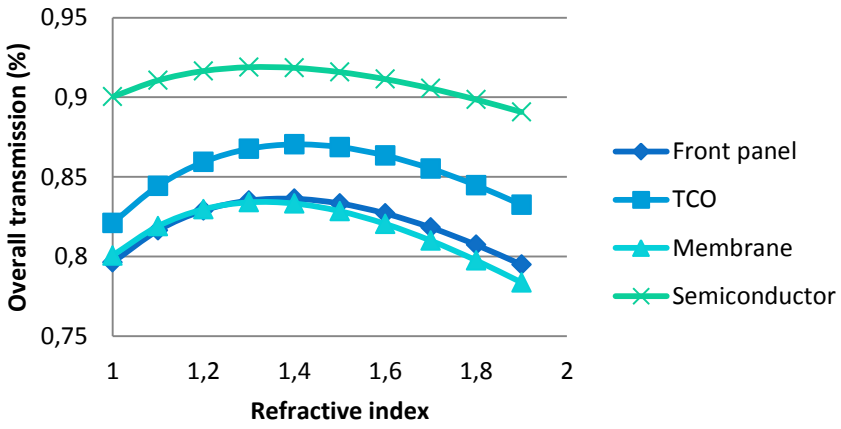

Figure 90. Effect of the refractive index of each component on the overall light transmission

Absorption losses

These losses depend on the absorption coefficient of the material (α) as well as on its thickness (t).

$$T = T_0 \cdot \exp(-t \cdot \alpha)$$

For PMMA, the bulk absorption is very low and can be neglected. According to the physical properties of Plexiglas® given by Arkema (http://www.plexiglas.com/en/), the bulk absorption of a sheet of even one inch thickness is less than 0.5%. Furthermore, the bulk light losses at of the TCO layer can be neglected compared to the losses at the optical boundaries (Luque & Hegedus, 2011).

The light absorption of water films of different thickness has been modelled by Doscher *et al.* (2014). The transmittance of the various water film thicknesses is shown in Figure 91. It can be observed in this figure that water films of thickness larger than 2 cm would carry significant losses for wavelengths above 700 nm. If the water film thickness is in the order of 1 mm, the losses will not be important below 1200 nm. It can be concluded that using a film of water as low as 1 mm, the bulk absorption losses will be neglectable when compared to the losses at the Fresnel losses.

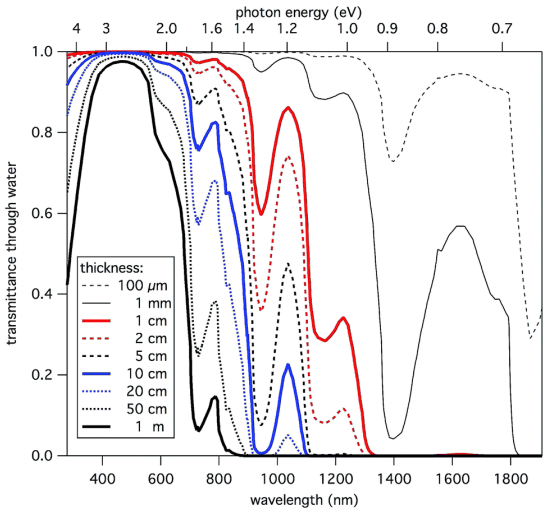

Figure 91. Light transmittance of different water film thicknesses (Doscher, 2014)

Appendix N – Ohmic losses due to ion transport in the selected device

Here the Ohmic losses in a faced-electrodes configuration, for different electrolyte conductivities and membrane thickness, are calculated. The conductivity of the membrane has been assume 42 mS/cm [Tokuyama Corporation ((http://www.tokuyama.co.jp)].

L_{el} represents the distance between the electrode and the membrane, and T_{mem} is the thickness of the membrane. Therefore, the total distance between the electrodes is $2xL_{el}+T_{mem}$.

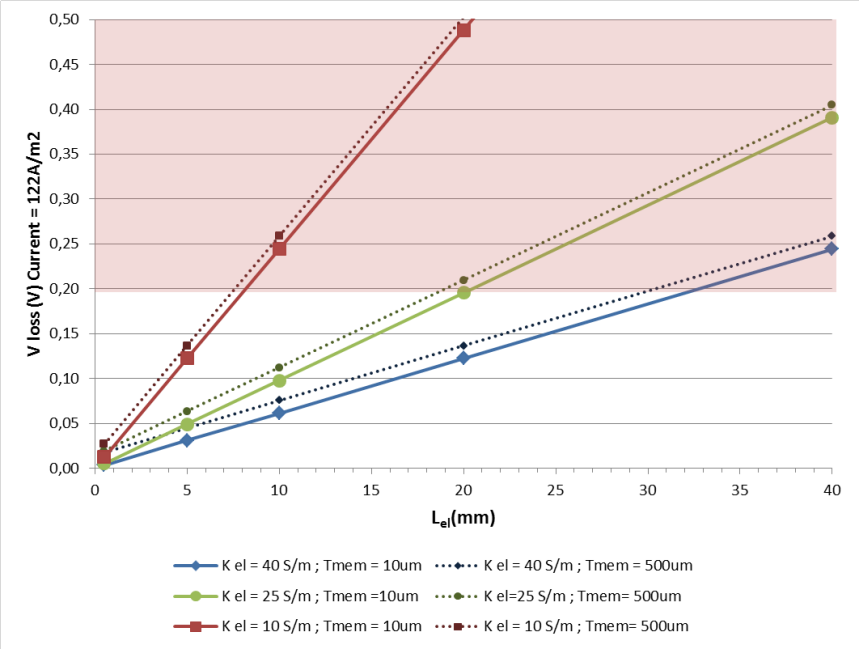

Figure 92. Ohmic losses vs distance between electrodes for different electrolyte conductivities and membrane thickness

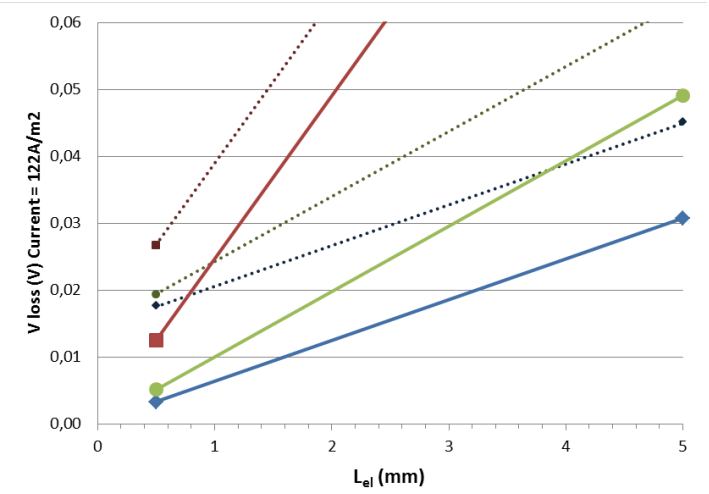

Figure 93. Zoom of the previous graph showing the ohmic losses for electrodes distance < 5 mm